UNICAMP

UNIVERSIDADE ESTADUAL DE CAMPINAS

Faculdade de Ciências Farmacêuticas

JULIANA SOUZA RIBEIRO COSTA

DEVELOPMENT OF FREEZE-DRIED DOSAGE FORMS FOR LOCAL DELIVERY
OF ANTI-INFLAMMATORY MOLECULES

DESENVOLVIMENTO DE FORMAS DE DOSAGEM LIOFILIZADAS PARA
ENTREGA LOCAL DE MOLÉCULAS ANTI-INFLAMATÓRIAS

CAMPINAS

2021

JULIANA SOUZA RIBEIRO COSTA

DEVELOPMENT OF FREEZE-DRIED DOSAGE FORMS FOR LOCAL DELIVERY OF ANTI-INFLAMMATORY MOLECULES

DESENVOLVIMENTO DE FORMAS DE DOSAGEM LIOFILIZADAS PARA ENTREGA LOCAL DE MOLÉCULAS ANTI-INFLAMATÓRIAS

Thesis presented to the Faculty of Pharmaceutical Sciences of the University of Campinas in partial fulfillment of the requirements for the degree of Doctor, in the area of Drugs, Medicines and Health Supplies.

Tese apresentada à Faculdade de Ciências Farmacêuticas da Universidade Estadual de Campinas como parte dos requisitos exigidos para a obtenção do título de Doutora em Ciências, na Área de Fármacos, Medicamentos e Insumos para a Saúde.

Supervisor: PROFA. DRA. LAURA DE OLIVEIRA NASCIMENTO

ESTE TRABALHO CORRESPONDE À VERSÃO FINAL DA TESE DEFENDIDA PELA ALUNA JULIANA SOUZA RIBEIRO COSTA, E ORIENTADA PELA PROFA. DRA. LAURA DE OLIVEIRA NASCIMENTO

CAMPINAS

2021

Informações para Biblioteca Digital

Título em outro idioma: Desenvolvimento de formas de dosagem liofilizadas para entrega local de moléculas anti-inflamatórias
Palavras-chave em inglês:
Dosage forms
Freeze drying
Área de concentração: Fármacos, Medicamentos e Insumos para Saúde
Titulação: Doutora em Ciências
Banca examinadora:
Karina Cogo Müller
Daniele Ribeiro de Araujo
Arnóbio Antônio da Silva Junior
Paulo Cesar Pires Rosa
Francisco Benedito Teixeira Pessine
Data de defesa: 09-02-2021
Programa de Pós-Graduação: Ciências Farmacêuticas

Identificação e informações acadêmicas do(a) aluno(a)
- ORCID do autor: https://orcid.org/0000-0002-2211-4493
- Currículo Lattes do autor: http://lattes.cnpq.br/3044932396498190

FOLHA DE APROVAÇÃO

Profa. Dra. Karina Cogo Müller

Profa. Dra. Daniele Ribeiro de Araujo

Prof. Dr. Arnóbio Antônio da Silva Junior

Prof. Dr. Paulo Cesar Pires Rosa

Prof. Dr. Francisco Benedito Teixeira Pessine

A ata de defesa, com as respectivas assinaturas dos membros, encontra-se no SIGA/ Sistema de Fluxo de Dissertação/ Tese e na Secretaria do Programa da Unidade.

Aos meus pais, meus irmãos e meu marido, que não mediram esforços para que eu chegasse até aqui. Este trabalho é dedicado a vocês.

AGRADECIMENTOS

que me ajudou sempre que possível; e a toda equipe do LRAQ-FEQ pela ajuda com diversas análises.

Aos amigos que deixei em Greifswald, em especial minha supervisora dra. Sandra Klein, meus colegas de laboratório Lisa, Erik, Katharina, Frank e Ulrike, à *Frau* Lange, técnica do laboratório, e todos os colegas do departamento. Vocês fizeram toda a diferença, me propiciando uma experiência internacional além dos muros da faculdade. Obrigada por toda a ajuda! Adrian, obrigado por me ajudar com todos os trâmites legais, e por me proporcionar momentos com sua família!

Aos membros da banca examinadora, pelo tempo dedicado a avaliação deste trabalho.

A todos que, direta ou indiretamente, fizeram parte da minha formação, o meu muito obrigada.

RESUMO

Os sistemas de entrega de fármaco são uma ferramenta eficaz para direcionar e manter a ação local de fármacos que seriam aplicados sistemicamente, evitando assim a exposição de todo o organismo aos potenciais efeitos colaterais dos fármacos. Para cuidados pós cirúrgicos, a ação anti-inflamatória geralmente é desejada, sendo a administração local do fármaco tida como a mais desejável. A lidocaína, fármaco utilizado na prática dental desde 1950 como anestésico e analgésico, apresenta atividade antibacteriana, desejável para aplicação local em lesões pós-cirúrgicas, sendo utilizada como fármaco modelo nesse trabalho. A curcumina é um fármaco muito utilizado na medicina oriental, com diversas utilidades, entre elas a atividade anti-inflamatória, porém com grande limitação na administração oral, por ter baixíssima solubilidade em água, e baixa biodisponibilidade. Nesse contexto, as ciclodextrinas surgem como boa alternativa para complexar com a curcumina, aumentando sua solubilidade e possivelmente sua biodisponibilidade. A complexação de curcumina em ciclodextrinas permitiu uma maior solubilidade da curcumina em água, facilitando a sua incorporação nos wafers liofilizados. Também foram estudadas a afinidade das duas ciclodextrinas (hidroxipropil-beta-cyclodextrina e sulfobutileter-beta-ciclodextrina) com os três curcuminóides (curcumina, demetoxicurcumina e bisdemetoxicurcumina) presentes em maior concentração na curcumina. Através de extensa caracterização físico-química dos biopolímeros foi possível desenvolver wafers biopoliméricos como sistemas de entrega para os fármacos aqui estudados. Os wafers apresentaram baixa atividade antimicrobiana, tempo de desintegração satisfatório para aplicação bucal, além de liberação do fármaco em tempo adequado para as aplicações desejadas.

ABSTRACT

Drug delivery systems (DDS) are an effective tool to direct and maintain the local action of drugs that would be applied systemically, thus avoiding the exposure of the entire organism to potential side effects of drugs. For post-surgical care, anti-inflammatory action is generally desired, with local administration of the drug being considered the most desirable. Lidocaine, a drug used in dental practice since 1950 as an anesthetic and analgesic, has antibacterial activity, desirable for local application in post-surgical injuries, being used as a model drug in this work. Curcumin is a drug widely used in oriental medicine, with several uses, including anti-inflammatory activity, but with great limitation in oral administration, because it has very low solubility in water, and low bioavailability. In this context, cyclodextrins appear as a good alternative to complex with curcumin, increasing its solubility and possibly its bioavailability. The complexation of curcumin in cyclodextrins allowed a greater solubility of curcumin in water, facilitating its incorporation in lyophilized wafers. The affinity of the two cyclodextrins (hydroxypropyl-beta-cyclodextrin and sulfobutyleter-beta-cyclodextrin) with the three curcuminoids (curcumin, demetoxycurcumin and bisdemetoxycurcumin) present in higher concentration in curcumin was also studied. Through extensive physical-chemical characterization of biopolymers it was possible to develop biopolymeric wafers as delivery systems for the drugs studied here. The wafers showed low antimicrobial activity, satisfactory disintegration time for oral application, in addition to the release of the drug in a timely manner for the desired applications.

SUMMARY

1 INTRODUCTION

Drug delivery systems (DDS) became a crucial tool for therapy enhancements. When potent drugs must be applied systemically to prevent local damage, the whole body gets exposed to possible side effects and biological action that is not needed on other sites. DDS can then direct and maintain local action without relevant systemic exposure, which also aids in decreased doses and consequent reduction of drug waste. If the substance has also antibacterial action, its systemic use can unbalance the natural microbiota and provoke undesired physiological outcomes. An unnecessary systemic exposure to anti-inflammatory substances causes the patient to be exposed to its potential adverse effects, most commonly gastrointestinal adverse effects, including ulceration, bleeding, or perforation. Other events may include nausea, dyspepsia, loss of appetite, abdominal pain, and diarrhea from erosion of the digestive tract. Though these risks can occur at any time in patients of any age, these adverse events tend to be more present in the elderly. Nonetheless, serious cardiovascular adverse events may also be associated with the use of anti-inflammatory drugs [1].
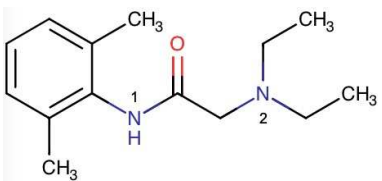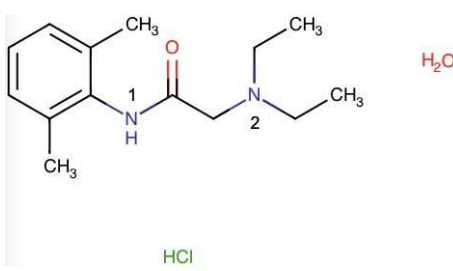
Anti-inflammatory action can be required for post-surgical care or over inflammation caused by infection, among other physiological disturbances. If infection and inflammation is localized or can be impaired by *in situ* intervention, local drug delivery should be evaluated as a feasible alternative. Here, in this thesis, we focused on two local medical conditions: post-surgical dental procedures and pulmonary infections, aiming to explore lidocaine and curcumin in lyophilized carriers as treatment options.

1.1   LIDOCAINE

Lidocaine hydrochloride was introduced in dental practice in the 1950s and became the main local anesthetic thanks to its effectiveness and safety, providing an anesthesia of 1.5-3 hours in duration when used in its injectable form [2,3]. Lidocaine (Table 1) is also used in formulations for other routes of administration and applications, such as injectable solution for local anesthesia [4–6], nasal aerosol [7], spray [8], transdermal microneedles [9], topical cream [10,11], among others. This variety of dosage forms shows the versatility of the molecule and facilitates comparisons of bioavailability in different routes of administration.

Table 1. Structural and physicochemical characteristics of lidocaine [12,13].

	Lidocaine	Lidocaine Hydrochloride
Chemical structure		
Molar mass (g/mol)	234.3	270.8
pKa	13.78 (1); 7.75 (2)	13.78 (1); 7.75 (2)
Water solubility (30 °C)	0.593 mg/mL	Soluble
LogP	2.84	-0.66 (ionic specie); 2.84 (non- ionic)
Melting point (°C)	68.5	81

Concerning the local use of lidocaine, it can anesthetize the mucosa before an incision, eliminating the pain of anesthetic injection or reducing the discomfort of an intravenous cannulation [14]. The transmucosal adhesive of the anesthetic lidocaine was the first medication in this pharmaceutical form to be approved by the FDA [15], capable of achieving moderate analgesia for up to 45

minutes if fixed for 15 minutes. However, one research has shown that the adhesive has low mucoadhesiveness [16].

Although the lidocaine is not an antibiotic agent, its anesthetic dose [17–19] inhibits bacterial growth and offers dual action during its use in dental procedures. Lidocaine can also be used as a postoperative analgesic and can be applied directly to the site of action, eliminating pain and first-pass effects [20,21]. Lidocaine undergoes extensive first-pass hepatic metabolism, where only 3% of orally administered lidocaine appear in plasma [22], so its use in pharmaceutical forms for local drug delivery is much more interesting.

In this work, lidocaine was used as a drug model since it is extensively characterized, a standard in dental practice and a multifunctional molecule, including anti-inflammatory properties. Lidocaine can be incorporated into oral wafers, which can be used as a dressing in the postoperative period, so that lidocaine would not need to cross the mucosa, avoiding first-pass metabolism, and maintaining the appropriate concentration of the drug at the site of action. The hydrochloride version was chosen for this project, instead of base lidocaine, mainly due to its solubility in water (Table 1), which facilitates its formulation in oral wafers, the chosen carrier for this study.
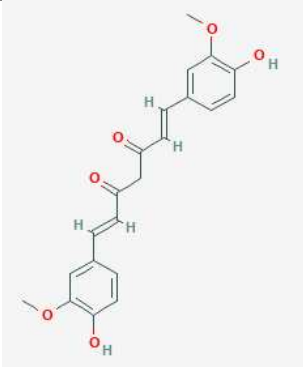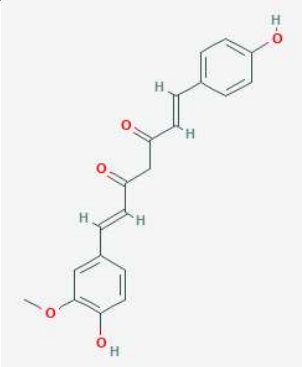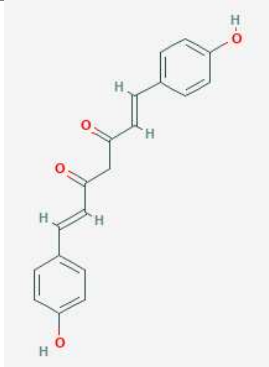
1.2   CURCUMIN

The dye extracted from the dry rhizome of *Curcuma longa L*, mainly constituted of curcumin, has been used in traditional Indian medicine as an antimicrobial and anti-inflammatory agent. Curcumin also acts on metabolism function, such as increased fecal excretion of cholesterol and bile acids in rats [23]. In addition, this drug eliminates reactive oxygen species, protecting hemoglobin from nitrite-induced oxidation, inhibiting lipid peroxidation and protecting DNA from damage caused by free radicals [24]. Another pharmacological activity found was the modulation of the activity of xenobiotic metabolizing enzymes in liver tissues of rats fed with turmeric [25]. Conney and his colleagues [26] also demonstrated that curcumin acts in tumors, inhibiting growth, invasion and metastasis due to the negative regulation of epidermal growth factor receptor expression [27]. However, the mechanism of action of curcumin in cancer in the oral cavity remains inconclusive [28].

The anti-inflammatory effect observed in studies was due to multiple actions. A reduction in the secretion of collagenase, elastase and hyaluronidase enzymes in activated macrophages has been reported [27]. However, the main action seems to be the modulation of NF-kB, with consequent inhibition of pro-inflammatory cytokines.

Curcuma longa L extract is constituted of three main curcuminoids: curcumin, demethoxycurcumin and bisdemethoxycurcumin. Their characteristics is showed in the Table 2.

Table 2. Structural and physicochemical characteristics of curcuminoids [29–32].

	Curcumin	Demethoxycurcumin	Bisdemethoxy curcumin
Chemical structure			
Molar mass (g/mol)	368.4	338.4	308.3
pKa	9.54 (1); 8.79 (2); 10.13 (3)	8.84 (strongest acidic)	8.64 (strongest acidic)
Water solubility	0.006 g/L (30 °C)	0.007 g/L	0.014 g/L
logP	4.12	4.28	4.07
Melting point (°C)	183	168	224

The next items (1.3 and 1.4) were written by me and belong to a review article entitled "Curcumin encapsulation in nanostructures for cancer therapy: a 10-year overview" [33].

1.2.1   Limitations of curcumin administration

Oral administration for systemic effects presupposes minimum water solubility, chemical stability under acidic (stomach) or around neutral pH (terminal jejunum, and ileum) and mucosal absorption. Curcumin is practically water-insoluble, approximately 1.34 mg/L [34], unstable in neutral and mild alkaline pH, with 25% degradation after 10 h in pH 8.0 at 25 °C [35] and presents a debatable stability under acidic pH [35–37]. As expected from its physicochemical profile, curcumin results in poor bioavailability for the human body and it is mostly found in feces after oral ingestion. Several clinical trials evaluated oral intake, from 0.5 to 12 g/day, finding plasma peak levels between 1-2 hours and traces or undetectable curcumin up to 2 g/day. Studies vary on their dosage forms (tablets/capsules, food), different food intake regimes (empty stomach, with fat

rich meals, etc.) and curcumin source (chemically synthetized, standardized extracts with other curcuminoids). Therefore, comparisons of peak levels between them should be cautious. Low plasma levels also derive from an extensive metabolism of curcumin mainly in liver, followed by intestine and gut microbiota. However, several metabolic products do have pharmacological properties, so metabolism itself may not impair treatment efficacy [38].

Low percutaneous permeation does not favor skin as a route for curcumin administration. An *in vitro* study with rat skin showed that even an emulsion brings only a small increment to permeation, which indicates that solubility would not be the limiting factor; however, microemulsion increased permeation substantially, paving a way for transdermal application by decreasing droplets average size [39]. In blood, curcumin seems to be highly stable by binding to human serum albumin (HSA) and fibrinogen, which precludes its degradation through hydrolysis [40]. Protein (bovine serum albumin - BSA) binding did not hamper curcumin antioxidant and antiproliferative (cancer cells) activities *in vitro* [41]. Therefore, the parenteral administration of curcumin would pose solubility as the main barrier. At last, toxicity studies in clinical trials pose no limitations to curcumin administration in humans so far; for oral administration it is already classified as Generally Recognized as Safe (GRAS). Noteworthy, high concentrations of curcumin induced mitochondrial and nuclear DNA damage in hepatoma G2 cells, but the phenomenon was not observed *in vivo* [42].

In this context, to enhance curcumin potential as a therapeutic agent in face of the above considerations, curcumin encapsulation in nanostructures is an excellent alternative, not only to facilitate its absorption by the organism but to protect it from degrading agents.

1.2.2   Curcumin nanocomplexes

In this topic, we will consider nanometric structures formed by one type of carrier molecule (protein or oligosaccharide), which interacts/aggregates with curcumin by non-covalent interactions to form a nanoaggregate (or nanocomplexes), as can be seen in Figure 1. In this sense, the most relevant nanocomplexes that enhance curcumin solubility relates to cyclodextrins (CD). CDs are cyclic glucose polymers consisting of six (α-), seven (β-) or eight (γ-) units linked by α-(1,4) glycosidic bonds, with an inner cavity that can bind

hydrophobic molecules and form stable hydrophilic complexes, which enhances their water solubility (Table 3) and dissolution kinetics [43,44]. Noteworthy, curcumin studies focus on solubility and inclusion characterization, rarely measuring diameter size; however, this measure is essential to characterize the aggregation state, since particle size depend on CD concentration, complexed drugs and excipients of the formulation. In addition, particle size can change internalization pathways and targeting, highlighting the need for better characterization of theses complexes in relation to their size profile [45].
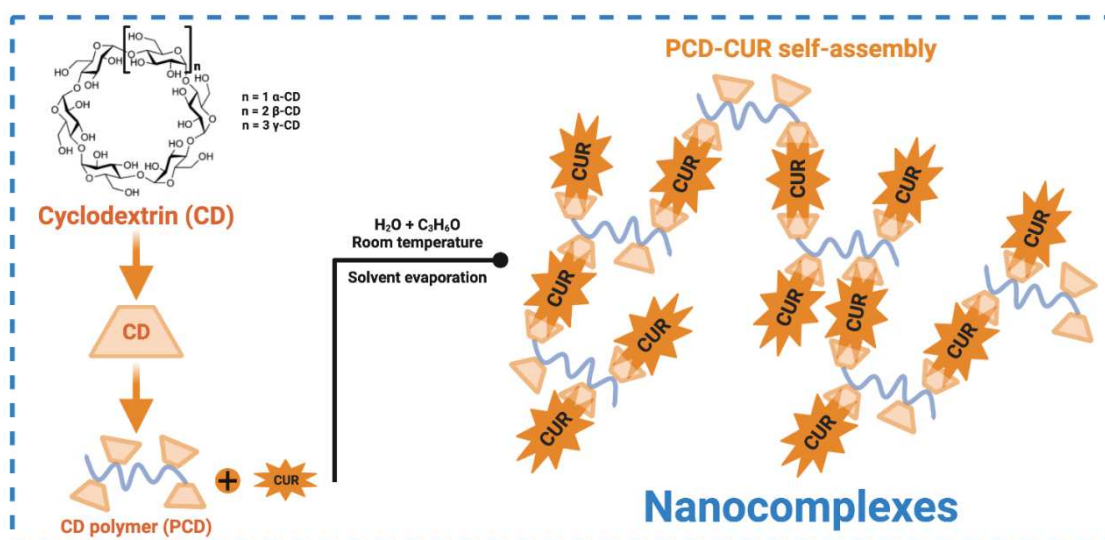
Figure 1. Schematic representation of polymeric β-cyclodextrin/ curcumin (PDC/CUR) self-assembly (inclusion complexation) formation (based on Yallapu et al., 2010 [46]).

Table 3. Curcumin solubility in different cyclodextrins (CD).

CD type	Solubility (mM)	Obs
β-CD	1.12 (60 mM CD)	Solubility in water [47]
β-CD	~ 0.05 (20 mM CD)	Solubility in water. Values obtained from the phase solubility diagram of curcumin–CD complexes [48]
γ-CD	~ 0.15 (20 mM CD)	
Hydroxypropyl-β-CD	~ 0.32 (20 mM CD)	
Methyl-β-CD	~ 0.51 (20 mM CD)	
Hydroxypropyl-α-CD	0.115±0.02 (92 mM CD)	Solubility in aqueous solution, pH 5. In this work, curcumin was synthesized according to the method of Pabon [49] in order to avoid interference from demethoxy- and bisdemethoxycurcumin [50].
Hydroxypropyl-β-CD	0.122±0.08 (79 mM CD)	
Hydroxypropyl-γ-CD	0.382±0.52 (70 mM CD)	
Hydroxytrimethyl-amoniumpropyl-β-CD	0.041±0.03 (68 mM CD)	
Randomly methylated β-CD	0.810±0.60 (84 mM CD)	
Sulfobutylether-β-CD	0.123±0.07 (46 mM CD)	
Hydroxypropyl-γ-CD	1.98 (57 mM CD)	Solubility in phosphate buffer (0.1 M, ionic strength 0.3) pH 6.0 [51]
Hydroxypropyl-β-CD	0.27 (70 mM CD)	

Curcumin-β-CD complexes (drug loading of 15%) were shown to increase molecule solubility and antitumor activity against lung tumor provoked by H22 cells in mice. The enhancement elucidated in vitro (A549 cells) was related to improved cellular uptake and modified release kinetics [52]. Polymeric β-CD were also complexed with curcumin and formed nanostructures of 250 nm in higher curcumin concentrations, with a drug loading of 23% (223.2 µg of curcumin per mg of CD). It reached an 80-fold enhanced solubility and an improved in vitro stability at physiological pH conditions: after 72 h immersed in PBS buffer, almost 100% of free curcumin was precipitated, whereas only 11% of the complexed curcumin precipitated. As for monomeric β-CDs, the polymeric complex showed higher antitumor and cytotoxic activities than free curcumin in prostate cancer cells. The IC50 (50% cell growth inhibitory concentration) for prostate cancer cell lines C4-2, DU145 and PC3 was 19.6, 19.25, and 19.4×10^{-6} M for free curcumin and 12.5, 15.9, and 16.1×10^{-6} M for curcumin complexed with β-CD, respectively [46].

Curcumin-hydroxypropyl-β-CD (HP-β-CD) complexes showed an even higher solubility (202-fold) and a modified dissolution profile of 50% release

in 6 h, with 100% of curcumin dissolved in 12 h. In addition, complexation increased the biological effects, demonstrated by greater antiangiogenic effects than free curcumin in chick chorioallantoic membrane model and decrease in the extent and severity of the disease in a rat colitis model (histopathological outcomes) [48].

Concerning other nanoaggregates, the stability and aqueous solubility of curcumin was significantly improved in the presence of proteins, which are folded in nanostructured particles. As in most CDs studies, protein-curcumin complexes generally lack physicochemical measurements such as size, particle charge or drug release kinetics. For instance, curcumin-casein complexes do not present these physicochemical indications. The work, however, showed that complexation increased the half-life of curcumin in Tris-HCl buffer pH 7.2 approximately 39-fold, from 8.8 min to 340 min, and degradation rates decreased from 90% after 30 min to 55% after 6 h of incubation [53]. Curcumin combined with BSA was also protected from degradation, showing only 24% degradation after 1,000 min in sodium phosphate buffer pH 7.0, whereas free curcumin decomposes practically 53% [54].

Curcumin encapsulated in the inner cavity of recombinant human H-chain ferritin presented the smallest size of measured curcumin-protein complexes (12 nm), but low encapsulation efficiency (14.7%), and drug loading of 1.07%. These nanoparticles increase curcumin water solubility about 492-fold, with photostability improvements: 69% of free curcumin degraded after 50 min exposed to an incandescent lamp, whereas only 11% of curcumin degraded when complexed with ferritin [28].

Protein complexes may perform better with surfactants like dextran, which diminish undesired aggregation. Yi et al. [55] studied the effect of curcumin coating with α-lactalbumin or α-lactalbumin-dextran complex on its stability. The protein coating formed a nanocomplex of 63.5 nm (PDI of 0.108, ζ potential of -13.9 mV, and encapsulation efficiency of 97.5%), while curcumin coated with α-lactalbumin and dextran showed a size of 68.1 nm (PDI of 0.161, ζ potential of -10.5 mV, and encapsulation efficiency of 98.8%). Curcumin coated with α-lactalbumin-dextran presented no changes in the mean particle diameters upon heating for 30 min (70, 80, and 90ºC) or when submitted to pH variations, performing better than the pure protein coating. However, both nanocomplexes

exhibit less degradation in water dispersion after 4 h storage: 91.7% of curcumin remained in α-lactalbumin complex, and 92.1% in α-lactalbumin-dextran conjugates, while only 24.8% was left of the amount of free curcumin.

A study of curcumin bonded in another globulin (β) presented formation of bigger nanoparticles (142 nm) but also high encapsulation efficiency (>96%). Curcumin stability in buffer Tris-HCl 50 mM pH 7.0 was increased by 6.7 times when in complex form, and its water solubility was enhanced by ~20,800 times [56]. Another high encapsulation formulation was curcumin-soy protein complex (96.8 to 99.1%, with drug loading of 1.743 to 1.784 µg/mg of soy protein). The dried nanocomplex prepared with a protein concentration of 1.0% (w/v), improved the curcumin water solubility about 1600-fold. The size of the complex was about 90 nm, and the ζ potential was between -10.95 to -13.20 mV.

Therefore, the nanocomplexation is an alternative to curcumin administration. In this work, we choose the nanocomplexation with cyclodextrin to future incorporation of curcumin, a hydrophobic drug, in hydrophilic wafers, leading to a satisfactory drug release.

1.3   ORAL WAFERS AS DRUG DELIVERY SYSTEMS

Drugs have a therapeutic concentration range above which they are toxic and below which they are ineffective. To keep the drug concentration within its therapeutic range for a longer time, modified DDS were developed. These systems also aim to direct the drug to the desired location, reducing the number of doses, toxicity and adverse and/ or side effects.

Lyophilized wafers are formulations prepared by the lyophilization of polymeric solutions or gels, to form a porous solid cake that can be easily applied to mucous surfaces [57]. They allow the delivery of drugs through the mucosal surface for local or systemic applications. Unlike semi-solid polymeric gels, wafers can maintain their structure for a longer period, increasing the residence time, allowing an effective absorption of the drug. Due to their porosity and large surface area, wafers have a good drug loading capacity [58].

Freeze-dried oral wafers are not washed out by saliva and provides dosage accuracy since they are unitary. When produced, they do not require environmentally inappropriate solvents, present few production steps and in a reproducible and scalable way. When it comes to formulation, they allow modulation of drug release according to type and concentration of the excipients, besides the rate of freezing [59,60], among other advantages.

Freeze-drying is the main step in structuring the wafers. This process removes the solvent from the frozen sample by sublimation and desorption under vacuum, enabling its storage and increasing the shelf life of the formulations. The process involves three basic steps: freezing, primary drying and secondary drying. First, the sample is frozen, which immobilizes the product to be lyophilized and decreases or reduces chemical and biological reactions. Then there is the primary drying (dehydration), which is the longest step in the process, and the reduction of bulk water/ solvent by sublimation occurs. For this, low temperatures and low pressures are used [61]. In secondary drying, the material is dehydrated by desorption of the bound water, reaching levels that do not allow biological growth or chemical reactions [62].

1.4   OBJECTIVES

Develop DDS (mucoadhesive polymeric wafers and cyclodextrin complex) to release drugs through mucosa, promoting longer residence time of the drug at the site of action, greater permeability and sustained release appropriate to prevent and/ or treat local inflammations in the mouth or the lung.

1.4.1   Specific objectives

• Carry out a bibliographic review on wafers technology;

• Adapt and validate published methods for the quantification of lidocaine and curcumin;

• Characterize the selected polymers: zeta potential, pH in solution and thermal properties;

• Develop polymeric wafers based on a factorial experimental design, considering the concentration of excipients (inputs), and the outputs: pH, residual moisture, zeta potential and thermal properties;

• Incorporate the drug in the selected wafers and evaluate the incorporation efficiency and *in vitro* release profile;

• Develop and characterize the curcumin-cyclodextrin nanocomplexes;

• Perform the physical-chemical quality control of the selected formulation;

• Evaluate the *in vitro* antimicrobial activity of the selected formulations.

1.5   REFERENCES

1.   Saad, J. & Mathew, D. Nonsteroidal Anti-Inflammatory Drugs Toxicity. in *StatPearls* (StatPearls Publishing, 2020).

2.   Kanaa, M. D., Whitworth, J. M., Corbett, I. P. & Meechan, J. G. Articaine and Lidocaine Mandibular Buccal Infiltration Anesthesia: A Prospective Randomized Double-Blind Cross-Over Study. *Journal of Endodontics* **32**, 296–298 (2006).

3.   Okamoto, H., Nakamori, T., Arakawa, Y., Iida, K. & Danjo, K. Development of polymer film dosage forms of lidocaine for buccal administration: II. Comparison of preparation methods. *J. Pharm. Sci.* **91**, 2424–2432 (2002).

4.   Ga, H., Choi, J.-H., Park, C.-H. & Yoon, H.-J. Acupuncture needling versus lidocaine injection of trigger points in myofascial pain syndrome in elderly patients – a randomised trial. *Acupunct Med* **25**, 130–136 (2007).

5.   Kamanli, A. *et al.* Comparison of lidocaine injection, botulinum toxin injection, and dry needling to trigger points in myofascial pain syndrome. *Rheumatol Int* **25**, 604–611 (2004).

6.   Wei, Y., Nedley, M. P., Bhaduri, S. B., Bredzinski, X. & Boddu, S. H. S. Masking the Bitter Taste of Injectable Lidocaine HCl Formulation for Dental Procedures. *AAPS PharmSciTech* **16**, 455–465 (2014).

7.   Rabinowitz, J. D. & Zaffaroni, A. C. Delivery of anti-migraine compounds through an inhalation route. (2004).

8.   Karasahin, K. E. *et al.* Lidocaine spray in addition to paracervical block reduces pain during first-trimester surgical abortion: a placebo-controlled clinical trial. *Contraception* **83**, 362–366 (2011).

9.   Nayak, A. & Das, D. B. Potential of biodegradable microneedles as a transdermal delivery vehicle for lidocaine. *Biotechnol Lett* **35**, 1351–1363 (2013).

10.   Rowbotham, M. C. & Fields, H. L. Topical lidocaine reduces pain in post-herpetic neuralgia. *Pain* **38**, 297–301 (1989).

11.   Sicherer, S. H. & Eggleston, P. A. EMLA Cream for Pain Reduction in Diagnostic Allergy Skin Testing: Effect on Wheal and Flare Responses. *Annals of Allergy, Asthma & Immunology* **78**, 64–68 (1997).

12.   Lidocaine hydrochloride - DrugBank. https://www.drugbank.ca/salts/DBSALT000900.

13. Lidocaine - DrugBank. https://www.drugbank.ca/drugs/DB00281.

14. Donaldson, D. & Meechan, J. G. A comparison of the effects of EMLA cream and topical 5% lidocaine on discomfort during gingival probing. *Anesth Prog* **42**, 7–10 (1995).

15. FDA (U. S. Food & Drug Administration). Drug Approval Package: Lidoderm (Lidocaine) NDA# 20-612. (1999).

16. Stecker, S. S., Swift, J. Q., Hodges, J. S. & Erickson, P. R. Should a mucoadhesive patch (DentiPatch) be used for gingival anesthesia in children? *Anesth Prog* **49**, 3–8 (2002).

17. Schmidt, R. M. & Rosenkranz, H. S. Antimicrobial activity of local anesthetics: lidocaine and procaine. *J. Infect. Dis.* **121**, 597–607 (1970).

18. Sculley, P. D. & Dunley, R. E. Antimicrobial Activity of a Lidocaine Preparation. *Anesth Prog* **27**, 21–23 (1980).

19. Johnson, S. M., Saint John, B. E. & Dine, A. P. Local anesthetics as antimicrobial agents: a review. *Surg Infect (Larchmt)* **9**, 205–213 (2008).

20. Okamoto, H., Taguchi, H., Iida, K. & Danjo, K. Development of polymer film dosage forms of lidocaine for buccal administration: I. Penetration rate and release rate. *Journal of Controlled Release* **77**, 253–260 (2001).

21. Sinclair, R., Westlander, G., Cassuto, J. & Hedner, T. Postoperative pain relief by topical lidocaine in the surgical wound of hysterectomized patients. *Acta Anaesthesiol Scand* **40**, 589 (1996).

22. Abu-Huwaij, R., Assaf, S., Salem, M. & Sallam, A. Mucoadhesive Dosage form of Lidocaine Hydrochloride: I. Mucoadhesive and Physicochemical Characterization. *Drug Development and Industrial Pharmacy* **33**, 855–864 (2007).

23. Srinivasan, K. & Sambaiah, K. The effect of spices on cholesterol 7 alpha-hydroxylase activity and on serum and hepatic cholesterol levels in the rat. *Int J Vitam Nutr Res* **61**, 364–369 (1991).

24. Reddy, S. & Aggarwal, B. B. Curcumin is a non-competitive and selective inhibitor of phosphorylase kinase. *FEBS Lett.* **341**, 19–22 (1994).

25. Goud, V. K., Polasa, K. & Krishnaswamy, K. Effect of turmeric on xenobiotic metabolising enzymes. *Plant Foods Hum Nutr* **44**, 87–92 (1993).

26. Conney, A. H. *et al.* Inhibitory effect of curcumin and some related dietary compounds on tumor promotion and arachidonic acid metabolism in mouse skin.

Adv. Enzyme Regul. **31**, 385–396 (1991).

27.   Joe, B. & Lokesh, B. R. Effect of curcumin and capsaicin on arachidonic acid metabolism and lysosomal enzyme secretion by rat peritoneal macrophages. *Lipids* **32**, 1173–1180 (1997).

28.   Zhen, L. *et al.* Curcumin inhibits oral squamous cell carcinoma proliferation and invasion via EGFR signaling pathways. *Int J Clin Exp Pathol* **7**, 6438–6446 (2014).

29.   Curcumin - DrugBank. https://www.drugbank.ca/drugs/DB11672.

30.   Foodb - Bisdemethoxycurcumin. https://foodb.ca/compounds/FDB011961 (2019).

31.   PubChem. PubChem. https://pubchem.ncbi.nlm.nih.gov/.

32.   Foodb - Demethoxycurcumin. https://foodb.ca/compounds/FDB011964 (2019).

33.   D'Angelo, N. A. *et al.* Curcumin encapsulation in nanostructures for cancer therapy: a 10-year overview. *International Journal of Pharmaceutics* 120534 (2021) doi:10.1016/j.ijpharm.2021.120534.

34.   Carvalho, D. de M. *et al.* Production, solubility and antioxidant activity of curcumin nanosuspension. *Food Science and Technology* **35**, 115–119 (2015).

35.   Kurnik, I. S. *et al.* Separation and purification of curcumin using novel aqueous two-phase micellar systems composed of amphiphilic copolymer and cholinium ionic liquids. *Separation and Purification Technology* **250**, 117262 (2020).

36.   Martínez-Guerra, J. *et al.* New insights on the Chemical Stability of Curcumin in Aqueous Media at Different pH: Influence of the Experimental Conditions. *Int. J. Electrochem. Sci.* **14**, 13 (2019).

37.   Schneider, C., Gordon, O. N., Edwards, R. L. & Luis, P. B. Degradation of Curcumin: From Mechanism to Biological Implications. *J Agric Food Chem* **63**, 7606–7614 (2015).

38.   Dei Cas, M. & Ghidoni, R. Dietary Curcumin: Correlation between Bioavailability and Health Potential. *Nutrients* **11**, 2147 (2019).

39.   Sintov, A. C. Transdermal delivery of curcumin via microemulsion. *International Journal of Pharmaceutics* **481**, 97–103 (2015).

40.   Leung, M. H. M. & Kee, T. W. Effective stabilization of curcumin by association to plasma proteins: human serum albumin and fibrinogen. *Langmuir*

25, 5773–5777 (2009).

41.   Mirzaee, F. *et al.* Diverse Effects of Different 'Protein-Based' Vehicles on the Stability and Bioavailability of Curcumin: Spectroscopic Evaluation of the Antioxidant Activity and Cytotoxicity In Vitro. *Protein Pept. Lett.* **26**, 132–147 (2019).

42.   Damarla, S. R., Komma, R., Bhatnagar, U., Rajesh, N. & Mulla, S. M. A. An Evaluation of the Genotoxicity and Subchronic Oral Toxicity of Synthetic Curcumin. *Journal of Toxicology* vol. 2018 e6872753 https://www.hindawi.com/journals/jt/2018/6872753/ (2018).

43.   Rocks, N. *et al.* Curcumin–cyclodextrin complexes potentiate gemcitabine effects in an orthotopic mouse model of lung cancer. *Br J Cancer* **107**, 1083–1092 (2012).

44.   Ndong Ntoutoume, G. M. A. *et al.* Development of curcumin–cyclodextrin/cellulose nanocrystals complexes: New anticancer drug delivery systems. *Bioorganic & Medicinal Chemistry Letters* **26**, 941–945 (2016).

45.   Zaman, H., Bright, A. G., Adams, K., Goodall, D. M. & Forbes, R. T. Characterisation of aggregates of cyclodextrin-drug complexes using Taylor Dispersion Analysis. *International Journal of Pharmaceutics* **522**, 98–109 (2017).

46.   Yallapu, M. M., Jaggi, M. & Chauhan, S. C. Poly(β-cyclodextrin)/Curcumin Self-Assembly: A Novel Approach to Improve Curcumin Delivery and its Therapeutic Efficacy in Prostate Cancer Cells. *Macromolecular Bioscience* **10**, 1141–1151 (2010).

47.   Mangolim, C. S. *et al.* Curcumin–β-cyclodextrin inclusion complex: Stability, solubility, characterisation by FT-IR, FT-Raman, X-ray diffraction and photoacoustic spectroscopy, and food application. *Food Chemistry* **153**, 361–370 (2014).

48.   Yadav, V. R., Suresh, S., Devi, K. & Yadav, S. Effect of Cyclodextrin Complexation of Curcumin on its Solubility and Antiangiogenic and Anti-inflammatory Activity in Rat Colitis Model. *AAPS PharmSciTech* **10**, 752 (2009).

49.   Pabon, H. J. J. A synthesis of curcumin and related compounds. *Recueil des Travaux Chimiques des Pays-Bas* **83**, 379–386 (1964).

50.   Tønnesen, H. H., Másson, M. & Loftsson, T. Studies of curcumin and curcuminoids. XXVII. Cyclodextrin complexation: solubility, chemical and photochemical stability. *Int J Pharm* **244**, 127–135 (2002).

51.   Singh, R., Tønnesen, H. H., Vogensen, S. B., Loftsson, T. & Másson, M. Studies of curcumin and curcuminoids. XXXVI. The stoichiometry and complexation constants of cyclodextrin complexes as determined by the phase-solubility method and UV–Vis titration. *J Incl Phenom Macrocycl Chem* **66**, 335–348 (2010).

52.   Zhang, L. *et al.* Curcumin-cyclodextrin complexes enhanced the anti-cancer effects of curcumin. *Environmental Toxicology and Pharmacology* **48**, 31–38 (2016).

53.   Sneharani, A. H., Singh, S. A. & Appu Rao, A. G. Interaction of αS1-Casein with Curcumin and Its Biological Implications. *J. Agric. Food Chem.* **57**, 10386–10391 (2009).

54.   Yang, M., Wu, Y., Li, J., Zhou, H. & Wang, X. Binding of Curcumin with Bovine Serum Albumin in the Presence of ι-Carrageenan and Implications on the Stability and Antioxidant Activity of Curcumin. *J. Agric. Food Chem.* **61**, 7150–7155 (2013).

55.   Yi, J. *et al.* Glycosylated α-lactalbumin-based nanocomplex for curcumin: Physicochemical stability and DPPH-scavenging activity. *Food Hydrocolloids* **61**, 369–377 (2016).

56.   Sneharani, A. H., Karakkat, J. V., Singh, S. A. & Rao, A. G. A. Interaction of Curcumin with β-Lactoglobulin—Stability, Spectroscopic Analysis, and Molecular Modeling of the Complex. *J. Agric. Food Chem.* **58**, 11130–11139 (2010).

57.   Boateng, J. S. *et al.* Characterisation of freeze-dried wafers and solvent evaporated films as potential drug delivery systems to mucosal surfaces. *Int J Pharm* **389**, 24–31 (2010).

58.   Ayensu, I., Mitchell, J. C. & Boateng, J. S. Development and physico-mechanical characterisation of lyophilised chitosan wafers as potential protein drug delivery systems via the buccal mucosa. *Colloids and Surfaces B: Biointerfaces* **91**, 258–265 (2012).

59.   Boateng, J. S. *et al.* In vitro drug release studies of polymeric freeze-dried wafers and solvent-cast films using paracetamol as a model soluble drug. *Int J Pharm* **378**, 66–72 (2009).

60.   Boateng, J. S. *et al.* Comparison of the in vitro release characteristics of mucosal freeze-dried wafers and solvent-cast films containing an insoluble drug.

Drug Dev Ind Pharm **38**, 47–54 (2012).

61. Tattini Jr, V., Parra, D. F. & Pitombo, R. N. de M. Influência da taxa de congelamento no comportamento físico-químico e estrutural durante a liofilização da albumina bovina. *Brazilian Journal of Pharmaceutical Sciences* **42**, 127–136 (2006).

62. Rey, L. *Freeze-Drying/Lyophilization of Pharmaceutical and Biological Products, Third Edition*. (CRC Press, 2016).

2. A MINI-REVIEW ON DRUG DELIVERY THROUGH WAFER TECHNOLOGY: FORMULATION AND MANUFACTURING OF BUCCAL AND ORAL LYOPHILIZATES

This chapter was published as a mini-review in the Journal of Advanced Research [1].

A mini-review on drug delivery through wafer technology: Formulation and manufacturing of buccal and oral lyophilizates

Juliana Souza Ribeiro Costa [a,b], Karen de Oliveira Cruvinel [a], Laura Oliveira-Nascimento [a]

[a] Faculty of Pharmaceutical Sciences, University of Campinas, Rua Candido Portinari 200, 13083-871 Campinas, São Paulo, Brazil

[b] Institute of Biology, University of Campinas, Rua Monteiro Lobato 255, 13083-970 Campinas, São Paulo, Brazil

ABSTRACT

A great number of patients have difficulty swallowing or needle fear. Therefore, buccal and orodispersible dosage forms (ODFs) represent an important strategy to enhance patient compliance. Besides not requiring water intake, swallowing or needles, these dosage forms allow drug release modulation. ODFs include oral lyophilizates or wafers, which present even faster disintegration than its compressed counterparts. Lyophilization can also produce buccal wafers that adhere to mucosa for sustained drug release. Due to the subject relevance and recent research growth, this review focused on oral lyophilizate production technology, formulation features, and therapy gains. It includes Critical Quality Attributes (CQA) and Critical Process Parameters (CPP) and discusses commercial and experimental examples. In sum, the available commercial products promote immediate drug release mainly based on biopolymeric matrixes and two production technologies. Therapy gains include substitution of traditional treatments depending on parenteral administration and patient preference over classical therapies. Experimental wafers show promising advantages as controlled release and drug enhanced stability. All compiled findings encourage the development of new wafers for several diseases and drug molecules.

Keywords: wafer; buccal; lyophilization; freeze-drying; drug delivery; oral lyophilizates.

2.1 INTRODUCTION

American surveys have shown that 8% of patients skip doses and 4% discontinue therapy due to difficulties in swallowing tablets [2]. Another barrier for therapy efficacy relates to patient aversion to injectable medications [3]. As buccal administration does not require swallowing nor needles, adherence to dosing regimens is likely to increase with buccal delivery. Buccal delivery provides easy access to highly vascularized tissue, avoiding first-pass metabolism and concomitant liquid intake. Furthermore, the neutral environment of the mouth allows for administration of acid-sensitive active pharmaceutical ingredients (APIs) [4]. Drugs can permeate the buccal mucosa more rapidly than they permeate the skin, but less rapidly than they permeate the intestinal wall. Absorption rates depend on drug physicochemical properties, such as molecular size, hydrophobicity, susceptibility to enzymatic degradation, and region of delivery inside the oral cavity [5,6]. Noteworthy, a buccal dosage form can release drug to the oral cavity and promote absorption throughout the gastrointestinal tract.

Buccal dosage forms include mucoadhesive tablets, films, patches, ointments, and hydrogels, each of which has limitations [7]. For instance, ointments and hydrogels are semi-solids that lack dosage precision or adequate hardness to resist tongue removal [5,8]. Although precision can be increased with mucoadhesive tablets, they are often uncomfortably large, limiting long-term residence and release time [7,9]. These disadvantages can be overcome with the use of films, patches, and wafers [7,10]. Buccal films are currently the preferred commercial dosage form for extended transmucosal delivery; their action depends on slow matrix erosion, high mucoadhesiveness, and adequate drug loading. However, these carriers contain enough water to favor microbial contamination or degradation of sensitive APIs [11]. Lyophilized wafers can sustain drug release as well, with the benefits of low residual moisture and increased drug loading (for low solubility drugs) [4,12]. To date, extended release wafers have been restricted to noncommercial formulations.

For rapid onset of drug action, several companies rely on orodispersible dosage forms (ODFs). These systems disintegrate rapidly in the mouth and increase therapy efficacy for disorders that require fast intervention [13]. ODFs include orally disintegrating tablets (ODTs), quick-dissolving lyophilized wafers (oral lyophilizates),

and thin films [14]. According to the FDA, an ODF must be small, lightweight (up to 500 mg), and must disintegrate within 30 seconds [15]. Among the options, wafers present highly porous solid matrixes obtained by freeze-drying of polymer gels or suspensions to an average of 3 mm thickness and 9 x 12 mm size [16,17] (Fig. 1). Owing to their potential therapeutic advantages and lack of review articles on wafer systems, this study focused on the production process, parameters, and formulation features of wafers.
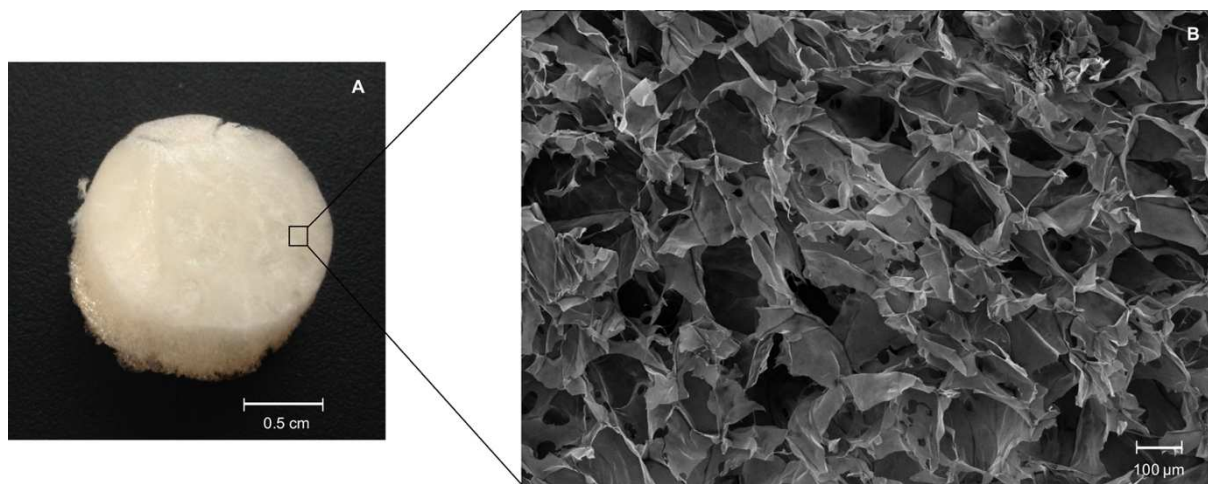
Fig. 1. An example of the macro and micro morphologies of wafers (A) Oral lyophilizate of gelatin and sodium alginate; (B) Micrograph of wafer pores obtained using a Leo 440i scanning electronic microscope (LEO Electron Microscopy/ Oxford, Cambridge, England) at 200x magnification. The figure was produced by the authors for the specific purpose of publication in this paper.

2.2   THERAPY GAINS

Wafer products are available to patients for immediate release of several APIs (Table 1). Most of these medicines showed better patient compliance, especially in acute pathologies or symptoms. For instance, acute attacks of migraine often come with nausea, which implicate in parenteral medication to avoid vomiting. With the advent of Rizatriptan wafers, pain decreases after around 20-30 minutes of drug administration, like standard subcutaneous sumatriptan. Although Rizatriptan is 45% bioavailable, compared to 95% of subcutaneous sumatriptan, its rapid onset of action, oral intake and similar efficacy pattern makes patients prefer the former [18,19]. To inhibit nausea and vomiting of migraine attacks and other medical conditions, fast-disintegrating antiemetics versions gained wide acceptance, including ondansetron

and domperidone. Oral ondansetron was as efficacious as its intravenous administration in prevent emesis after laparoscopic cholecystectomy [20].

Table 1. Examples of commercial oral lyophilizates (US and EU markets).

Drug (strength)	Indication	Trade name	Company	Excipients
Brompheniramine maleate – phenylpropanolamine HCl (1 mg – 6.25 mg)	Antihistamine, Decongestant	Dimetapp® Quick Dissolve	Whitehall-Robins	Aspartame, FDCA Blue No. 2, FDCA Red No. 40, flavors, gelatin, glycine, mannitol
Buprenorphine hydrochloride (2, 8 mg)	Opioid drug dependence	Espranor Oral lyophilisate	Martindale Pharma	Gelatin, mannitol, aspartame, mint flavour, citric acid
Clonazepam (0.125, 0.25, 0.5, 1, 2 mg)	Sedation, seizures, panic attacks	Klonopin® wafer	Roche	Gelatin, mannitol, methylparaben sodium, propylparaben sodium and xanthan gum
Desmopressin acetate (25, 50, 60, 120, 240 µg)	Vasopressin-sensitive cranial diabetes insipidus, nocturnal enuresis	Noqdirna Oral lyophilisate/ DDAVP Melt Oral lyophilisate/ DesmoMelt Oral lyophilisate	Ferring Pharmaceuticals Ltd	Gelatin, mannitol, citric acid
Famotidine (20, 40 mg)	Hearthburn, Indigestion	Pepcidine Rapitab	Cardinal/ Merck	Aspartame, mint flavor, gelatin, mannitol, red ferric oxide and xanthan gum
Loratadine (5, 10 mg)	Allergy	Claritin® Reditabs®	Schering	Citric acid, gelatin, mannitol, mint flavor
Loperamide (2 mg)	Diarrhea	Loperamide Lyoc®	Teva Santé	Aspartame, sorbitol, polysorbate 60, xanthan gum, sodium hydrogen phosphate, dextran 70, lactose monohydrate, raspberry flavor powder: ethyl acetate, isoamyl acetate, limonene, benzoic acid aldehyde, benzyl acetate, beta ionone, vanillin, propylene glycol, maltodextrin, vegetable gum
Loperamide (2 mg)	Diarrhea	Imodium®	Cardinal/ J&J	Gelatin, mannitol, aspartame, mentol flavour, sodium bicarbonate
Metopimazine (7.5 mg)	Nausea and vomiting	Vogalene Lyoc®	Teva Santé	Xantham gum, aspartame, sodium docusate, dextran 70, mannitol
Ondansetron (4, 8 mg)	Nausea and vomiting	Zofran ODT®	GlaxoSmithKline	Aspartame, gelatin, mannitol, methylparaben sodium, propylparaben sodium, strawberry flavor
Olanzapine (5, 10, 15, 20 mg)	Schizophrenia	Zyprexa® Zydis®	Eli Lilly	Gelatin, mannitol, aspartame, sodium methyl paraben, sodium propyl paraben
Piroxicam (20 mg)	Pain, inflammation	Feldene® Melt	Cardinal/ Pfizer	Gelatin, mannitol, aspartame, citric acid

Table 1. Examples of commercial oral lyophilizates (US and EU markets).

(continuation)

Drug (strength)	Indication	Trade name	Company	Excipients
Paracetamol (500 mg)	Pain fever	Paralyoc®	Cephalon	Aspartame, polysorbate 60, xanthan gum, dextran 70, orange flavouring, mono hydrous lactose
Piroxicam (10, 20 mg)	Osteoarthritis, rheumatoid arthritis, ankylosing spondylitis	Proxalyoc®	Cephalon	Aspartame, mannitol, povidone K30
Phloroglucinol (80, 160 mg)	Gastro-intestinal and biliary tract pain, renal colic, contraction during pregnancy	Spasfon-Lyoc®	Teva Santé	Dextran 70, mannitol (common), and for lyophilisate 160 mg: sucralose, macrogol 15-hydroxystearate.
Risperidone (2, 4mg)	Schizophrenia	Risperdal®/ M-Tab®	Janssen	Amberlite® resin, gelatin, mannitol, glycine, simethicone, carbomer, sodium hydroxide, aspartame, red ferric oxide, peppermint oil
Rizatriptan Benzoate (5, 10 mg)	Migraine	Maxalt-MLT®	Merck	Gelatin, mannitol, glycine, aspartame, peppermint flavor
Selegiline (1.25 mg)	Parkinson's	Zelapar®	Cardinal/ Elan	Gelatin, mannitol, glycine, aspartame, citric acid, yellow iron oxide, grapefruit flavor

Data collected from company sites and references [21–26].

A prolonged seizure (over 5 minutes) is another condition that requires rapid chemotherapy without tablet/liquid swallowing. Among the options, oral clonazepan wafers were as efficient as rectal diazepam in stopping seizures. This data alone is meaningful because it reduces patient embarrassment related to the rectal administration [27]. As a last case for illustration, the antihistaminics desloratadine and loratadine have wafer and tablet versions for relief of allergy symptoms. Wafers did not decrease the time to achieve a maximum concentration in plasma (Tmax) when compared to traditional tablets; however, a 5mg loratadine version resulted in 25% more drug bioavailability than its tablet counterpart. Since allergy symptoms include itchy throat, a fast-disintegrating dosage form can also decrease discomforts related to medicine administration [28].

Mucoadhesive wafers (without fast disintegration) were tested in few clinical trials, with no commercial representatives. Current research focuses consists of wound healing enhancement and pain management. On this matter, ketorolac/lidocaine

polymeric wafers reduced pain and enhanced tissue healing in dental patients previously subjected to gingivectomy [29].

2.3   FORMULATION FEATURES

2.3.1   Matrix forming polymers

Concerning excipients, gelatin is the most used matrix-forming polymer (Table 1) of commercial oral lyophilisates. It is abundant in animals, cost-effective, biocompatible, biodegradable, and has favorable physicochemical properties (forms hydrogels and is hydrophilic, translucent, colorless, and flavorless). Gelatin forms physical crosslinks that break at body temperature [30]. This effect "melts" the dosage form, resulting in drug release. Zydis® was the first gelatin-based technology available to patients. It can incorporate doses of up to 400 mg of poorly soluble drugs and 60 mg of water-soluble drugs. This technology has limitations: drug and excipient particles should be smaller than 50 µm; hot packaging increase costs; inadequate friability is a common product defect [31]. Quicksolv® technology also uses gelatin as matrix (table 1, Risperidone), but relies on more excipients and a second solvent to obtain a less friable product and facilitated packaging. In exchange, it limits drug options to the ones with low doses and immiscible in the second solvent [32]. The third and last technology (Lyoc®) with commercial medicines relies on xanthan gum as the matrix polymer (Fig. 2A). This polysaccharide forms coherent and stable freeze-dried forms, with the advantage of production and sustainability of a microbial source [33]. The apparent yield stress was reported as higher than for gelatin based products, which results in less friable wafers and facilitated storage/package conditions [34]. A few Lyoc® products use polivinilpirrolidone instead of xantam gum or even no polymers at all (Table 1). Although there are many other wafer technologies on the market, we could not find commercial products using them.
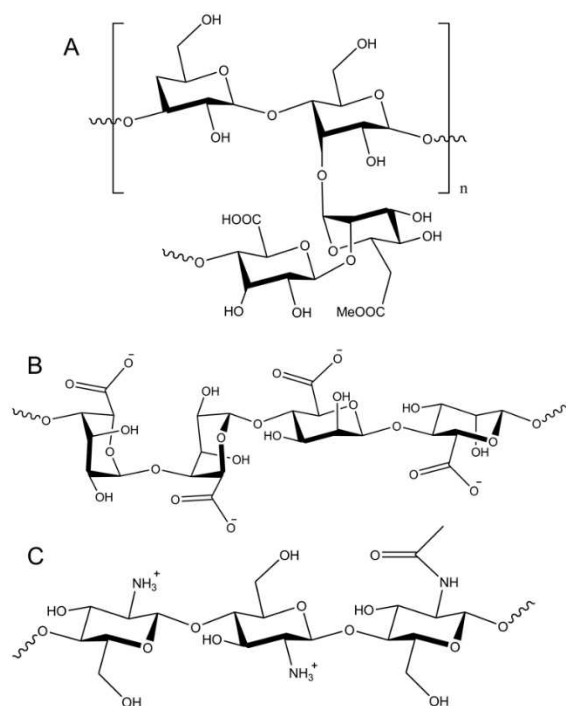
Fig. 2. Structural features of natural matrix polysaccharides. (A) Molecular structure of xanthan gum, (B) molecular structure of sodium alginate and (C) molecular structure of chitosan.

Alternative experimental polysaccharides include the algal derived alginate (Fig. 2B) and chitosan (Fig. 2C). For example, combination of alginate with magnesium aluminum silicate improved the stability of nicotine used for replacement therapy [35]. Extended release versions require mucoadhesiveness, which allows for longer swelling time in the buccal cavity. Experimental wafers can also be formulated with synthetic polymers, such as thiolated chitosan, which is reported to be up to 10 times more bioadhesive than chitosan, but still biodegradable. Hydrophilic sodium carboxymethyl cellulose delivers drugs effectively through gastrointestinal mucosal tissue absorption. Sodium carboxymethyl cellulose does not require organic solvents and is usually combined with other matrix-formers, such as alginate [12,35–37].

As polymers constitute a large portion of the carrier, the following characteristics must be considered: molecular weight (adhesiveness increases above 100,000 Da), chain flexibility (related to polymer diffusion through the mucosal surface), hydrogen bond formation capacity (greater hydrogen bonding augments interactions with the mucosal surface), and hydration capacity (favors increased contact with the barrier surface) [4,5]. Accordingly, natural cationic chitosan allows for

extensive mucoadhesion, and provides permeation enhancement and inhibition of peptidases [6,38]. The performance of chitosan makes it an excellent candidate for use in prolonged release wafers, which is supported by at least 45 papers (PubMed search, October 25, 2018) and over 40 patents (Orbit software search, October 25, 2018). Gelatin can be used to prepare extended release wafers when combined with other excipients, including chitosan, which can enhance its mechanical properties and mucoadhesiveness [39,40].

Matrix pore size, interconnections, and erosion/swelling of the polymeric chain determine drug-matrix interactions and release rates. Crosslinkers in wafers are mainly ionic in nature and include divalent cations (such as $CaCl_2$ for use with alginate) or polyanions (such as sodium tripolyphosphate, TPP, for use with chitosan) [41]. Alginate crosslinking occurs at physiological pH and room temperature, which are desired properties for biological applications and drug stability. In turn, chitosan crosslinks with TPP under mild acidic conditions, which limits labile drugs incorporation in the gel phase. Chemical crosslinking changes the polymer network and increases resistance to disintegration, which is why orodispersible forms do not include this additive [42].

2.3.2   Other excipients

Freeze-dried formulations have low water content, and do not support microbial growth, precluding the need for inclusion of these additives. However, some formulations (e.g. Zydis® technology) use these additives to inhibit microbial growth during manufacturing [43]. Oral lyophilizates generally contain taste-masking agents, lyoprotectors, and pH adjusters. Sweeteners mask unpleasant taste and are essential for patient compliance. Yet, most of these compounds have multifunctional roles. Xylitol has the added benefit of antimicrobial action. Mannitol prevents structural collapse during freeze-drying (lyoprotector), enhances mechanical properties, accelerates disintegration, and facilitates removal of wafers from molds [44,45]. Another way to deal with unpalatable particles is by coating or encapsulation, as exemplified by the amberlite ion exchange resin in risperidone formulations [46].

Taste-masking can have the added benefit of drug solubility enhancement, as observed with cyclodextrin (CD)-drug complexation. CDs are soluble cyclic sugars that accommodate hydrophobic drugs/moieties inside their lipophilic cavities. CDs

enhance permeation [47,48] and are approved by the FDA for oral use. As most wafer-based polymers are hydrophilic, drug solubility affects not only dissolution and bioavailability but also drug incorporation/homogeneity. CD-econazole complexes increased drug solubility by 66-fold, which allowed for solubilization in pectin/carboxymethylcellulose gels prior to wafer freeze-drying [49]. Although we did not find any other wafers that included this kind of complexation, many buccal films use this complexation technique to enhance solubility. The addition of CD to a polyethylene oxide buccal film increased the release of triamcinolone acetonide in the presence of mucin from 7 % to 47 % [50].

Additional formulation techniques can be used to increase solubility, such as pH modifiers, emulsions, amorphization, co-solvents, solid dispersions, and nanotechnology [51,52]. Curcumin was solubilized in solid lipid nanoparticles prior to dispersion in freeze-dried wafers ("sponges") of polycarbophil. *In vivo* studies (with 5 adult volunteers) showed a buccal residence time of 15 h and sustained release over 14-15 h. However, studies demonstrating permeation or bioavailability were not performed, as the formulation was designed for local treatment of precancerous oral lesions [53]. Finally, another formulation strategy for sustained release is the use of beads. Beads offer a particulate matrix to sustain release and diminish burst effects (initial rapid release). Chitosan lactate beads loaded with tizanidine prevent burst release from chitosan lactate buccal wafers. An *in vivo* pharmacokinetics study (with six male volunteers) showed a considerable increase in T_{max} and an increase in the bioavailability of tizanidine (2.27 folds) compared to those of the immediate release product Sirdalud® [54].

2.4   PRODUCTION PROCESS

The process to obtain oral wafers has a few steps, as shown in Fig. 3. The most critical steps for stability are mixing, freezing and drying. Since many patent technologies perform slight variations of the presented backbone, we discuss some of the particularities along this topic.

Production at laboratory scale allows mixing in magnetically stirred beakers [55] with overhead mechanical stirring [33]. However, industrial production requires a temperature-controlled tank and mechanical agitation. The impeller geometry for

mixing depends mainly on the rheological properties of the resultant mixture. Low viscosity products can be mixed well by hydrofoil or pitch blades. When working with encapsulated or coated particles, a high shear mixer may disrupt the coating and should be avoided [56]. The target viscosity will depend on the presence of particles and consequent sedimentation rate, as well as disintegrating and mechanical performances. For gelatin-based formulations, patents describe planetary mixers (higher viscosities, low shear) [57,58], but most documents do not provide equipment details.

Gels are dried by lyophilization (or freeze-drying), in which water is removed from the frozen matrix by vacuum sublimation. This technique has many advantages, such as improved stability of thermolabile APIs [59] and final products with high porosity (which allows subsequent gain in loading capacity per weight) [59]. The entire process can occur inside a freeze-drier. As most industrial freeze-driers do not cool below -40°C, nitrogen tunnels or ultra-freezers can be required for specific freezing processes. Freezing shapes wafers and determines the porosity and surface topology. Therefore, target temperature, rate, and intermediate thermal procedures are entered as settings in advance. Fast rates produce smaller particles and more crystals, which dry slower, resulting in increased drying time. Although slow freezing results in larger crystals, thermal treatments (such as annealing) could result in homogeneity and reduced drying rates [60]. A recent innovation in pharmaceutical freeze-drying processes refers to nucleation control of ice crystals upon freezing. Because nucleation occurs in a wide range of temperature, its occurrence provokes batch heterogeneity and prolonged process. Therefore, inducing simultaneous nucleation can increase product homogeneity and significantly reduce process time/cost [61]. The technologies with proven scalability to induced nucleation are depressurization, ice fog and temperature quench freezing [62].

```
┌─────────────────────────┐
│ Separation/ weighting of │
│      raw materials       │
└─────────────────────────┘
```

```
┌─────────────────────────┐     ┌─────────────────────────┐
│ Bulk mixing (dissolution/ │     │   Bulk mixing (drug      │
│      gel forming)        │     │ dispersion/ dissolution) * │
└─────────────────────────┘     └─────────────────────────┘
```

```
┌─────────────────┐
│  Blister filling │
└─────────────────┘
```

```
┌───────────────────────────────────────┐
│   ┌─────────────────────────┐          │
│   │   Freeze-drier loading   │          │
│   └─────────────────────────┘          │
│                                        │
│   ┌─────────────────────────┐          │
│   │       Freezing **        │          │
│   └─────────────────────────┘          │
│                                        │
│   ┌─────────────────────────┐          │
│   │         Drying           │          │
│   └─────────────────────────┘          │
│                                        │
│   ┌─────────────────────────┐          │
│   │  Freeze-drier unloading  │          │
│   └─────────────────────────┘          │
└───────────────────────────────────────┘
```

```
┌─────────────────┐
│     Sealing      │
└─────────────────┘
```

```
┌─────────────────┐
│     Packing      │
└─────────────────┘
```
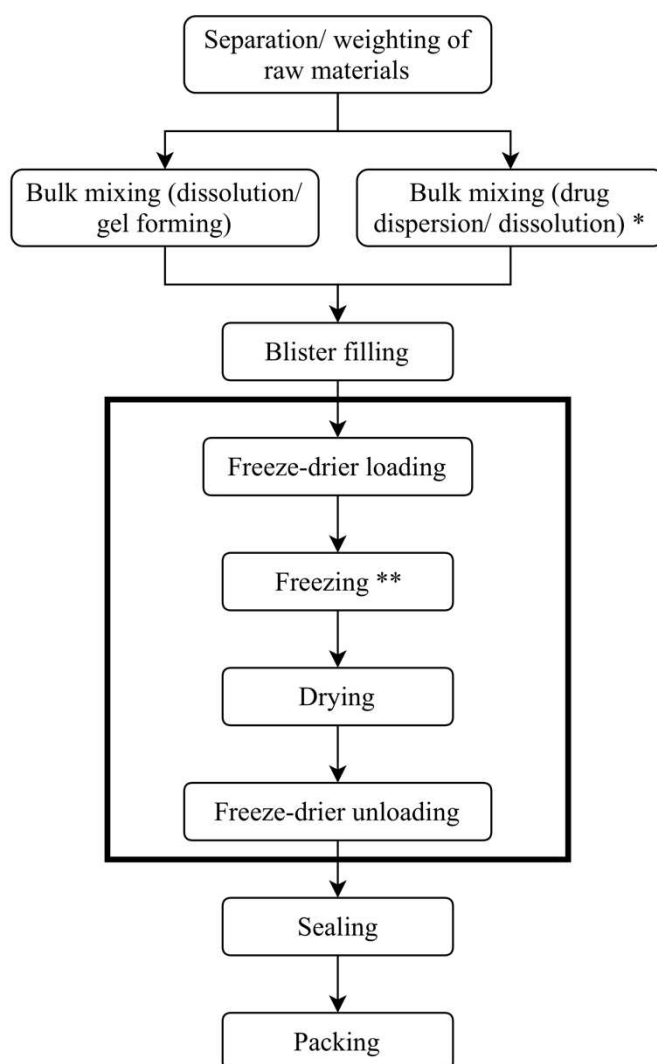
Fig. 3. Flowchart of the production process. The steps inside the highlighted box are performed inside the freeze-drier. *Drug dispersion/dissolution can be accomplished in a separate tank or directly in the gel. Liquid preparations can be solution, suspension or emulsion. Alternatively, blank wafers can be embedded in drug solutions after the lyophilization step. **Some process designs include freezing samples outside the freeze-drier (e.g. Zydis®), before the freeze-drier loading step [63].

After freezing, the product is placed under deep vacuum. Solvent removal occurs in two steps: primary (free solvent removal) and secondary drying (bound solvent removal). The former should start below the collapse temperature (Tc) of the formulation to assure structural integrity and adequate residual moisture. Although biopolymers used in wafers have high Tcs, drugs generally have lower Tc values. Primary drying is time-consuming because bulk water sublimates in larger amounts and at lower temperatures unlike bound solvent. Higher starting temperature results in shorter drying time and lower cost [64]. As such, when Tc is close to or lower than -40°C,

reformulation often occurs. Quicksolv® patent claims to facilitate drying using a second solvent, which must be miscible with water, present a lower vapor pressure and do not dissolve the other components. However, the patent of the technology does not limit freeze-drying as the only method possible; it is unclear which combinations of claims were really tested and result in optimal formulations [65]. Concerning packaging, the oral lyophilizate fragility demands specific blisters that resist physical stress and humidity [21]. Special packaging is not necessary for modified released forms due to enhanced mechanical strength, but they still need to resist water entrance.

2.5   QUALITY ATTRIBUTES AND RELATED PROCESS/MATERIAL PARAMETERS

International drug-related agencies recommend the Quality by Design (QbD) approach to assure product quality. Quality, safety, and efficacy must define pharmaceutical product attributes for the intended dose, administration route, and patient profile (Quality Target Product Profile). Then, the identified Critical Quality Attributes (CQA) are correlated with Critical Material Attributes (CMA) and Critical Process Parameters (CPP). Risk analysis and experimental designs help define ranges and actions for CPP/CMA that produce desired results for the CQAs (design space) [66]. CQAs include physical, chemical, biological, or microbiological properties that may impact product quality depending on its range/limit/distribution. Thus, direct or indirect quality control are required. Identification of CPPs relies on a set of tools. Scientific literature and team experience support first conclusions, whereas risk management aids final decisions and further actions [67]. For oral lyophilizates, Table 2 shows the common CQAs and the most relevant operation units associated with these CQAs [68].

CPPs relate to process steps that consequently impact CQAs; therefore, they must be well-established and monitored. Fig. 4 shows process parameters relevant to most common issues in wafer development and production. Cassian and coworkers observed that inadequate mixing time can lead to incomplete polymer hydration. As a result, viscosity may be variable and affect inter/intra-batch mechanical resistance and disintegration/dissolution [45]. In addition to process parameters, CMAs affect several quality attributes. For instance, particle size and excipient solubility can

influence disintegration and should be specified [15]. In the case of polymorphisms, the final product may disintegrate/dissolve slower than desired. An evaluation of gelatin-based ODTs demonstrated that low bloom strength and polymer concentration increased disintegration time. This study also showed that some saccharides confer lyoprotection and enhance hardness, but each saccharide had an optimal concentration for effective disintegration of lyophilizates. Mannitol (30-40%) was the top filler in this study for 2-5% low bloom gelatin gels [69]. Another impact of CMAs relates to process adjustments. Previous studies have demonstrated that PVP can suppress metastable forms of mannitol and eliminate the need for an annealing step in freezing [70].

Table 2. Main unit operations related to quality attributes and correlated analytical evaluations [15,71–74].

Critical Quality Attributes	Operation unit	Analytical evaluation
Appearance (macrostructure)	Primary drying	Visual analysis [I]
Microbial contamination	Transference/ mixture	Microbial limits
Content uniformity	Mixture	Assay [II] (10 units)
API concentration	Mixture	Assay
Drug release profile	Freezing	USP Dissolution methods [III]
Oral residence time	Secondary drying	Mucoadhesiveness*/ USP disintegration methods [IV]
Residual moisture	Secondary drying	Karl Fischer/ Thermogravimetry
Mechanical resistance	Secondary drying	Texture profile

[I] Color, presence of collapse, shape, dimensions.
[II] Assay is drug specific and performed as described in compendiums. Common analyses include HPLC, UV-vis, infrared.
[III] For wafers loaded with nanoparticles, this assay can be performed in Franz cells or dialysis bags.
[IV] FDA recommendation. Other methods that provide results equivalent to the USP method can be used to determine disintegration time.
*Extended release versions.
Highlighted attributes are those that differ between orodispersible and extended release wafers. Obs: Drug Identification is a CQA that cannot be changed by process; therefore, it does not appear in the table.
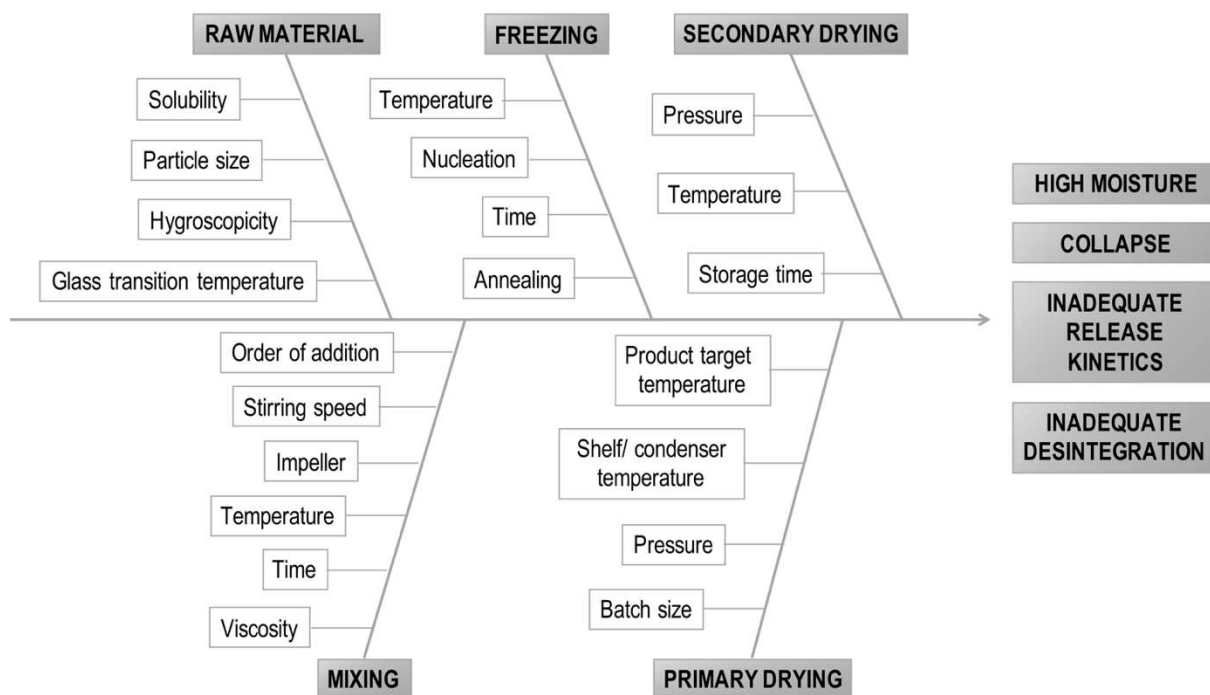
Fig. 4. Ishikawa for process parameters related to the most important quality deviations [45].

Studies on wafer development that use QbD principles are scarce. A recent paper provided a complete assessment, which included risk analysis (Ishikawa-FMEA), D-optimal designs, screening of excipients, and determination of a design space for a blank formulation. These researchers found that alginate/mannitol formulations had high mechanical strength and disintegration time, whereas xanthan-gum/mannitol formulations rapidly dispersed, but maintained structural stability [45]. Another interesting study combined formulation with process parameters as the basis for developing a design space. They observed that slow freezing of methylcellulose/mannitol wafers improved mechanical strength and the dissolution profile of meloxicam [75]. In another study, an experimental design was developed to generate an optimal predicted formulation of low-methoxy amidated pectin/carboxymethylcellulose wafers to increase mucoadhesitivity. The optimal polymer ratio showed similar performance to the predicted formulation, validating the mathematical approach [44].

2.6 CONCLUSION AND FUTURE PERSPECTIVES

Freeze-dried wafers can provide immediate or sustained delivery of APIs for local or systemic action. These wafers allow for ease of administration, protection against mechanical removal, and high drug loading. Although production of freeze-dried wafers requires few, inexpensive excipients that are widely available commercially, freeze drying is a high-cost and long process. Therefore, wafers are generally reserved for drugs susceptible to degradation/crystallization during manufacturing by other methods, or for market product differentiation. Gelatin and xanthan gum are the most commonly used polymers in commercial products and sodium alginate is the most commonly used natural polymer for experimental formulations. Production of wafers requires few steps, mainly mixing and freeze-drying. The wafers are shaped in the freezing step, which is crucial for process cost and time. In addition to process parameters, several material attributes are critical, such as thermal transitions, crystallinity, and hygroscopicity.

Mucoadhesive buccal wafers are typically designed for sustained release and consist of coated APIs and particulate carriers. As this trend is consistent in ODTs and buccal films [76], wafers will probably follow them. The advantage of wafers lies in the process, as the absence of compression and heating stresses protect particles from deformation and aggregation. Development of experimental wafers is increasing within the framework of QbD, a trend based on recent guidelines from regulatory agencies. While few articles detail development of wafers, these studies provide a framework for rational improvements and optimal formula prediction. These studies also highlight the relevance of new excipients, such as chitosan lactate, to augment formulation efficacy. Nevertheless, *in vivo* experiments have been scarce, and should increase in frequency in the future. Overall, buccal wafers are good candidates as dosage forms for commercial drugs, similar to their fast-disintegrating counterparts. Increasing scientific evidence will help sustained release buccal wafers reach clinical trials, allowing for verification of their performance in humans.

2.7   REFERENCES

1.   Costa, J. S. R., de Oliveira Cruvinel, K. & Oliveira-Nascimento, L. A mini-review on drug delivery through wafer technology: Formulation and manufacturing of buccal and oral lyophilizates. *Journal of Advanced Research* **20**, 33–41 https://doi.org/10.1016/j.jare.2019.04.010 (2019).

2.   U.S. Department of Health and Human Services. Guidance for Industry - Size, Shape, and Other Physical Attributes of Generic Tablets and Capsules. (2015).

3.   Spain, C. V., Wright, J. J., Hahn, R. M., Wivel, A. & Martin, A. A. Self-reported Barriers to Adherence and Persistence to Treatment With Injectable Medications for Type 2 Diabetes. *Clinical Therapeutics* **38**, 1653-1664.e1 (2016).

4.   Andrews, G. P., Laverty, T. P. & Jones, D. S. Mucoadhesive polymeric platforms for controlled drug delivery. *Eur. J. Pharm. Biopharm.* **71**, 505–518 (2009).

5.   Salamat-Miller, N., Chittchang, M. & Johnston, T. P. The use of mucoadhesive polymers in buccal drug delivery. *Adv. Drug Deliv. Rev.* **57**, 1666–1691 (2005).

6.   Ayensu, I., Mitchell, J. C. & Boateng, J. S. Development and physico-mechanical characterisation of lyophilised chitosan wafers as potential protein drug delivery systems via the buccal mucosa. *Colloids Surf B Biointerfaces* **91**, 258–265 (2012).

7.   Montero-Padilla, S., Velaga, S. & Morales, J. O. Buccal Dosage Forms: General Considerations for Pediatric Patients. *AAPS PharmSciTech* **18**, 273–282 (2017).

8.   Laffleur, F. Mucoadhesive polymers for buccal drug delivery. *Drug Dev Ind Pharm* **40**, 591–598 (2014).

9.   Aher, B. D., Shinkar, D. M., Kothawade, P. D. & Maru, A. D. A review on mucoadhesive buccal drug delivery system. *World J Pharm Pharm Sci* **7**, 305–320 (2018).

10.   Nafee, N. A., Ismail, F. A., Boraie, N. A. & Mortada, L. M. Mucoadhesive buccal patches of miconazole nitrate: in vitro/in vivo performance and effect of ageing. *Int J Pharm* **264**, 1–14 (2003).

11.   Mukherjee, D. & Bharath, S. Design and Characterization of Double Layered Mucoadhesive System Containing Bisphosphonate Derivative. *ISRN Pharm* **2013**, (2013).

12. Boateng, J. S. *et al.* Characterisation of freeze-dried wafers and solvent evaporated films as potential drug delivery systems to mucosal surfaces. *Int J Pharm* **389**, 24–31 (2010).

13. Nagar, P. *et al.* Orally disintegrating tablets : formulation, preparation techniques and evaluation. *J Appl Pharm Sci* 35–45 (2011).

14. WHO Expert Committee on Specifications for Pharmaceutical Preparations. WHO Technical Report - Annex 5: Development of paediatric medicines: points to consider in formulation. (2012).

15. U.S. Department of Health and Human Services. Guidance for Industry - Orally Disintegrating Tablets. (2008).

16. Hoffman, A. S. Hydrogels for biomedical applications. *Adv. Drug Deliv. Rev.* **64**, 18–23 (2012).

17. Lerner, E. I., Rosenberger, V. & Flashner, M. Pharmaceutical oral patch for controlled release of pharmaceutical agents in the oral cavity. (2001).

18. Hay, E. *et al.* Rizatriptan RPD for severe migraine in the emergency department—a multicenter study. *The Journal of Emergency Medicine* **25**, 245–249 (2003).

19. Evans, R. W. & Mathew, N. T. *Handbook of Headache*. (Lippincott Williams & Wilkins, 2005).

20. Grover, V. K., Mathew, P. J. & Hegde, H. Efficacy of orally disintegrating ondansetron in preventing postoperative nausea and vomiting after laparoscopic cholecystectomy: a randomised, double-blind placebo controlled study. *Anaesthesia* **64**, 595–600 (2009).

21. Ghosh, T. K. & Pfister, W. R. *Drug delivery to the oral cavity: molecules to market*. (CRC Press, 2005).

22. Barua, S. *et al.* Drug delivery techniques for buccal route: formulation strategies and recent advances in dosage form design. *J Pharm Investig* **46**, 593–613 (2016).

23. Datapharm Communications Limited, Medicines and Healthcare products Regulatory Agency & European Medicines Agency. Electronic Medicines Compendium (eMC) [homepage on the Internet]. https://www.medicines.org.uk/emc/ (2019).

24. U. S. Food and Drug Administration. U. S. Food and Drug Administration [homepage on the Internet]. https://www.fda.gov/ (2019).

25.   RxMed. RxMed: Diseases and Preparations' Description [homepage on the Internet]. https://www.rxmed.com/ (2018).

26.   EMA. European Medicines Agency [homepage on the Internet]. *European Medicines Agency* https://www.ema.europa.eu/en (2019).

27.   Troester, M. M., Hastriter, E. V. & Ng, Y.-T. Dissolving oral clonazepam wafers in the acute treatment of prolonged seizures. *J. Child Neurol.* **25**, 1468–1472 (2010).

28.   Center for Drug Evaluation and Research. Clinical Pharmacology Review: Claritin® Reditab® 12 Hour Tablet. (2006).

29.   El-Feky, G. S., Abdulmaguid, R. F., Zayed, G. M. & Kamel, R. Mucosal co-delivery of ketorolac and lidocaine using polymeric wafers for dental application. *Drug Delivery* **25**, 35–42 (2018).

30.   Xing, Q. *et al.* Increasing Mechanical Strength of Gelatin Hydrogels by Divalent Metal Ion Removal. *Sci Rep.* **4**, 4706 (2014).

31.   Habib, W., Khankari, R. & Hontz, J. Fast-dissolve drug delivery systems. *Crit Rev Ther Drug Carrier Syst* **17**, 61–72 (2000).

32.   Saharan, V. A. *Current Advances in Drug Delivery Through Fast Dissolving/Disintegrating Dosage Forms*. (Bentham Science Publishers, 2017).

33.   Matthews, K. H., Stevens, H. N. E., Auffret, A. D., Humphrey, M. J. & Eccleston, G. M. Lyophilised wafers as a drug delivery system for wound healing containing methylcellulose as a viscosity modifier. *Int J Pharm* **289**, 51–62 (2005).

34.   Matthews, K. H., Stevens, H. N. E., Auffret, A. D., Humphrey, M. J. & Eccleston, G. M. Gamma-irradiation of lyophilised wound healing wafers. *International Journal of Pharmaceutics* **313**, 78–86 (2006).

35.   Boateng, J. S. *et al.* In vitro drug release studies of polymeric freeze-dried wafers and solvent-cast films using paracetamol as a model soluble drug. *Int J Pharm* **378**, 66–72 (2009).

36.   Boateng, J. S. *et al.* Comparison of the in vitro release characteristics of mucosal freeze-dried wafers and solvent-cast films containing an insoluble drug. *Drug Dev Ind Pharm* **38**, 47–54 (2012).

37.   Aravamudhan, A., Ramos, D. M., Nada, A. A. & Kumbar, S. G. Chapter 4 - Natural Polymers: Polysaccharides and Their Derivatives for Biomedical Applications. in *Natural and Synthetic Biomedical Polymers* (eds. Kumbar, S. G., Laurencin, C. T. & Deng, M.) 67–89 (Elsevier, 2014). doi:10.1016/B978-0-12-396983-5.00004-1.

38.   Boateng, J. S. & Areago, D. Composite Sodium Alginate and Chitosan Based Wafers for Buccal Delivery of Macromolecules. *Austin J Anal Pharm Chem* **1**, 1022 (2014).

39.   Cohen, B., Pinkas, O., Foox, M. & Zilberman, M. Gelatin–alginate novel tissue adhesives and their formulation–strength effects. *Acta Biomater* **9**, 9004–9011 (2013).

40.   Bae, S. K., Sung, T.-H. & Kim, J.-D. A soft-tissue gelatin bioadhesive reinforced with a proteinoid. *J Adhes Sci Technol* **16**, 361–372 (2002).

41.   Shaikh, R. P. *et al.* The application of a crosslinked pectin-based wafer matrix for gradual buccal drug delivery. *J Biomed Mater Res B Appl Biomater* **100B**, 1029–1043 (2012).

42.   Ullah, F., Othman, M. B. H., Javed, F., Ahmad, Z. & Md Akil, H. Classification, processing and application of hydrogels: A review. *Mater Sci Eng C Mater Biol Appl* **57**, 414–433 (2015).

43.   Seager, H. Drug-delivery products and the Zydis fast-dissolving dosage form. *J. Pharm. Pharmacol.* **50**, 375–382 (1998).

44.   Sznitowska, M., Płaczek, M. & Klunder, M. The physical characteristics of lyophilized tablets containing a model drug in different chemical forms and concentrations. *Acta Pol Pharm* **62**, 25–29 (2005).

45.   Casian, T. *et al.* QbD for pediatric oral lyophilisates development: risk assessment followed by screening and optimization. *Drug Dev Ind Pharm* **43**, 1932–1944 (2017).

46.   Tawakkul, M. A., Shah, R. B., Zidan, A., Sayeed, V. A. & Khan, M. A. Complexation of risperidone with a taste-masking resin: novel application of near infra-red and chemical imaging to evaluate complexes. *Pharm Dev Technol* **14**, 409–421 (2009).

47.   Másson, M., Loftsson, T., Másson, G. & Stefánsson, E. Cyclodextrins as permeation enhancers: some theoretical evaluations and in vitro testing. *J Control Release* **59**, 107–118 (1999).

48.   Khadka, P. *et al.* Pharmaceutical particle technologies: An approach to improve drug solubility, dissolution and bioavailability. *Asian Journal of Pharmaceutical Sciences* **9**, 304–316 (2014).

49.   Mura, P. *et al.* Amidated pectin-based wafers for econazole buccal delivery: Formulation optimization and antimicrobial efficacy estimation. *Carbohydr Polym* **121**, 231–240 (2015).

50.   Jain, A. C., Aungst, B. J. & Adeyeye, M. C. Development and in vivo evaluation of buccal tablets prepared using danazol–sulfobutylether 7 β-cyclodextrin (SBE 7) complexes. *J Pharm Sci* **91**, 1659–1668 (2002).

51.   Fahr, A. & Liu, X. Drug delivery strategies for poorly water-soluble drugs. *Expert Opin Drug Deliv* **4**, 403–416 (2007).

52.   Kalepu, S. & Nekkanti, V. Insoluble drug delivery strategies: review of recent advances and business prospects. *Acta Pharm Sin B* **5**, 442–453 (2015).

53.   Hazzah, H. A., Farid, R. M., Nasra, M. M. A., EL-Massik, M. A. & Abdallah, O. Y. Lyophilized sponges loaded with curcumin solid lipid nanoparticles for buccal delivery: Development and characterization. *Int J Pharm* **492**, 248–257 (2015).

54.   El-Mahrouk, G. M., El-Gazayerly, O. N., Aboelwafa, A. A. & Taha, M. S. Chitosan lactate wafer as a platform for the buccal delivery of tizanidine HCl: In vitro and in vivo performance. *Int J Pharm* **467**, 100–112 (2014).

55.   Ng, S.-F. & Jumaat, N. Carboxymethyl cellulose wafers containing antimicrobials: A modern drug delivery system for wound infections. *Eur J Pharm Sci* **51**, 173–179 (2014).

56.   Davidson, R. & Rousset, J. Oral films – A multi-faceted drug delivery system and dosage form. *CURE Pharmaceutical* 14–17 (2018).

57.   Ishii T. & 石井徹弥. Water-bearing gel and its production method. (2006).

58.   Amos, S. & Goldwater, F. A. Gelating adhesive pharmaceutical preparations. (1962).

59.   Bunte, H. *et al.* Key considerations when developing freeze-dried formulation and current trends. *Pharm Technol Europe Digital* **22**, 2–4 (2010).

60.   Kianfar, F., Antonijevic, M., Chowdhry, B. & Boateng, J. S. Lyophilized wafers comprising carrageenan and pluronic acid for buccal drug delivery using model soluble and insoluble drugs. *Colloids Surf B Biointerfaces* **103**, 99–106 (2013).

61.   Konstantinidis, A. K., Kuu, W., Otten, L., Nail, S. L. & Sever, R. R. Controlled nucleation in freeze-drying: Effects on pore size in the dried product layer, mass transfer resistance, and primary drying rate. *J. Pharm. Sci.* **100**, 3453–3470 (2011).

62.   Geidobler, R. & Winter, G. Controlled ice nucleation in the field of freeze-drying: Fundamentals and technology review. *European Journal of Pharmaceutics and Biopharmaceutics* **85**, 214–222 (2013).

63.   Kearney, P. & Wong, S. K. Method for making freeze dried drug dosage forms. (1997).

64.   Tang, X. (Charlie) & Pikal, M. J. Design of Freeze-Drying Processes for Pharmaceuticals: Practical Advice. *Pharm Res* **21**, 191–200 (2004).

65.   Gole, D. J., Levinson, R. S., Carbone, J. & Davies, J. D. Preparation of pharmaceutical and other matrix systems by solid-state dissolution. (1993).

66.   U.S. Department of Health and Human Services. Guidance for Industry - Q8 (R2) Pharmaceutical Development. (2009).

67.   Yu, L. X. Pharmaceutical Quality by Design: Product and Process Development, Understanding, and Control. *Pharm Res* **25**, 781–791 (2008).

68.   Maguire, J. & Peng, D. How to Identify Critical Quality Attributes and Critical Process Parameters. in (The AAPS Journal, 2015). doi:10.1208/s12248-016-9874-5.

69.   AlHusban, F., Mohammed, A. R. & Perrie, Y. Preparation, Optimisation and Characterisation of Lyophilised Rapid Disintegrating Tablets Based on Gelatin and Saccharide. *Curr Drug Deliv* **7**, 65–75 (2010).

70.   Borges, P. F. *et al.* The role of SeDeM for characterizing the active substance and polyvinyilpyrrolidone eliminating metastable forms in an oral lyophilizate—A preformulation study. *PLOS ONE* **13**, e0196049 (2018).

71.   Suciu, T., Iurian, S., Bogdan, L., Moldovan, M. & Tomu, I. QbD Approach in the Development of Oral Lyophilisates with Ibuprofen for Paediatric Use. *Farmacia* **66**, 10 (2018).

72.   Patel, S. M. & Pikal, M. J. Lyophilization Process Design Space. *J Pharm Sci* **102**, 3883–3887 (2013).

73.   Patel, S. M. *et al.* Lyophilized Drug Product Cake Appearance: What Is Acceptable? *J Pharm Sci* **106**, 1706–1721 (2017).

74.   Jug, M. *et al.* In vitro dissolution/release methods for mucosal delivery systems. *ADMET and DMPK* **5**, 173–182 (2017).

75.   Iurian, S. *et al.* Defining the design space for freeze-dried orodispersible tablets with meloxicam. *Drug Dev Ind Pharm* **42**, 1977–1989 (2016).

76.   Elwerfalli, A. M., Ghanchi, Z., Rashid, F., Alany, R. G. & ElShaer, A. New Generation of Orally Disintegrating Tablets for Sustained Drug Release: A Propitious Outlook. *Curr Drug Deliv* **12**, 652–667 (2015).

3 BIOPOLYMERIC WAFERS AS DRUG DELIVERY SYSTEMS FOR POST DENTAL PROCEDURES

Biopolymeric wafers as drug delivery systems for post dental procedures

Juliana Souza Ribeiro Costa[a,b], Karen de Oliveira Cruvinel[a], Karina Cogo Muller[a], Sandra Klein[c], Laura Oliveira-Nascimento[a]

[a] Faculty of Pharmaceutical Sciences, University of Campinas, Campinas, São Paulo, Brazil.

[b] Institute of Biology, University of Campinas, Campinas, São Paulo, Brazil.

[c] Center of Drug Absorption and Transport (C_DAT), Department of Biopharmaceutics and Pharmaceutical Technology, Institute of Pharmacy, University of Greifswald, Greifswald, Germany.

ABSTRACT

After dental surgical procedures, the wound occlusion protects the site from contamination and promotes homeostasis. Buccal wafers composed by biopolymers present a promising solution as dressings, since replacing the suture with biodegradable dressings loaded with drugs can provide less systemic exposure to medication, absorption of exudates and better recovery from laceration or wound. For this work, biopolymers were chosen and characterized upon an experimental design to form freeze-dried buccal wafers to act as dressing and drug carriers. Lidocaine hydrochloride and curcumin presented antimicrobial activity against some common oral bacteria, which reinforces their use as drug to dressings. The developed wafers were characterized by visual analysis, near infrared spectroscopy, scanning electron microscopy, and X-ray diffraction. The resulting dosage forms presented a good visual homogeneity, a porous surface, high drug loading (of at least up to 20 mg/mL of lidocaine hydrochloride) and disintegration time up to 80 minutes in artificial saliva with mucin. Although this formulation can be well suited for application over sutures, possibly improving healing, further studies with chemical crosslinking can enhance the disintegration time and allow suture substitution.

Keywords: Biopolymeric wafer, freeze-drying, lidocaine.

3.1 INTRODUCTION

Closing a surgical incision or healing a wound goes through the stages of homeostasis, inflammation, cell proliferation and remodeling. Homeostasis can be impaired by diseases or chronic use of anticoagulants, as well as by microbial contamination, generating chronic and painful wounds. The inflammation phase can also be influenced by contamination or disease, and its exacerbation is a major cause of the appearance of chronic wounds [1], in addition to the post-surgical implications. The union of tissues by suture can cause tissue tension and generally requires the removal of stitches, in addition to not allow intermediate checks. Therefore, replacing the suture with biodegradable dressings loaded with drugs presents greater flexibility, less systemic exposure to medication, absorption of exudates and better recovery from laceration or wound [2–4].

The pharmaceutical form must remain fixed long enough to guarantee occlusion and pharmacological action, in addition to present biodegradability, biocompatibility, acceptable taste, non-interaction with the loaded drugs and increase their permeation. Occlusion aids homeostasis, protects the site from contamination and provides a basis for the cell proliferation phase [2]. Buccal wafers, composed of lyophilized biopolymeric gels, meet these requirements and present a promising solution as dressings.

Given the above, this work focused on formulation and process development for the manufacture of freeze-dried biopolymeric buccal wafers as post-surgical oral dressings. The chosen drugs to be loaded were lidocaine, a local anesthetic/ analgesic, and curcumin, with anti-inflammatory and antimicrobial action. Lidocaine is the local anesthetic/ analgesic most used in dental practice worldwide and the first medication in transmucous adhesive pharmaceutical form approved by the FDA [5]. Despite lidocaine is not an antibiotic agent, its anesthetic dose inhibits bacterial growth and offers dual action during its use in dental procedures [6]. The choice of curcumin is based on the various scientific reports of its application in topical formulations for the treatment of wounds, showing benefits in the prevention of chronic inflammation and the consequent pain generated [1,7]. In addition, curcumin present antimicrobial properties [8,9], a desirable feature for a post trauma treatment. The choice of curcumin is based on the various scientific reports of its application in topical

formulations for the treatment of wounds, showing benefits in the prevention of chronic inflammation and the consequent pain generated [1,7]. In addition, both drugs present antimicrobial properties, a desirable feature for a post trauma treatment, which were tested in this paper to address the oral microbiota.

3.2 METHODS

3.2.1 Wafer formulation and polymer screening

For the formation of the gel, bovine gelatin type B (Gelita, Brazil) was dissolved in 10 mL of distilled water (50 °C), followed by the addition of sodium alginate (Dinamica, Brazil) dissolved in 10 mL of distilled water. After homogenization, the drug (lidocaine hydrochloride (Sigma-Aldrich, USA) or curcumin C3 complex (Infinity Pharma, USA) – dissolved in 1% ethanol in the final solution) was added, while stirring. The gel formed was lyophilized to form the wafer. Likewise, wafers of chitosan (Sigma-Aldrich, USA; medium molecular weight, 75-85% deacetylation), wafers using xylitol (Sigma Aldrich, USA – from 1 to 10 mg/mL in the final solution) as a sweetener, and wafers using calcium chloride (Sigma Aldrich, USA – 0.01% in the final solution) as a crosslinker were formulated, from which the best formulation for the delivery of the drug was analyzed. Statistical analyses and designs were performed with the aid of the software Prisma, Origin, and Minitab.

3.2.1.1 Bilayer wafers

Bilayer wafers were produced in two different ways: i) Spraying an ethanolic ethyl cellulose solution on the freeze-dried wafers, ii) Casting an ethyl cellulose film on wells overnight, over-layering it with the gelatin-alginate-lidocaine solution and freeze drying it.

3.2.1.2 Freeze-drying of formulations

The formulations were lyophilized in a 24-well plate. The process was carried out in the Lyostar 3 lyophilizer (SP scientific), which contains shelves with computational pressure control and temperature ramps. The samples were subjected to different rates of freezing and heating, according to the previous results of the thermal analyses. From their evaluation, the formulations were

lyophilized following the coming protocol: freezing at -45 °C for 5 hours, primary drying at -45 °C for 24 hours, secondary drying at -20 °C for 16 hours and at 20 °C for 20 hours, at 100 mTorr.

3.2.2 Characterization of polymers (Zeta potential)

The Zeta potential was measured on the Zetasizer Nano ZS equipment (Malvern Instruments, Malvern, UK) by electrophoretic mobility. The samples (isolated polymers or in association) were measured in suspension immediately after preparation, diluted 1:10 in ultrapure water.

3.2.3 Determination of critical temperatures of formulations

To determine the collapse temperature of the samples, a microscope attached to a lyophilization module, Lyostat 2, model FDCS 196, Linkam Instruments, Surrey, UK, equipped with a liquid nitrogen freezing system (LNP94/2) and temperature controller, was used programmable (TMS94, Linkam). The pressure was monitored through a Pirani valve. The equipment was calibrated with aqueous NaCl solution (eutectic temperature of –21.1 °C). Direct observation of freezing and lyophilization was performed using a Nikon polarized light microscope, model Elipse E600 (Nikon, Japan), and heating-cooling ramps of 2.5 °C/min, 5 °C/min and 10 °C/min.

The glass/ eutectic transition temperature was performed in DSC (Differential Scanning Calorimetry – Mettler Toledo, model DSC1, Schwerzenbach, Switzerland). For weighing the samples in an aluminum sample holder (approximately 20 mg), a microanalytical balance was used (Mettler Toledo, model MX5, Schwerzenbach, Switzerland). The blank was automatically discounted in each analysis. The analyses were carried out in a nitrogen atmosphere, at a flow of 50 mL/min, in different temperature ranges (cooling from 25 to –65 °C, at a rate of 5 °C/min; 2–minute isotherm at –65 °C; heating from –65 to 25 °C, at a rate of 5 °C/min).

3.2.4 Rheological analysis

The analyses were performed on the HAAKE ™ MARS ™ Rheometer (Thermo Scientific ™) with a cone-type apparatus (4 °/ 40 mm) – plate (20 mm), with a gap of 1 mm. The data were collected on a computer connected to it, for

later analysis. The analysis time was 300 seconds and the shear gradient were 50 [1/ s] to 1000 [1/ s]).

3.2.5   Visual assessment

Visual analysis of the drug wafers was performed to verify if there is matrix collapse, in addition to visual homogeneity.

3.2.6   Polymeric distribution in the matrix

The analysis of the distribution of the components of the wafer was performed by near infrared (NIR) spectroscopy and the chemometric tool Multivariate Resolution of Curves (MRC).   For this, the wafer and pure substances spectra were obtained using the Spotlight 400N FT-NIR Imaging System, Perkin-Elmer spectrometer. The operating conditions were a 50 μm pixel size, 32 scans, 16 cm^{-1} resolution and a spectral range of 7800-4000 cm^{-1}. The image analysis of the center (1000 x 1000 μm) and the edges of the wafers (3000 x 3000 μm) was performed. The spectra were obtained in reflectance (R) and converted to pseudo-absorbance (log 1/ R). As pre-processing, the normal standard variation was applied to correct the physical effects (radiation scattering and particle size). The spectra were also analyzed by Savitzky-Golay, with a 19-point window (removal of experimental noise).

3.2.7   Scanning electron microscopy morphology

The structural analysis of the wafers was performed by scanning electron microscopy (model Leo 440i, LEO Electron Microscopy/ Oxford, Cambridge, England). The sample was cut into small, thin pieces and placed on double-sided carbon tape in 15 mm aluminum stubs. The sample was analyzed at different points to obtain representative images of the whole.

3.2.8   X-ray diffraction characterization

This test was carried out to investigate the physical form (crystalline or amorphous) of the wafer with and without drug, using a table X-ray diffractometer (Rigaku Miniflex II, Japan) in Bragg-Brentano reflection mode, equipped with a source of Cu Kα x-ray radiation. The samples were compressed by placing them

in the sample holder. Diffractograms were acquired for each sample within a 2-theta range of 10-40 °.

3.2.9 Residual moisture of wafers

The residual moisture of the lyophilized samples was determined using a thermogravimetric analyzer (TGA, model TGA-50M, Shimadzu, Kyoto, Japan). For weighing the samples in an alumina sample holder, a microanalytical balance was used (Mettler Toledo, model MX5, Schwerzenbach, Switzerland). The samples were heated from 25 to 150 °C at a rate of 10 °C per minute.

3.2.10 Disintegration test

To determine the disintegration time, one wafer was placed in 5 mL of artificial saliva solution (with or without mucin), at 37 °C, in an orbital shaker, and the time necessary to disintegrate was observed. The artificial saliva was composed by 2.38 g of Na_2HPO_4, 0.19 g of KH_2PO_4, and 8.00 g of NaCl (and 1.8 g of mucin in tests in artificial saliva with mucin) in 1L of distilled water, the pH was set to 6.8.

3.2.11 Drug content

3.2.11.1 Curcumin

Incorporation efficiency (IE) refers to the percentage of the curcumin that was incorporated into the wafers. The IE was determined by UV-vis spectroscopy at 430 nm. For this, curcumin was extracted from lyophilized wafers and the resulting solution was subjected to drug dosing. IE was calculated by the following the Equation 1:

$$IE(\%) = \frac{(drug\ in\ the\ extracted\ solution)}{added\ drug} * 100 \qquad \text{Equation 1}$$

3.2.11.2 Lidocaine

The wafer was dissolved in 5 mL of water for disintegration and release of the incorporated lidocaine, this solution was taken to HPLC, following the method parameters defined above (Table 1).

Table 1. Chromatographic conditions for quantification of lidocaine.

Sample	Lidocaine diluted in mobile phase
Mobile phase	Glacial acetic acid 5% in water (adjusted pH to 3.4 with NaOH 1N) and acetonitrile (4:1, v/v)
Injection volume	20 µL
Run time	8 minutes
Flow	1.5 mL/min
Detector	254 nm
Column	C18 – 250 mm x 4.6 mm x 5 µm (L1)

The analytical methodology by HPLC for lidocaine quantification was applied according United States Pharmacopeia (USP29) [10], with modifications, aiming to obtain a symmetrical peak and within the required standards. The analytical curve was constructed by taking increasing concentrations of lidocaine between 12 and 380 µg/mL.

3.2.12 Drug release

3.2.12.1 Vertical diffusion cell

The dissolution studies were performed in triplicate, on the vertical diffusion cells (Hanson), with 2 mL of artificial saliva pH 6.8 as a media in the donor compartment, and phosphate buffer pH 7.2 as an acceptor media (7.5 mL), at 37°C, using a Supor® membrane (0.45µm 25mm) separating the compartments. The samples of both compartments were withdrawn at predetermined times (15 min, 30 min, 45 min, 1h, 1h30, 2h, 3h, 4h, 5h, 6h), and the volume was replaced with fresh medium. The samples were filtered (0.45 µm PVDF syringe filters) and diluted with mobile phase for HPLC analysis.

3.2.12.2 USP Apparatus 4

The dissolution studies were performed on the USP Apparatus 4 equipment (Erweka), using a glass microfiber filter (Whatman™ GF/F, 25mm). All the tests were performed in quadruplicate, with artificial saliva pH 6.8 as a dissolution media, in closed loop, flow of about 2.4 mL/min, at 37°C. The samples were withdrawn at predetermined times (t = 0 min, 10 min, 20 min, 30 min, 40

min, 50 min, 1h, 1h30, 2h, 3h, 4h, 5h, 6h), and the volume was replaced with fresh medium. The samples were filtered (0.45 μm PVDF syringe filters) and diluted with mobile phase for HPLC analysis.

3.2.13 Minimum inhibitory concentration (MIC)

The determination of the minimum inhibitory concentration (MIC) was made by the microdilution method in 96-well plates as described by the Clinical and Laboratory Standards Institute (CLSI) [11]. All tests were performed in triplicates. The bacteria and the medium used were described in the Table 2.

Table 2. Culture media and conditions for bacterial growth.

Bacteria	Culture media	Growth conditions
S. oralis ATCC 10557 S. mitis NCTC 12261 S. salivarius ATCC 7073 S. sanguinis 3K36 S. gordonii Chali ATCC 35105	Brain heart infusion (BHI) and brain hearth infusion agar (BHI agar)	CO_2 5 %, 37 °C, for 24 hours
P. gingivalis ATCC 33277 P. gingivalis W83	Supplemented TSB-BHI broth: 1.55% Tryptone Soy Broth (TSB – Tryptic Soy Broth, Difco Co., Detroit, MI, USA), Brain-Heart Broth 1.48% (BHI – Brain Heart Infusion, Difco Co., Detroit, MI, USA), 0.2% Yeast Extract, 5 μg/mL of Hemine and 1 μg/mL of Menadione.	Anaerobic chamber for 48h

Lidocaine was dissolved in sterile distilled water. The concentrations of lidocaine varied from 20 to 0.01 mg/mL. Curcumin was first dissolved in 50% absolute ethanol. The concentrations of curcumin varied from 500 to 0.24 μg/mL (with 5% ethanol final concentration in the wells). The plates were incubated for 24 hours in a CO_2 oven. The experimental groups tested were: A. Test group (culture medium + bacteria + lidocaine in different concentrations); B. Vehicle control group (culture medium + bacteria + sterile distilled water); C. Substance control group (culture medium + lidocaine); D. Culture medium control group and E. Inoculum control group (culture medium + inoculum). To verify the minimum

inhibitory concentration, optical density readings were made on a spectrophotometer (550 nm) and then stained with 30 μL of resazurin in each well at 0.01% in aqueous solution, for better visualization of bacterial growth.

3.3   RESULTS

3.3.1   Screening of biopolymers for wafers matrix

3.3.1.1   Theoretical screening

Current scientific literature points to chitosan as one of the biopolymers with the greatest mucoadhesive potential [12–15]. Thus, chitosan was used as a keyword in the search for existing patents for lyophilized polymeric pharmaceutical forms. The research was carried out on the Orbit platform, with the keywords "chitosan, wafer, lyophilized OR freeze-dried and buccal" (307 patents). A new screen was applied so that the final documents contained the words "claims and description", excluding documents with only citations or examples with those words; patents were also excluded if related to new diagnostic methods, of products for veterinary use only, for exclusive use in culture media or carrying genes. The selected patents are cited in the bibliography, adding up to 15 relevant documents [16–30].

All selected patents have oral or buccal application. In addition to these application routes, some still have other possibilities, such as topical, parenteral or through other mucous membranes, such as vaginal and anal for example. Among the biopolymers found in the patents are sodium alginate, gelatin, pectin, carrageenan, among others. Chitosan was found both isolated and combined with other polymers. Based on this review of patents and review of articles, three polymers with potential for the formulation of wafers were selected: chitosan, alginate and gelatin.

3.3.1.2   Experimental screening

In order to verify the viability of the gels, binary combinations between polymers were performed, based on the literature [13,31,32]: CHSA (chitosan 6 mg/mL + sodium alginate 4 mg/mL); CHGE (chitosan 5 mg/mL + gelatin 10 mg/mL); and SAGE (4 mg/mL sodium alginate + 10 mg/mL gelatin).

The gelatin and alginate mixture (SAGE) formed a translucent, homogeneous and stable gel for at least 24 hours. On the other hand, all chitosan combinations were heterogeneous right after preparation, showing white branched solids (Figure 1). It is likely that this phenomenon is due to the formation of complexes between chitosan (cationic) and sodium alginate (anionic), as

reported by other groups [33–35], as well as with gelatin (anionic). This failure in homogeneity was not avoided by varying the type of stirring (magnetic, manual with a glass stick, or ultra-turrax® (high-performance dispersing instrument)), by changing the order of polymer addition or temperature change (23 to 40 °C).
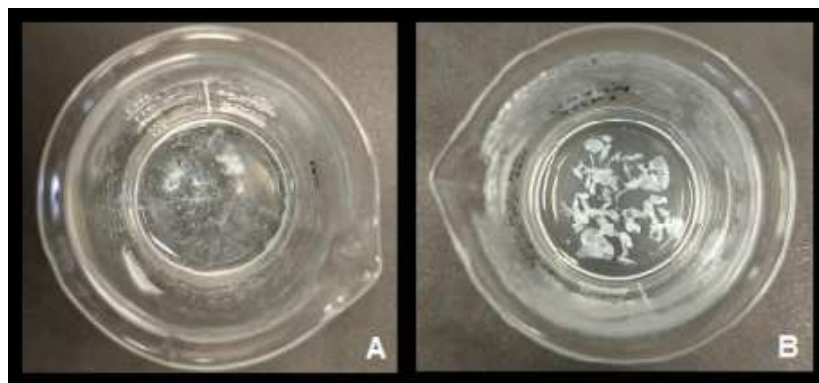
Figure 1. Heterogeneous chitosan and sodium alginate formulations, with complex formation. (A) Chitosan 6 mg/mL + sodium alginate 4 mg/mL; (B) Chitosan 0.4 mg/mL + sodium alginate 1.6 mg/mL.

3.3.1.3   Zeta potential and pH

The zeta potential of polymers (Table 3) were consistent with those previously reported [36,37]. The values confirm the negative charge of gelatin, reinforcing the thesis of chitosan complexation by electrostatic interaction to a lesser extent than alginate, given the lower ionic density. The zeta potential is a function of the polymer charge, which in turn is related to mucoadhesive properties. According to the scientific literature, the greater the charge (positive or negative), the greater the probability of being mucoadhesive, although this effect is not completely understood [12,13,15]. Nevertheless, actual mucoadhesiveness can only be proven by *ex vivo* tests on animal mucous membranes, or even by *in vivo* tests.

Table 3. Potential zeta values (mV) and pH of polymeric solutions.

Polymer/ Polymeric combination	Zeta potential (mV)	pH
Gelatin 10 mg/mL (GE)	-6.89 ± 0.57	5.85
Chitosan 5 mg/mL (CH)	64.5 ± 3.81	3.80
Chitosan 6 mg/mL (CH)	56.6 ± 2.76	3.78
Sodium alginate 4 mg/mL (SA)	-58.2 ± 6.73	5.02
CHSA	60.9 ± 3.19	3.92
CHGE	42.6 ± 6.24	4.02
SAGE	-38.6 ± 1.33	5.63

The pH values of the solutions were measured to check their compatibility with the oral mucosa, considering that the pH of this medium varies between 5.5 and 7 [38]. Although the final dosage form is lyophilized, the saliva soaks the matrix, which should dehydrate at a solution pH close to the range found in the mouth, avoiding discomfort to the patient.

3.3.1.4   Rheological analysis

Rheology is the study of the flow and deformation properties of matter in a solid, semi-solid or liquid system [39]. Viscosity is a measure of the product's resistance to flow: the higher the viscosity, the greater the resistance. At last, the shear stress (τ) is the force applied to the product to flow, which generates a speed, or rate, of shear (γ). High shear stresses cause the curve to tend to linearity, indicating that a minimum viscosity value has been reached [39,40].

A rheological analysis of the SAGE formulation was carried out, without (Figure 2A) or with xylitol (Figure 2B), a sweetener added to the formulation so that the patient's acceptability to the pharmaceutical form is improved [41] (Item 2, review article).
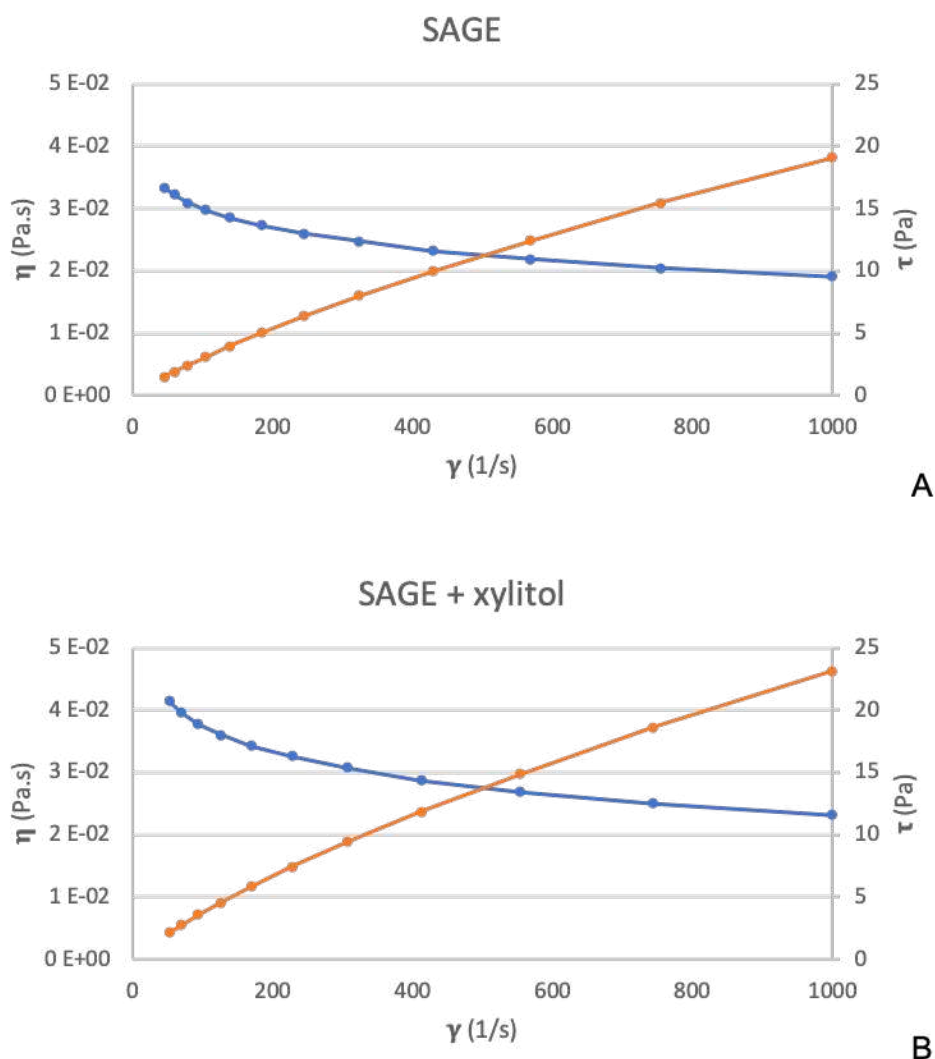
Figure 2. Graph of rheological analysis of the formulations: (A) gelatin 1% + sodium alginate 4 mg/mL, and (B) gelatin 1% + sodium alginate 4 mg/mL + xylitol 10 mg/mL; which illustrates the value of the viscosity (η, in blue) and the shear stress (τ, in orange), given the variation of the shear rate (γ).

Both formulations were presented as non-Newtonian fluids, like most pharmaceutical fluids, presenting a pseudo plastic behavior. This behavior, characterized by the decrease in viscosity with the increase of the applied shear stress, is adequate because it facilitates filling, presenting a lower viscosity when passing through the injector nozzle [39].

3.3.2 Wafer optimization

The experimental design was done with a focus on the SAGE formulation with xylitol. This was the formulation of choice, since the formulation with gelatin 10 mg/mL and sodium alginate 4 mg/mL was the one that showed the best visual homogeneity of the mixture. In addition, this formulation showed the pH values closest to the oral mucosa, being one more indication of better compatibility with the site of action. Thus, the experimental design described in Table 4 was elaborated to optimize the placebo formulation. The outputs analyzed were pH, zeta potential, critical temperatures, residual moisture.

Table 4. Experimental design to optimize blank wafer formulation (2^3, with a central point in triplicate).

Formulation		Gelatin (mg/mL)	Sodium alginate (mg/mL)	Xylitol (mg/mL)	pH	Zeta potential (mV)	Residual moisture (%)
1	+1/+1/+1	17	6	10	6.1	-62.2 $\pm$ 1.6	15.426
2	-1/-1/+1	3	2	10	6.8	-54.4 $\pm$ 1.6	13.038
3	-1/+1/-1	3	6	1	6.6	-66.2 $\pm$ 0.8	19.206
4	+1/-1/+1	17	2	10	6.0	-42.4 $\pm$ 2.3	16.012
5	0/0/0	10	4	5.5	6.2	-54.8 $\pm$ 1.3	18.686
6	-1/+1/+1	3	6	10	6.5	-65.8 $\pm$ 1.0	20.382
7	+1/-1/-1	17	2	1	6.0	-39.1 $\pm$ 0.1	17.694
8	0/0/0	10	4	5.5	6.2	-58.0 $\pm$ 1.0	17.633
9	+1/+1/-1	17	6	1	6.1	-55.8 $\pm$ 3.1	17.732
10	0/0/0	10	4	5.5	6.1	-59.3 $\pm$ 1.5	16.961
11	-1/-1/-1	3	2	1	6.6	-47.9 $\pm$ 0.2	17.068

After formulating the samples of the experimental design, the pH and zeta potential were measured. The results are shown in Table 4. As observed in the screening of polymers, the formulations showed pH values close to that of the oral mucosa, an indication of compatibility with the site of action. Considering the pH, gelatin had the largest influence in the wafer and, to a lesser extent, the combination of alginate and gelatin (Figure 3A).
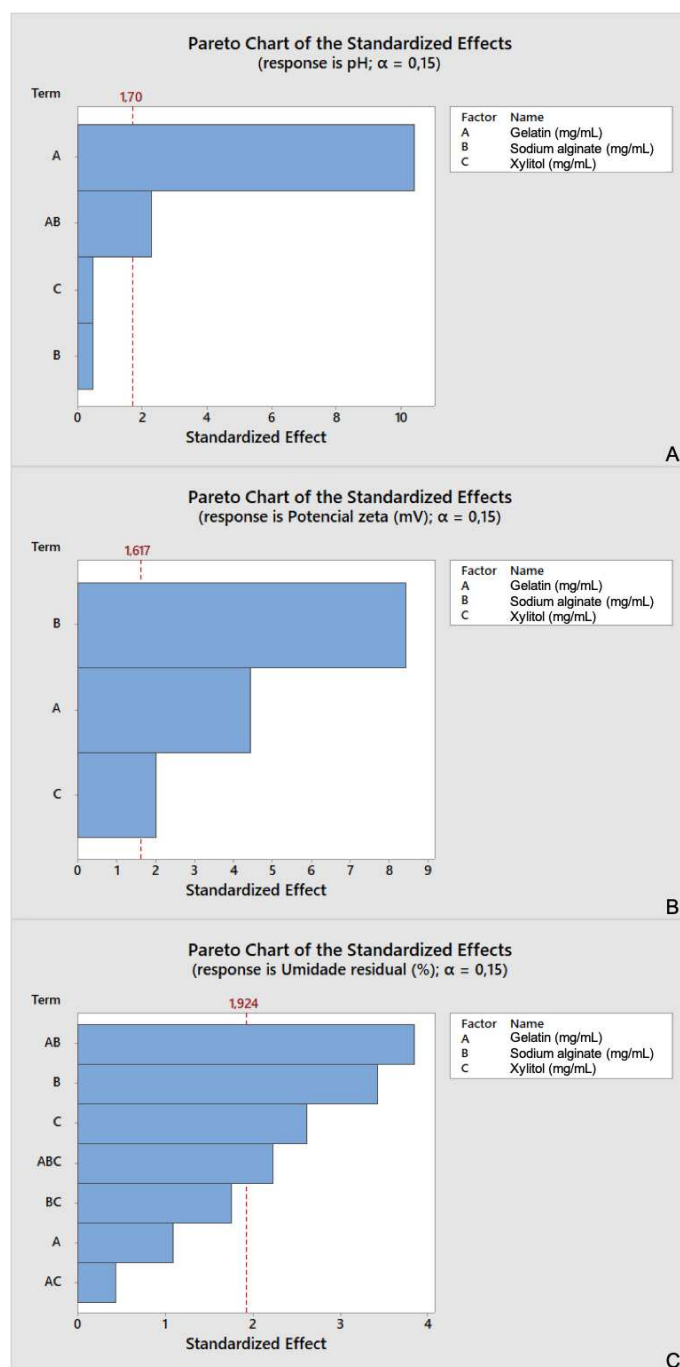
Figure 3. Pareto graph of the standardized effects, facing (A) pH, (B) zeta potential, and (C) residual moisture responses.

The results of the zeta potential were negative, and have high absolute value, indicating mucoadhesivity [12,13,15]. When considering the zeta potential response, the parameters that have the greatest influence are the concentration of sodium alginate, the concentration of gelatin and the concentration of xylitol in the wafer, respectively (Figure 3B).

The wafers presented high residual moisture (Table 4), between 13.0% and 20.3%. The formulation with the lowest residual moisture was

formulation 2, with the lowest concentration of alginate and gelatin, and the highest concentration of xylitol. Even so, the residual moisture response was influenced by the combination of gelatin and sodium alginate in the wafer, the concentration of sodium alginate, xylitol and the combination of the three components (Figure 3C). One possibility is the rise of the product resistance of the formulation during the primary drying, with higher concentration of components resulting in higher resistance during drying and higher residual moisture in the freeze-dried product [42]. From these data, residual moisture optimization will be necessary, increasing the secondary drying time, which removes the adsorbed water in the matrix [43].

Lyophilization microscopy is performed to predict the maximum temperature the sample can be submitted to in the primary drying stage of lyophilization without collapse (loss of structure). However, with the ramp used (10 ºC/min to 60 ºC, holding for 1 minute, pressure of 100 MTorr, heating ramp to 0 ºC of 5 ºC/min) it was not possible to visualize the collapse temperatures of the samples, which indicates that the collapse is above the ice melting temperature (0 °C), which is not detectable in the equipment.

The test for determining the critical temperatures of all formulations in the experimental design was carried out using the Differential Scanning Calorimeter (DSC) Sup. Figure 1. The DSC was performed to complement the analysis of critical temperatures, and to try to identify the glass transition temperature of the solution. However, we also did not detect transitions prior to the peak of melting ice, which confirms the lyophilization microscopy. The analyses failed to translate the phenomenon quantitatively, however, the thermal transition being above or concomitant with the melting of the ice is an advantage for freeze drying, which can be done at temperatures above those that are commonly used. There is no data from the literature on thermal transitions of these gels to confirm this result. No graph was generated for this response for the experimental design because all samples behaved the same way, with no detectable glass or eutectic transition events.

3.3.3 Scanning electron microscopy morphology

The analyzed sample was formulation 5, referring to the central point of the experimental design. As expected, it presented a high porosity structure,

consistent with wafer formation (Figure 4). This is an important characteristic, as it provides high loading capacity of drugs for this pharmaceutical form.


```
100µm        EHT=15.00 kV                                    LRAC/FEQ
Mag=  200  X  I Probe=    50 pA    WD=  23 mm   Detector= SE1   UNICAMP
```
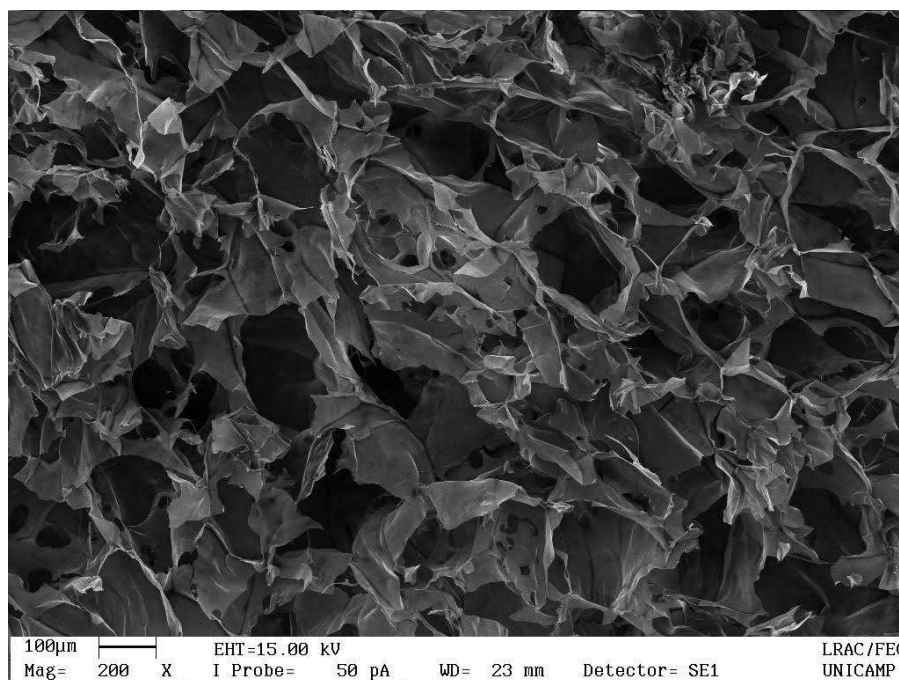
Figure 4. Scanning electron microscopy of the sodium alginate-gelatin wafer (formulation 5 of experimental design). Image acquired with magnification of × 200.

3.3.4 Production and visual evaluation of wafers

The SAGE samples (Figure 5) were lyophilized with or without curcumin (200 µg/mL), in a pilot freeze-dryer, using the lyophilization protocol described in the methodology. The choice of curcumin in this analysis facilitates the preliminary visualization of the homogeneity of the drug in the matrix, due to its color. Both formulations were porous, with a straight surface, easy to remove from the mold, without visual collapse and of uniform height between the units produced. Visual analysis of curcumin formulations confirms that the drug is distributed homogeneously throughout the matrix, even though it is hydrophobic.
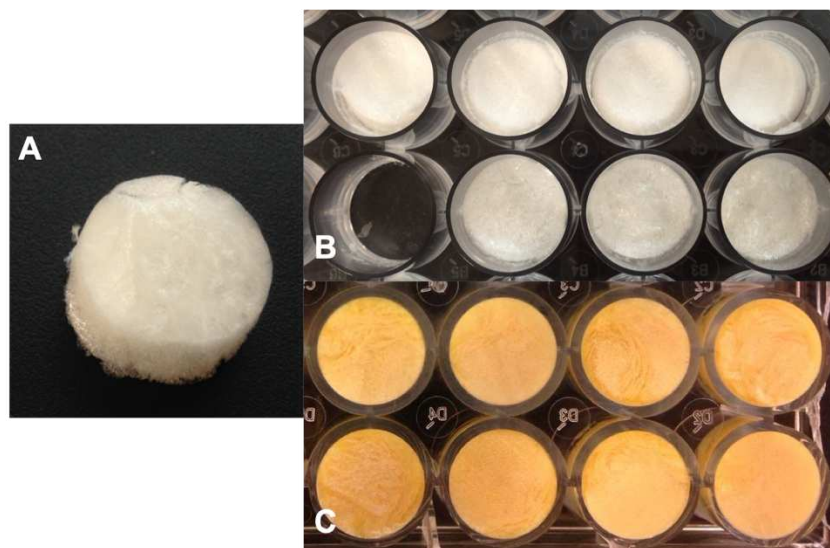
Figure 5. Alginate and chitosan wafers after lyophilization (A) without drug; (B) without drug, in the mold; (C) with curcumin, in the mold.

3.3.4.1 Polymeric distribution in the matrix

NIR spectroscopy was performed to analyze the distribution of alginate and chitosan in the SAGE wafer. For this purpose, the chemometric tool Multivariate Curves Resolution (MCR) was used. The data was taken from the center (Figure 6) and the edge (Figure 7) of the wafers to verify and compare their composition in these two regions regarding the degree of distribution. The figures show relatively homogeneous formulations, as can be seen by the images [44].

Figure 6. Comparison of the spectra of pure substances obtained experimentally (blue) and the spectra recovered by the MCR model (in red), in addition to the values of the correlation coefficients (r^2), referring to the center of the sodium alginate-gelatin wafer: (A) sodium alginate and (B) gelatin. Images of the center of the wafer, referring to (C) sodium alginate and (D) gelatin (the warm colors, red, indicate the presence of the component and the cold, blue, the absence).
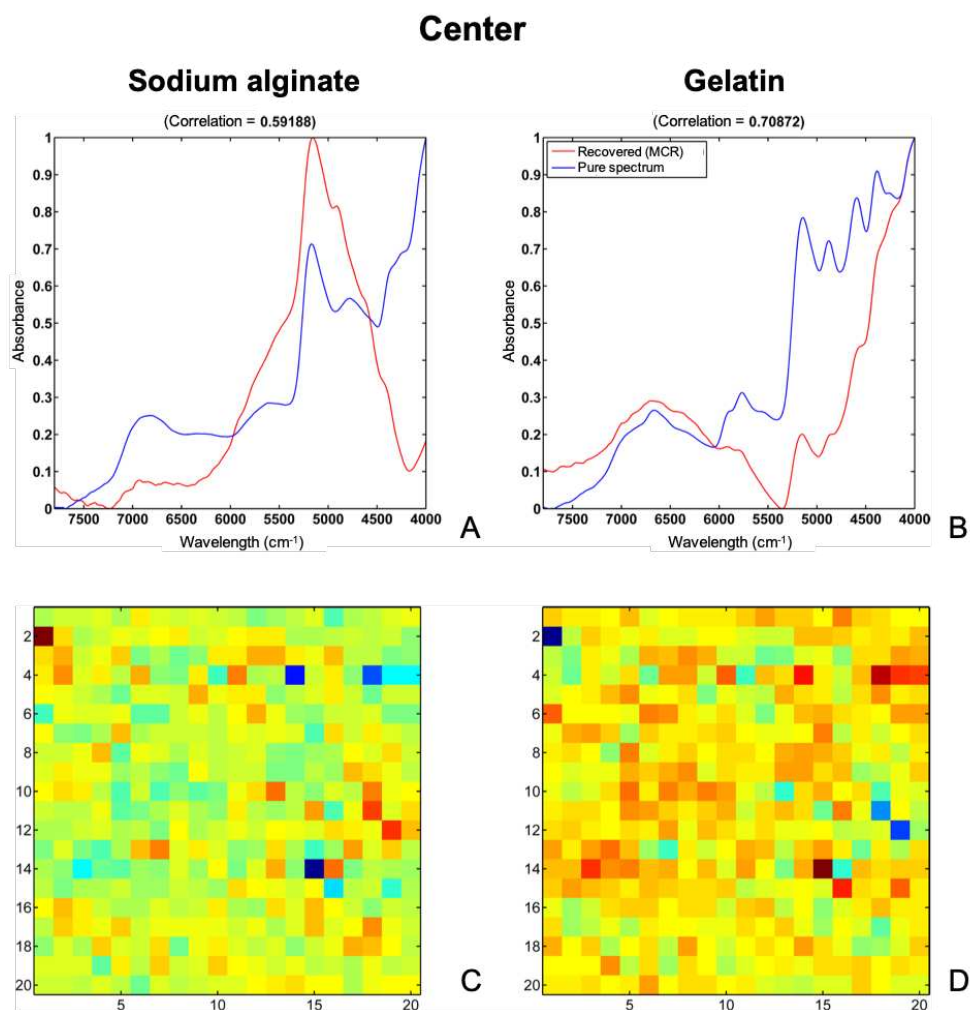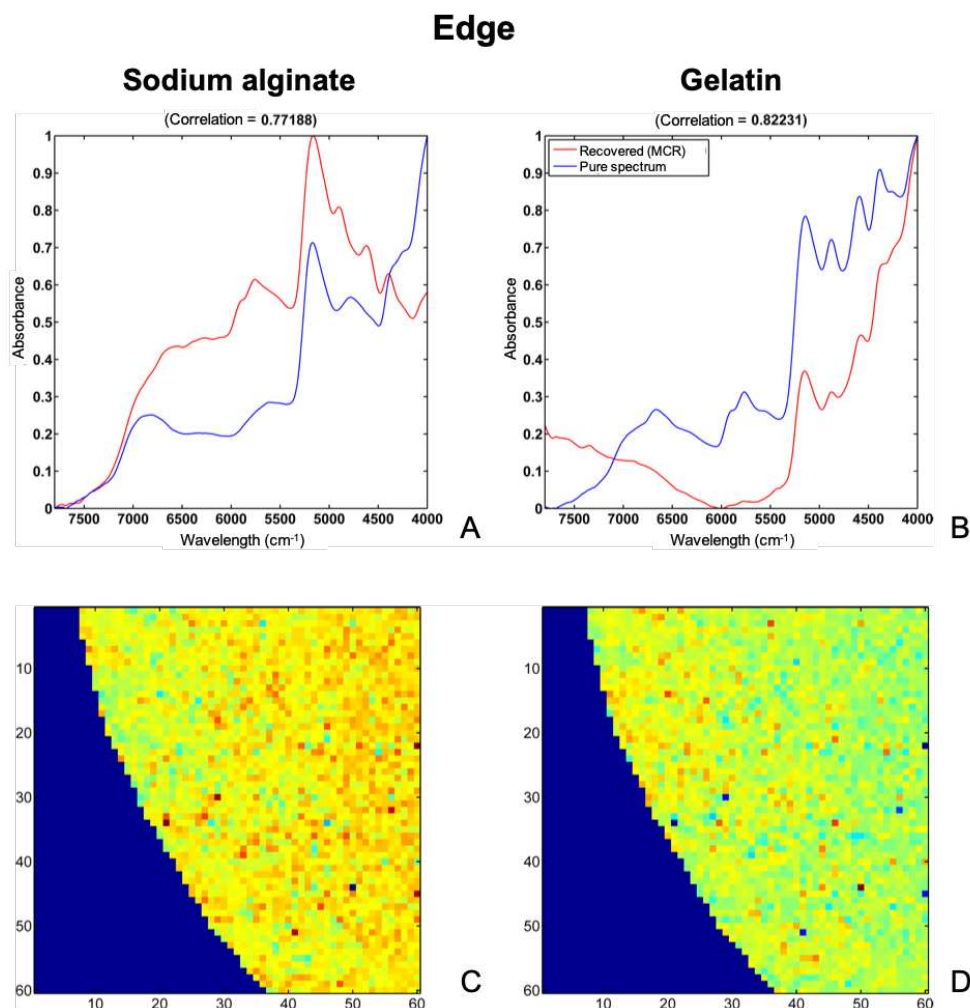
Figure 7. Comparison of the spectra of pure substances obtained experimentally (blue) and the spectra recovered by the MCR model (in red), in addition to the values of the correlation coefficients (r^2), referring to the sodium alginate-gelatin wafer edge: (A) sodium alginate, and (B) gelatin. Images of the center of the wafer, referring to (C) sodium alginate and (D) gelatin (the warm colors, red, indicate the presence of the component and the cold, blue, the absence).

The MCR model was made for two components in the central region and at the edge, with a non-negativity restriction for concentration, 0.1% error and a maximum of 100 iterations, generating the figures of merit. In the center the percentage of explained variance (% r^2) was 99.6% and the percentage of lack of adjustment (% LOF) was 5.4 x 10^{-14}. At the edges, the percentage of explained variance (% r^2) was 99.7% and the percentage of lack of adjustment (% LOF) was 1.4 x 10^{-13}.

3.3.5 Residual moisture optimization and disintegration test

After the results of experimental design, the freeze-drying protocol was improved to reduce the residual moisture of the wafers. These new wafers, formulated with sodium alginate 4 mg/mL and gelatin 10 mg/mL, were used for dissolution tests. The results were shown in Table 5.

Table 5. Disintegration time and residual moisture in wafers.

| Formulation | $CaCl_2$ | Disintegration time (min) | | Residual |
	(mg/mL)	Without mucin	With mucin	moisture (%)
WFBBL_011	-	< 23	20	11.78
WFBBL_012	0.1	40	80	9.63

The changes in the freeze-drying protocol were able to reduce the residual moisture in the wafers, from 13.04% (the lowest in the experimental design) to 11.78% (the highest after improvement). We were unable to reduce it further, perhaps because we cannot close the plates with the wafer inside the freeze dryer, so we have to open it, remove the plates, then close the wells manually, causing the wafers to collect water from the environment for a brief period.

The disintegration time measured for the wafers is suitable for use intended for local action of the drugs; however, even the longest time found would still not be sufficient for its use as dressing, as it would not allow adequate homeostasis time. The addition of $CaCl_2$ in the formulation, possibly reticulating with sodium alginate, improved the wafer disintegration time, in both mediums, leading to future studies using crosslinkers to increase the disintegration time.

With mucin, the artificial saliva became thicker, better representing the viscosity of the real saliva. For the wafer with $CaCl_2$, the disintegration time was two times the one without $CaCl_2$ showing the relevance of the physical crosslinking on wafer dissolution. There are no standardized tests for extend release buccal forms, therefore we were able to show the importance of mucin to evaluate this type of carrier.

3.3.6 X-ray diffraction characterization

X-ray diffraction was used to characterize the SAGE formulation, WFBBL formulation, and the pure drug (Figure 8). The polymeric matrix showed an expected amorphous sample pattern, with low counts per second, while lidocaine showed characteristic crystalline peaks, according to previously published data [45].
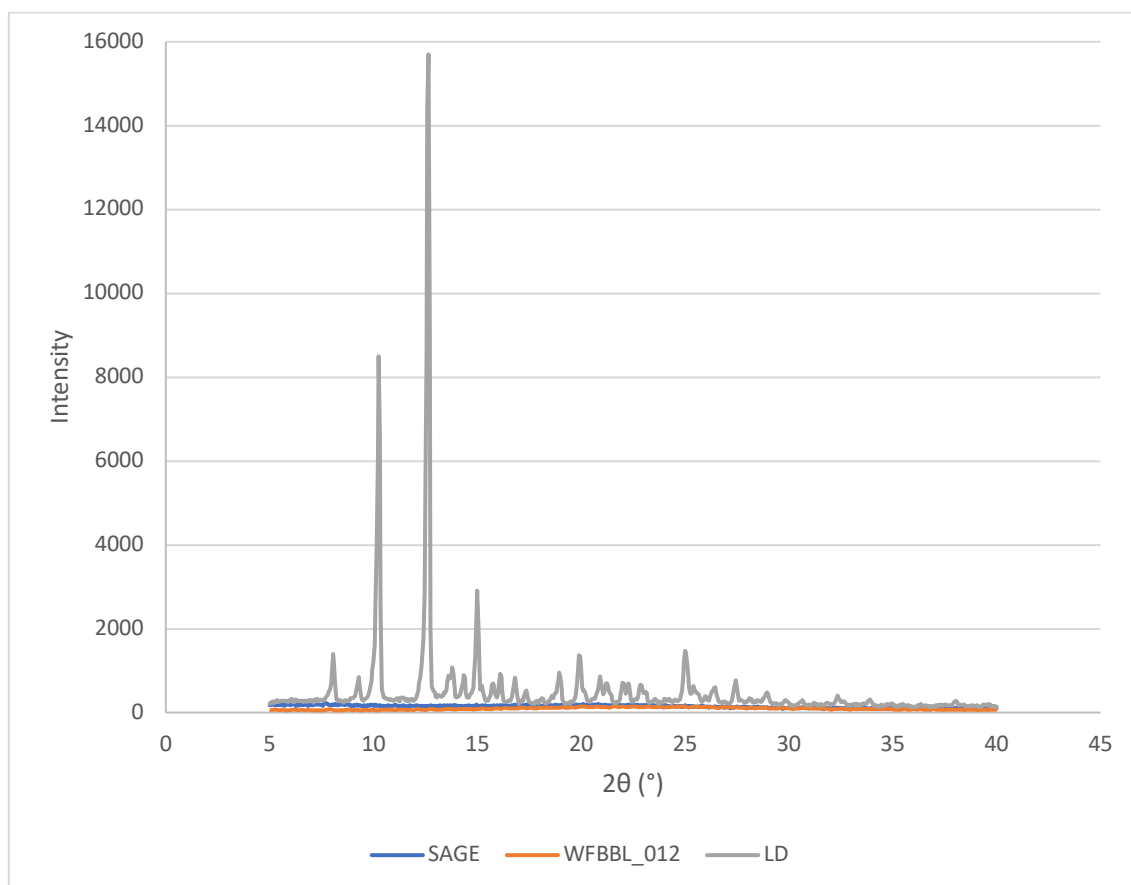
Figure 8. Graph of the X-ray diffraction analysis of the formulation of sodium alginate–gelatin wafer (SAGE), sodium alginate–gelatin–calcium chloride wafer (WFBBL_012), and lidocaine (LD).

3.3.7 Determination of drug content in wafers

UV-vis analysis was carried out to determine curcumin content in the wafer. The method was validated, and it is linear (between 20 μg/mL to 50 μg/mL of curcumin), specific, precise and reproductive, with an LOD of 1.45 μg/mL and an LOQ of 4.45 μg/mL (Sup. Table 1). Wafers produced with 200 μg/mL of curcumin, presented curcumin content of 187 μg/mL, and IE was 93.5%.

The HPLC method for lidocaine contents was linear (12 µg/mL to 380 µg/mL), with adequate correlation coefficient >0.99 (Sup. Table 2). The method was specific, without any other peaks in the same retention time (Sup. Figure 3), precise and reproductive. To determine the effect of the matrix on the quantification of lidocaine, wafers were produced with different concentrations of lidocaine hydrochloride. The values calculated for EI are shown in Table 6, and the chromatograms in Figure 9.

Table 6. Incorporation efficiency (IE) of lidocaine (LD) in alginate-gelatin wafers (SAGE).

	Theoretical LD (mg/mL)	LD content (mg/mL)	IE (%)
SAGE_02	10.0	10.2	102.0
SAGE_03	9.5	9.3	97.9
SAGE_04	15.1	15.2	100.7
SAGE_05	19.7	19.2	97.5
SAGE_06	19.7	20.2	102.5
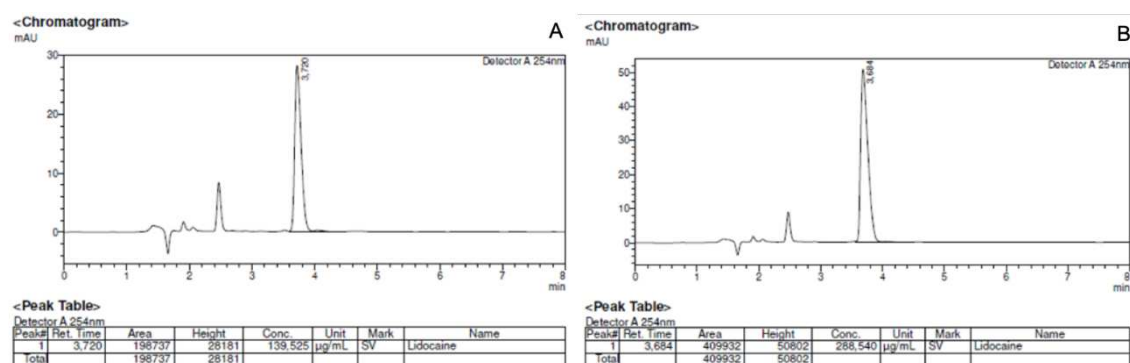
Figure 9. Chromatograms obtained from lidocaine-sodium alginate-gelatin wafers: (A) SAGE_03 and (B) SAGE_05.

3.3.8 Drug release

3.3.8.1 Curcumin

Curcumin has a very low aqueous solubility, which limits its pharmaceutical use [46,47]. Despite a good homogenization in the pharmaceutical formulation developed for visual analysis, the preliminary release test was ineffective, reaching low percentages of release (4.8% in 24 hours, Figure 10).

The use of 10% ethanol in the release medium was tested, but it maintained low percentages of release in 24 hours.

Curcumin release profile
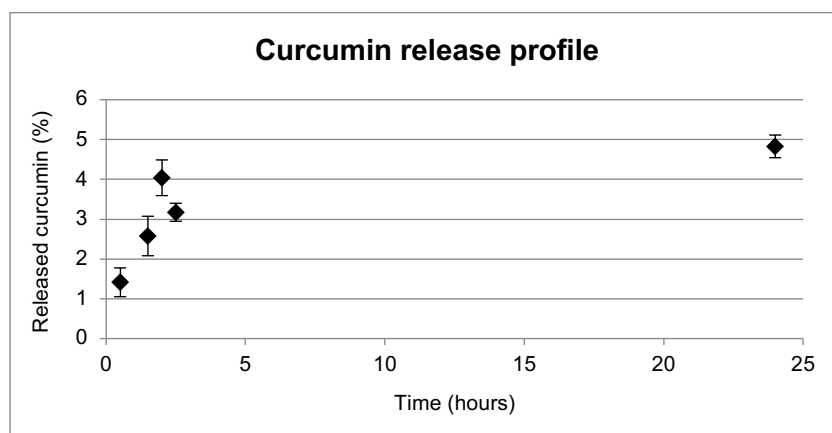
Figure 10. Release profile of curcumin loaded sodium alginate-gelatin (SAGE) wafer in artificial saliva, pH 6.8. Results showed as the average of duplicate.

3.3.8.2 Lidocaine hydrochloride

The release studies were carried out with the wafers with 10 mg/mL of LD. They were performed by two different apparatus: vertical diffusion cells and USP apparatus IV. The vertical diffusion cells were used to observe how much of the drug could overtake the mucous membrane of the mouth. The results showed that approximately 50% of the incorporated LD was released of the wafer in 15 minutes on the donor compartment (Figure 11). The released LD reached the equilibrium between both compartments in about 5 hours.
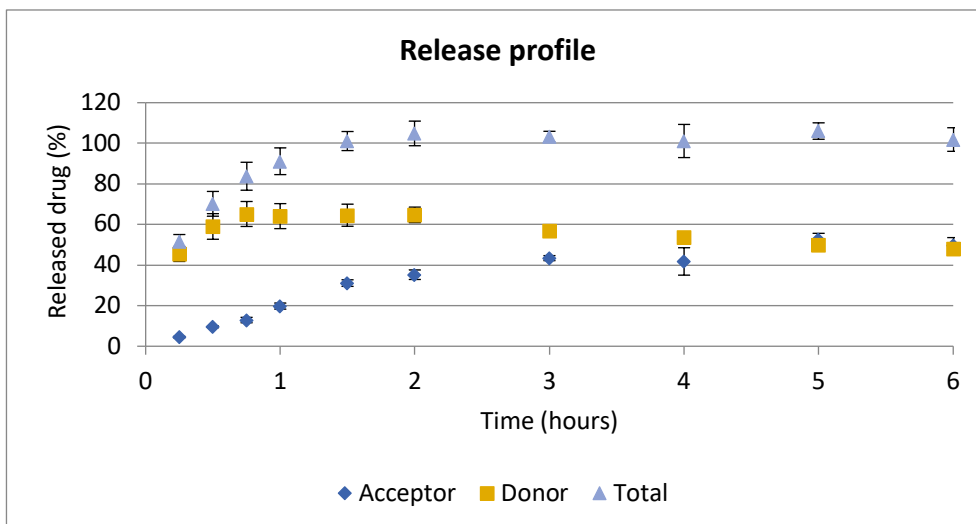
Figure 11. Release profile of lidocaine hydrochloride in phosphate buffer pH 7.2 on the acceptor compartment and artificial saliva on the donor compartment. Results showed as the average of triplicate.

Release tests with USP apparatus IV was performed using holders to fix the wafer in vertical position inside the cell. It was designed and 3-d printed two different types of holders: holder "A" (Figure 12A) has holes just in two sides, and holder "B" (Figure 12B) has holes in all directions and one "ring" to ensure that the holder stay in the exactly same place during all the test. To perform the test, the wafer was placed inside the holder, on a "bed" of glass beads (Figure 12C).
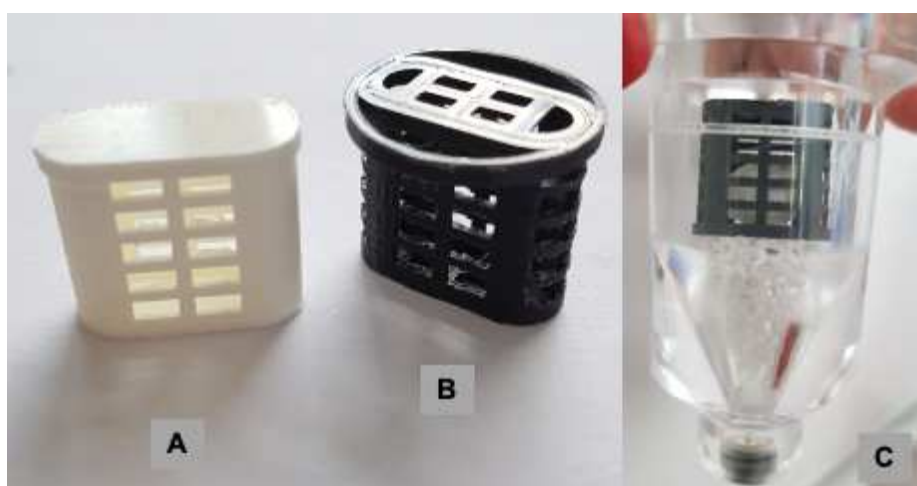
Figure 12. 3-D printed holders used for release test in USP Apparatus IV. (A) Holder A, with holes just in two sides; (B) Holder B, with holes in all directions, and the ring to ensure that the holder stay in the exactly same place during all the test (C) Cell from USP Apparatus IV with the wafer inside the holder B, on a "bed" of glass beads.

The results of the tests with the different holders clarify its influence on the release profile (Figure 13). It was possible to observe that they can impact on release profile: 50% of the wafer incorporated LD was released in 2 hours with holder A and in 30 minutes with holder B. The test with the holder A showed a delayed release of LD, compared to the test with holder B, probably because it does not allow a sink condition for the wafer in the medium.
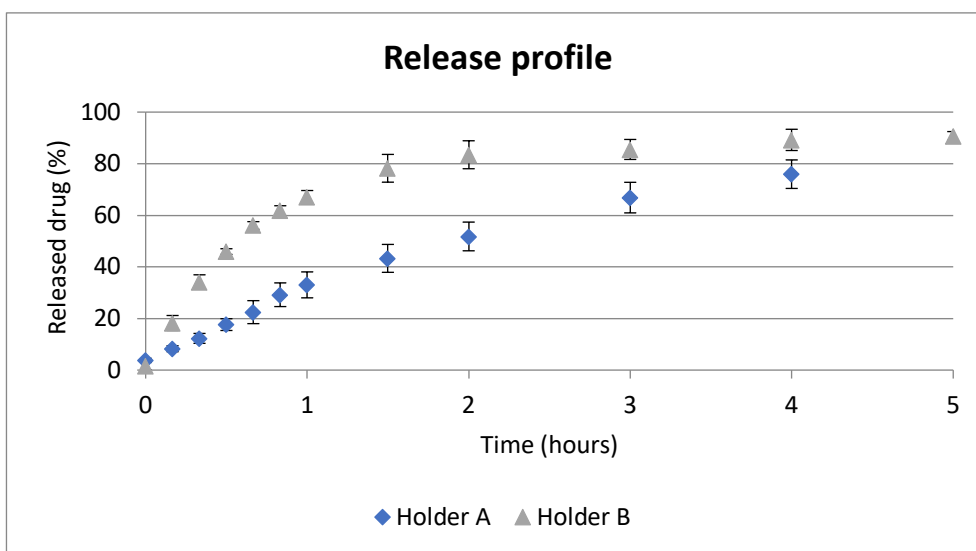

Figure 13. Release profile of lidocaine hydrochloride in artificial saliva medium pH 6.8, using two different types of holders: holder A, with holes just in two sides, and holder B, with holes in all directions, and the ring to ensure that the holder stay in the exactly same place during all the test. Results showed as the average of quadruplicate.

3.3.8.2.1 Bilayer wafers

The bilayer wafers were produced to observe if it is possible to obtain a unidirectional drug release, directed to the buccal mucosa.

The first release tests were performed in USP apparatus IV, to compare the release profile with the uncoated wafer. The dissolution studies were performed with the holder B, since it was determined that is the best option. The three different wafers (uncoated, bilayer by casting method and bilayer by spraying method wafers) were tested in the same conditions (Figure 14).
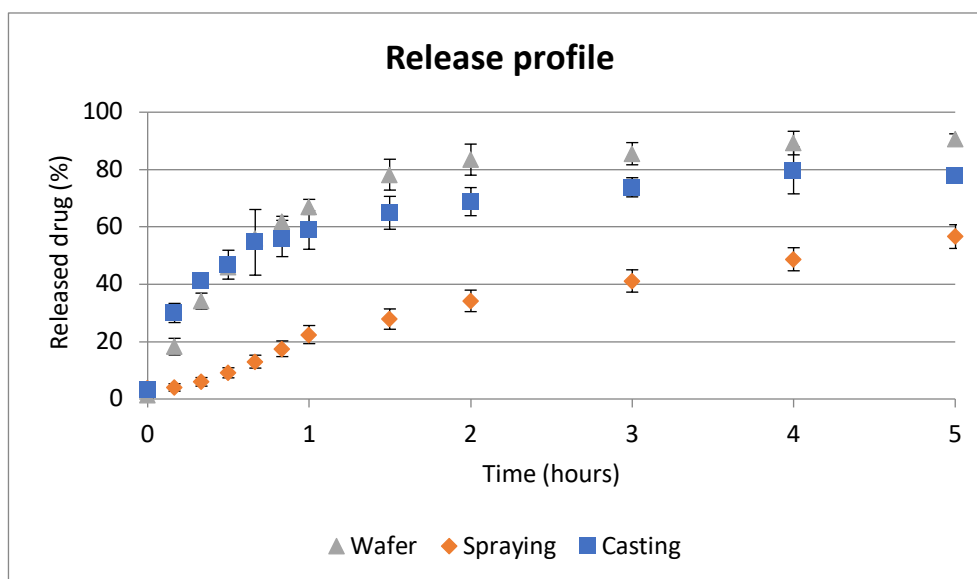
Figure 14. Release profile of lidocaine hydrochloride in artificial saliva medium pH 6.8, in three different batches of wafers. "Wafer" was produced by freeze-drying the gel solution; "Spraying" was produced by spraying an ethanolic ethyl cellulose solution on the freeze-dried wafer; "Casting" was produced by casting an ethyl cellulose film prior to freeze-drying, overlaying it with the gel solution and freeze-drying it. Results showed as the average of quadruplicate.

The bilayer wafers produced by casting method showed a similar release profile to uncoated wafer. The release in total is slower compared to the uncoated wafer, but in the USP apparatus IV experiments we could not detect a directed drug release.

In contrast, the spraying procedure led to a sustained release, but it was not suitable for this purpose since the ethyl cellulose solution penetrated the lyophilized product and did not form a real layer.

3.3.9 Minimum inhibitory concentration (MIC)

Minimum inhibitory concentration (MIC) experiments was conducted in order to explore the antimicrobial activity of lidocaine. The results are in Table 7.

Table 7. Lidocaine and curcumin minimal inhibitory concentration (MIC, mg/mL) against oral bacterial strains.

Strain	Lidocaine MIC (mg/mL)	Curcumin MIC (mg/mL)
S. sanguinis 3K36	20	0.250
S. mitis NCTC 12261	20	0.125
S. oralis ATCC 10557	20	> 0.500
S. salivarius ATCC 7073	10	> 0.500
S. gordonii Chali	20	0.500
P. gingivalis ATCC 33277	2.5	0.125
P. gingivalis W83	5	0.250

A previous study presented a lower lidocaine MIC against *S. sanguinis*, *S. mitis* and *S. oralis* (4.4, 4.8 and 4.8 respectively), but a MIC of 6.0 against *S. salivarius*, which is similar of what we found (less than 1-fold lower), and a MIC of 4 mg/mL against 8 different strains of *P. gingivalis*, with agree with that we found (2.5 and 5 mg/mL) [48].

These results show that a formulation with 20 mg/mL of lidocaine would be able to inhibit the growth of the studied bacteria, and a formulation with 10 mg/mL would still be able to inhibit the proliferation of the *S. salivarius* ATCC 7073, and mainly the strains of *P. gingivalis* ATCC 33277 and W83.

Kumbar et al. used a curcumin extract that had purity of ≥ 95% of curcuminoids, and found a curcumin MIC of 62.5 µg/mL against *P. gingivalis* ATCC 33277, which is one-fold less than that we found, and a minimum bactericidal concentration (MBC) of 125 µg/mL against the same strain. MBC is described as the minimum concentration, where 99.9% of the viable organisms get killed for a limited period relative to the starting inoculum [49]. Another study found a MIC of 15 µg/mL, but there is no information about curcumin origin and its purity; they also analyzed the biofilm formation, conducted with a confocal laser-scanning microscope (CLSM), showing that curcumin suppressed *P. gingivalis* homotypic and *P. gingivalis–S. gordonii* heterotypic biofilm formation in

a dose-dependent manner: a concentration of 20 µg/mL curcumin inhibited *P. gingivalis* biofilm formations by >80% [50].

Formulations with curcumin 200 µg/mL would be able to inhibit the growth of *S. mitis* NCTC 12261 and *P. gingivalis* ATCC 33277. If curcumin complexed with cyclodextrins can be incorporate in wafers, it is possible that we can increase the curcumin concentration, leading to a formulation with antimicrobial properties in a greater number of oral bacteria.

Future studies will be carried out with the two drugs incorporated in the buccal wafers, to verify if the antibacterial activity is maintained.

3.4 CONCLUSION

It was possible to produce wafers with a straight surface, easy to remove from the mold, without visual collapse and of uniform height between the units produced. The wafers disintegration was satisfactory to the buccal application. Electronic microscopy images exhibited high porosity, which allowed the loading of a good amount of drug in the wafer.

HPLC method was validated and suitable to determine lidocaine content in the wafer, as UV/Vis was for total curcumin content. The MIC results showed that lidocaine and curcumin have antimicrobial activity against some common oral bacteria strains in anesthetic concentrations. Future studies will confirm the antibacterial activity of the drugs incorporated in wafers. However, *in vitro* tests showed no relevant release for curcumin and ongoing studies are evaluating complexation of curcumin to cyclodextrins, such as hydroxypropyl-β-cyclodextrin or sulfobutylether-β-cyclodextrin, for further incorporation in the wafer matrix and consequent enhanced release.

There is no compendial test for wafers dissolution/ drug release, leading us to test two methods. The test in vertical diffusion cells showed 50% of lidocaine release in 15 minutes, and the same occur in USP apparatus IV with the use of an appropriate wafer holder. The use of holders for the USP apparatus IV dissolution tests is recommended and need to be holders that do not disrupt the pharmacodynamic, as the holder B. Noteworthy, disintegration time was enhanced by mucin in the medium, which may also change release behavior if present. This was the first study to address dissolution and disintegration challenges for these dosage form.

Concerning wafers with a back layer, it was possible to observe that the spraying procedure was not suitable for forming a bilayer wafer since the ethyl cellulose solution penetrated the lyophilized product. The bilayer wafers produced by casting method showed a slower release compared to the uncoated wafer, but the dissolution tests in USP apparatus IV could not detect a directed drug release of the bilayer wafer.

3.5 REFERENCES

1.   Mohanty, C. & Sahoo, S. K. Curcumin and its topical formulations for wound healing applications. *Drug Discov. Today* **22**, 1582–1592 (2017).

2.   Health (UK), N. C. C. for W. and C. Appendix C - Wound dressings for surgical site infection prevention. in *Surgical Site Infection: Prevention and Treatment of Surgical Site Infection.* (RCOG Press, 2008).

3.   Kumar, K. R. A., Kumar, J., Sarvagna, J., Gadde, P. & Chikkaboriah, S. Hemostasis and Post-operative Care of Oral Surgical Wounds by Hemcon Dental Dressing in Patients on Oral Anticoagulant Therapy: A Split Mouth Randomized Controlled Clinical Trial. *J Clin Diagn Res* **10**, ZC37–ZC40 (2016).

4.   Boateng, J. S., Matthews, K. H., Stevens, H. N. E. & Eccleston, G. M. Wound healing dressings and drug delivery systems: A review. *J Pharm Sci* **97**, 2892–2923 (2008).

5.   FDA (U. S. Food & Drug Administration). Drug Approval Package: Lidoderm (Lidocaine) NDA# 20-612. (1999).

6.   Johnson, S. M., Saint John, B. E. & Dine, A. P. Local anesthetics as antimicrobial agents: a review. *Surg Infect (Larchmt)* **9**, 205–213 (2008).

7.   Hewlings, S. J. & Kalman, D. S. Curcumin: A Review of Its' Effects on Human Health. *Foods* **6**, (2017).

8.   Shailendiran, D. *et al.* Characterization and Antimicrobial Activity of Nanocurcumin and Curcumin. in *2011 International Conference on Nanoscience, Technology and Societal Implications* 1–7 (IEEE, 2011). doi:10.1109/NSTSI.2011.6111984.

9.   Gunes, H. *et al.* Antibacterial effects of curcumin: An in vitro minimum inhibitory concentration study. *Toxicol Ind Health* **32**, 246–250 (2016).

10.   USP Monographs: Lidocaine. in *United States Pharmacopeia National Formulary USP29-NF24* (2007).

11.   CLSI. *Methods for Antimicrobial Susceptibility Testing of Anaerobic Bacteria; Approved Standard—Seventh Edition; CLSI document M11-A7*. vol. 27 (Clinical and Laboratory Standard Institute, 2007).

12.   Russo, E. *et al.* A focus on mucoadhesive polymers and their application in buccal dosage forms. *J Drug Deliv Sci Technol* **32**, 113–125 (2016).

13.   Ayensu, I., Mitchell, J. C. & Boateng, J. S. Development and physico-

mechanical characterisation of lyophilised chitosan wafers as potential protein drug delivery systems via the buccal mucosa. *Colloids Surf B Biointerfaces* **91**, 258–265 (2012).

14. Menchicchi, B. *et al.* Structure of chitosan determines its interactions with mucin. *Biomacromolecules* **15**, 3550–3558 (2014).

15. Bogataj, M. *et al.* The correlation between zeta potential and mucoadhesion strenght on pig vesical mucosa. *Biological and Pharmaceutical Bulletin* **26**, 743–746 (2003).

16. Abraham, S. *et al.* 1-(3-(6,7-dimethoxyquinazolin-4-yloxy)phenyl)-3-(5-(1,1,1-trifluoro-2-methylpropan-2-yl)isoxazol-3-yl)urea as raf kinase modulator in the treatment of cancer diseases. (2009).

17. Li, M. H. C. Oral film containing enteric release opiate resinate. (2013).

18. Chen, L. *et al.* Compositions and methods for mucosal delivery. (2003).

19. Li, M. Oral film containing opiate enteric-release beads. (2015).

20. Lance, K. D., Desai, T. A., Steedman, M. R., Bhisitkul, R. B. & Bernards, D. A. Multilayer thin film drug delivery device and methods of making and using the same. (2014).

21. Lee, J., Seo, M., Choi, I., Kim, J. & Pai, C. Locally administrable, biodegradable and sustained-release pharmaceutical composition for periodontitis and process for preparation thereof. (1997).

22. Reddy, D., Pillay, V., Choonara, V. & Adeleke, O. A. A transmucosal delivery system. (2011).

23. Dulieu, C., Durfee, S., Holl, R. & Nguyên, T. Lyophilized pharmaceutical compositions and methods of making and using same. (2008).

24. Lerner, E. I., Rosenberger, V. & Flashner, M. Tannic acid-polymer compositions for controlled release of pharmaceutical agents, particularly in the oral cavity. (2009).

25. Goldberg, M. N., Alonso, M. J. & Chen, K. Targeted buccal delivery of agents. (2014).

26. Lerner, E. I., Rosenberger, V. & Flashner, M. Pharmaceutical oral patch for controlled release of pharmaceutical agents in the oral cavity. (2001).

27. Bromberg, L. & Friden, P. Composite wafer for controlled drug delivery. (2002).

28. Glen Patrick Quadrant Drug Delivery Ltd. MARTYN & David John St.

Coghlan. Composition for delivery of an active agent. (2007).

29. Tester, R. & Qi, X. Chemical carrier based on a beta-limit dextrin. (2004).

30. Ellis-Behnke, R. *et al.* Compositions and methods for promoting hemostasis and other physiological activities. (2011).

31. Boateng, J., Burgos-Amador, R., Okeke, O. & Pawar, H. Composite alginate and gelatin based bio-polymeric wafers containing silver sulfadiazine for wound healing. *International Journal of Biological Macromolecules* **79**, 63–71 (2015).

32. Boateng, J. S. & Areago, D. Composite Sodium Alginate and Chitosan Based Wafers for Buccal Delivery of Macromolecules. *Austin J Anal Pharm Chem* **1**, 1022 (2014).

33. Shojaei, A. H. Buccal mucosa as a route for systemic drug delivery: a review. *J Pharm Pharm Sci* **1**, 15–30 (1998).

34. Van Roey, J., Haxaire, M., Kamya, M., Lwanga, I. & Katabira, E. Comparative efficacy of topical therapy with a slow-release mucoadhesive buccal tablet containing miconazole nitrate versus systemic therapy with ketoconazole in HIV-positive patients with oropharyngeal candidiasis. *J. Acquir. Immune Defic. Syndr.* **35**, 144–150 (2004).

35. Yang, Z. *et al.* Application of in vitro transmucosal permeability, dose number, and maximum absorbable dose for biopharmaceutics assessment during early drug development for intraoral delivery. *Int J Pharm* **503**, 78–89 (2016).

36. Carneiro-da-Cunha, M. G., Cerqueira, M. A., Souza, B. W. S., Teixeira, J. A. & Vicente, A. A. Influence of concentration, ionic strength and pH on zeta potential and mean hydrodynamic diameter of edible polysaccharide solutions envisaged for multinanolayered films production. *Carbohydr Polym* **85**, 522–528 (2011).

37. Chang, S.-H., Lin, H.-T. V., Wu, G.-J. & Tsai, G. J. pH Effects on solubility, zeta potential, and correlation between antibacterial activity and molecular weight of chitosan. *Carbohydr Polym* **134**, 74–81 (2015).

38. Pezzini, B. R., Silva, M. A. S. & Ferraz, H. G. Formas farmacêuticas sólidas orais de liberação prolongada: sistemas monolíticos e multiparticulados. *Revista Brasileira de Ciências Farmacêuticas* **43**, 491–502 (2007).

39. Lahoud, M. H. & Campos, R. Aspectos teóricos relacionados à reologia

farmacêutica. *Visão Acadêmica* **11**, (2010).

40.   Aulton, M. E. *Aulton Delineamento de Formas Farmacêuticas*. (Elsevier Brasil, 2016).

41.   Costa, J. S. R., de Oliveira Cruvinel, K. & Oliveira-Nascimento, L. A mini-review on drug delivery through wafer technology: Formulation and manufacturing of buccal and oral lyophilizates. *Journal of Advanced Research* **20**, 33–41 (2019).

42.   Bogner, R. Factors that influence product resistance and methods to measure product resistance. (2020).

43.   Empower pharmacy. Freeze drying (lyophilization). https://empower.pharmacy/freeze-drying-lyophilization.html.

44.   Da-Col, J. A., Dantas, W. F. C. & Poppi, R. J. Experimento didático de quimiometria para o mapeamento de pellets farmacêuticos utilizando espectroscopia de imagem na região do infravermelho próximo e resolução multivariada de curvas com mínimos quadrados alternantes: Um tutorial, parte IV. *Química Nova* **41**, 345–354 (2018).

45.   Magaña-Vergara, N. *et al.* Mechanochemical Synthesis and Crystal Structure of the Lidocaine-Phloroglucinol Hydrate 1:1:1 Complex. *Crystals* **8**, 130 (2018).

46.   Curcumin - DrugBank. https://www.drugbank.ca/drugs/DB11672.

47.   Baglole, K. N., Boland, P. G. & Wagner, B. D. Fluorescence enhancement of curcumin upon inclusion into parent and modified cyclodextrins. *Journal of Photochemistry and Photobiology A: Chemistry* **173**, 230–237 (2005).

48.   Pelz, K., Wiedmann-Al-Ahmad, M., Bogdan, C. & Otten, J.-E. Analysis of the antimicrobial activity of local anaesthetics used for dental analgesia. *J Med Microbiol* **57**, 88–94 (2008).

49.   Kumbar, V. M. *et al.* Effect of curcumin on growth, biofilm formation and virulence factor gene expression of Porphyromonas gingivalis. *Odontology* (2020) doi:10.1007/s10266-020-00514-y.

50.   Izui, S. *et al.* Antibacterial Activity of Curcumin Against Periodontopathic Bacteria. *Journal of Periodontology* **87**, 83–90 (2016).

51.   Brasil. ANVISA, I. Resolution RDC Nº 166. (2017).

52.   Abraham, J. International Conference On Harmonisation Of Technical Requirements For Registration Of Pharmaceuticals For Human Use. in

Handbook of Transnational Economic Governance Regimes (eds. Brouder, A. & Tietje, C.) 1041–1054 (Brill, 2009). doi:10.1163/ej.9789004163300.i-1081.897.

53.   ICH. Validation of analytical procedures: text and methodology Q2 (R1). (2005).

3.6   SUPPLEMENTARY FILES

3.6.1   Differential scanning calorimetry
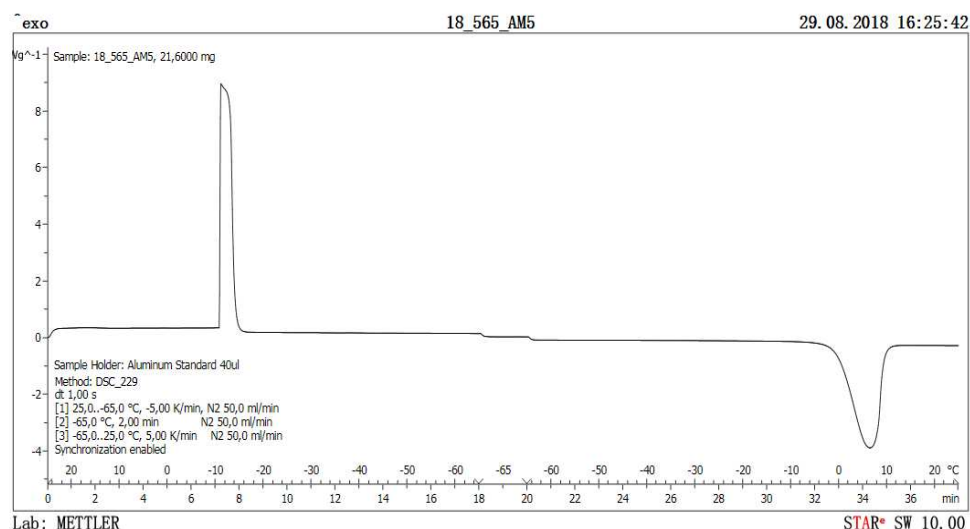
Sup. Figure 1. DSC result referring to the central point of the design (experiment 5). The conditions of the experiment are described in the figure and the blank was automatically discounted.

3.6.2   Drug content methods validation

The validation of the analytical method was performed as described in the guideline from *Agência Nacional de Vigilância Sanitária* (Brazilian Health Regulatory Agency) [51] and the International Conference on the Harmonization of Technical Requirements for the Human Use [52] were used in order to direct the validation of the method.

3.6.2.1   Specificity

Specificity was assessed to ensure that the method has the ability to measure exactly the compound of interest when others are present (for example, impurities, degradation products and matrix components) [51,53]. The mobile phase was used as a dispersant in the determination of lidocaine in wafer, to evaluate the specificity of the analytical method.

3.6.2.2   Linearity

The linearity of the method was determined in order to demonstrate that the results obtained were proportional to the concentration of the analyte in

the sample, within the specified interval. Different concentrations, carried out in triplicate and in three days, were used for the construction of the analytical curve, and the linear regression calculation was performed using the least squares method [51,53].

3.6.2.3   Precision

The precision, expressed by Sup. Equation 1, assesses the proximity of the results generated in several experiments of a multiple sampling of the same sample.

$$CV = \frac{SD}{DMC} * 100 \qquad \text{Sup. Equation 1}$$

The precision of an analytical method can be expressed as a standard deviation (coefficient of variation, CV) of various measures, where SD is the standard deviation and DMC, the determined mean concentration. Values greater than 5% are not allowed, which must be defined according to the methodology used, with the concentration of the analyte in the sample, with the type of matrix and the purpose of the method.

The agreement between the results within a short period of time with the same analyst and the same instrumentation is known as repeatability (or intra-run precision), whereas the agreement between the results of the same laboratory, but obtained on different days, is referred to as intermediate (or inter-run) precision [51].

3.6.2.4   Accuracy

The proximity of the results obtained by the method under study to the true value defines the accuracy of an analytical method. After establishing the linearity and specificity of the analytical method, its accuracy is determined from at least nine determinations, considering the linear range of the procedure, that is, three concentrations: low, medium and high, with three replicates of each. Accuracy (A) was obtained using Sup. Equation 2, which relates the average concentration determined experimentally and the theoretical concentration [51],

$$A = \frac{DAC}{TC} * 100 \qquad \text{Sup. Equation 2}$$

where, TC is the theoretical concentration and DAC is the determined average concentration.

3.6.2.5 Interval

The range between the limits of quantification used in the construction of the analytical curve is called the interval; this is derived from the linearity assessment, being dependent on the desired application [51,53]. The specified range was determined by confirming that the method has adequate accuracy, precision and linearity.

3.6.2.6 Detection and quantification limits

The detection limit (DL) refers to the smallest amount of the analyte in a sample that can be detected, but not necessarily quantified, under the established experimental conditions. By analyzing solutions of known and decreasing concentrations of the analyte, down to the lowest detectable level, the detection limit can be measured.

The limit of quantification (QL) is the smallest amount of the analyte in a sample to be determined with allowable precision and accuracy under the experimental conditions already determined.

In the case of instrumental methods (HPLC, CG, atomic absorption), the DL estimate can be made based on the ratio of 3 times the baseline noise. For the QL, the baseline noise is determined and the concentration that produces a signal-to-noise ratio greater than 10: 1 [53] is considered as the limit of quantification.

3.6.3 Validation of curcumin content

Method validation was performed, the wavelength used was 430 nm, confirmed by the scanning spectrum of the curcumin dissolved in 50% ethanol (Sup. Figure 2).
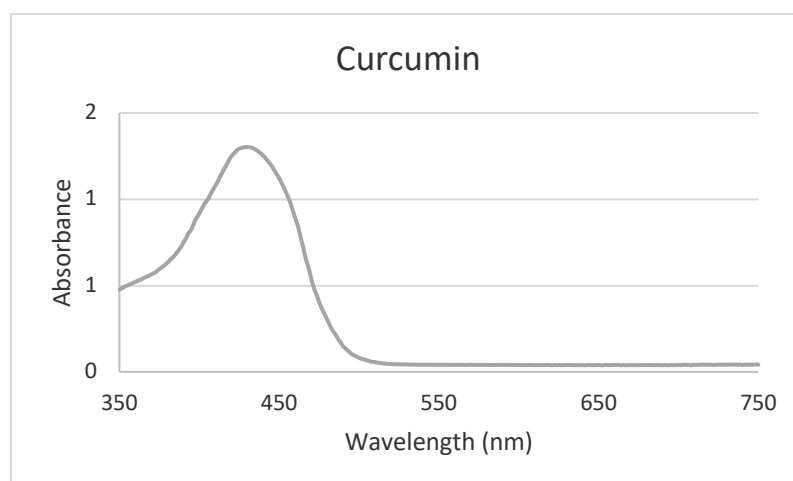
Sup. Figure 2. Scanning spectrum of curcumin, dissolved in ethanol 50%.

3.6.3.1   Linearity, limits of detection (LOD) and quantification (LOQ)

Curcumin solutions were prepared in ethanol 50%, containing between 20 µg/mL to 50 µg/mL of curcumin. The correlation coefficients (R^2) were > 0.99, according to the recommendations of RE 899 of ANVISA [51] (Sup. Table 1).

Sup. Table 1. Linearity, limit of detection (LOD) and limit of quantitation (LOQ) for curcumin.

Linear equation	y = 0.0344x – 0.1441
R^2	0.999
Range (µg/mL)	20 – 50
LOD (µg/mL)	1.47
LOQ (µg/mL)	4.45

3.6.3.1 Precision

The data are presented in Sup. Table 2, showing CV values below 5%, and accuracy results according to ANVISA's determination (between 95% and 105%).

Sup. Table 2. Results of the precision analysis (mean and standard deviation (SD) of triplicate), and accuracy for lidocaine.

Lidocaine (µg/mL)	Intraday		Interday		Accuracy (%)
	Mean ± SD (µg/mL)	CV (%)	Mean ± SD (µg/mL)	CV (%)	
50	53.09 ± 0.03	0.03	49.87 ± 0.01	0.20	99.7
40	41.66 ± 0.08	0.08	40.44 ± 0.04	0.10	101.1
20	20.60 ± 0.44	0.44	20.37 ± 0.01	0.07	101.6

3.6.4 Validation of lidocaine content

3.6.4.1 Specificity

Sup. Figure 3 shows the chromatogram of a standard lidocaine sample, the peak can be visualized in a retention time of 3.8 minutes. No other peaks were observed at the same retention time when samples of biopolymeric wafer without lidocaine were evaluated under the same conditions of chromatographic analysis, as well as impurities of the components were not observed, thus demonstrating specificity in the established technique.

Sup. Figure 3. HPLC chromatogram of (A) lidocaine (48 µg/mL), and (B) wafer sample (sodium alginate and gelatin) without lidocaine, showing that there are no peaks in the retention time of 3.8 minutes.

3.6.4.2   Linearity, limits of detection (LOD) and quantification (LOQ)

Lidocaine solutions were prepared containing between 12 µg/mL to 380 µg/mL of lidocaine. The correlation coefficients (R^2) were > 0.99, according to the recommendations of RE 899 of ANVISA [51] (Sup. Table 3).

Sup. Table 3. Linearity, limit of detection (LOD) and limit of quantitation (LOQ) for lidocaine.

Linear equation	y = 1417.27x – 992.198
R^2	0.9999
Range (µg/mL)	12 – 384
LOD (µg/mL)	2.18
LOQ (µg/mL)	6.61

3.6.4.3   Precision

The data are presented in Sup. Table 4, showing CV values below 5%, and accuracy results according to ANVISA's determination (between 95% and 105%).
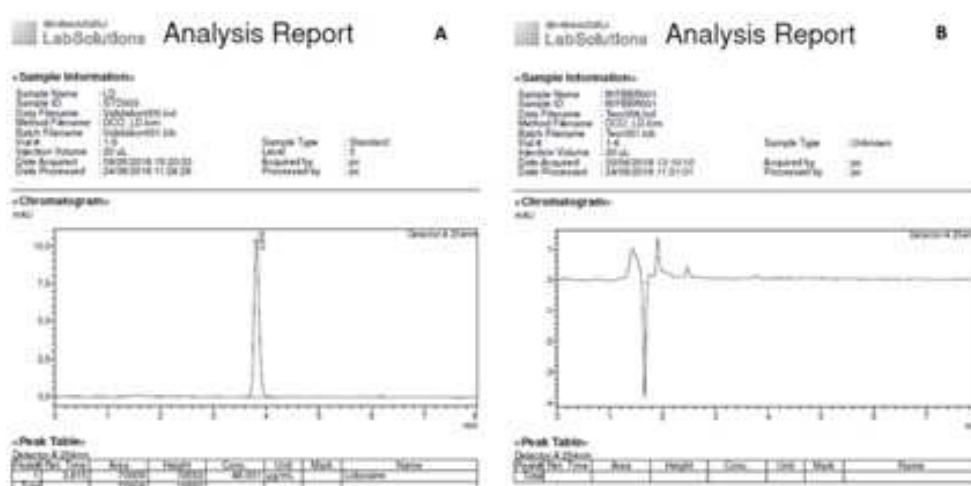
Sup. Table 4. Results of the precision analysis (mean and standard deviation (SD) of triplicate), and accuracy for lidocaine.

Lidocaine (µg/mL)	Intraday		Interday		Accuracy (%)
	Mean ± SD (µg/mL)	CV (%)	Mean ± SD (µg/mL)	CV (%)	
384	289.4 ± 2.01	0.51	390.61 ± 1.12	0.29	102.3
96	96.86 ± 1.70	1.75	98.38 ± 0.89	0.91	102.4
12	11.81 ± 0.54	4.61	11.68 ± 0.24	2.09	98.2

4 COMPLEXATION OF CURCUMIN EXTRACT WITH CYCLODEXTRINS AND THEIR EFFECT ON CURCUMINOID DISTRIBUTION AND ANTIMICROBIAL ACTIVITY

Complexation of curcumin extract with cyclodextrins and their effect on curcuminoid distribution and antimicrobial activity

Juliana Souza Ribeiro Costa, Danilo Costa Geraldes, Jeany Delafiori, Rodrigo Ramos Catharino, Daniel Fábio Kawano, Karina Cogo Muller, Laura Oliveira-Nascimento

Faculty of Pharmaceutical Sciences, University of Campinas, Campinas, Brazil.

ABSTRACT

Curcuma longa L. extract is widely used in oriental medicine due to its anti-inflammatory and antimicrobial activity. It is composed by three main curcuminoids: curcumin, demethoxycurcumin and bisdemethoxycurcumin, each one with different concentrations and characteristics, like molecular weight and water solubility. This work aimed to formulate curcumin-cyclodextrin complexes to improve its solubility and evaluate the impact of the process on curcuminoids distribution and a curcumin biological activity. Complexes with hydroxypropyl-beta-cyclodextrin and sulfobutylether-beta-cyclodextrin were analyzed by several physical-chemical methods and a HPLC method was used to determine each curcuminoid content. Mass spectroscopy confirmed the presence of the three curcuminoids in the extract. Nanocomplexes formation was confirmed by differential scanning calorimetry, but they did not modify the pattern of curcuminoids distribution. Between the two cyclodextrins tested, sulfobutylether-beta-cyclodextrin showed slightly greater capacity to increase the curcuminoids solubility in molar terms. Among the tested bacteria, nanocomplexes showed better antimicrobial activity against *K. pneumoniae* ATCC 700603. The studied complexes were successfully freeze dried and can be resuspended for further *in vivo* studies aiming antimicrobial action for pulmonary delivery, or incorporated in a pharmaceutical form, like freeze-dried wafers, for buccal infections treatment.

Keywords: curcumin, cyclodextrin, complexation, solubility, antimicrobial.

4.1   INTRODUCTION

Curcumin is the major curcuminoid component of turmeric (*Curcuma longa L*). It has been used in traditional medicine on the southeast Asian as an antimicrobial and anti-inflammatory [1,2]. Commercially available curcumin used for research and for clinical trials contains approximately 77% pure curcumin (CUR), 17% demethoxycurcumin (DMC) and 3% bisdemethoxycurcumin (BDC).

The anti-inflammatory effect observed in studies was due to multiple actions. The main action of curcumin reported is the modulation of NF-kB, with consequent inhibition of pro-inflammatory cytokines [3]. The different curcuminoids differ in anti-inflammatory activity: CUR is more effective suppressing TNF-induced NF-kB activation, followed by DMC and BDC, suggesting that the phenyl methoxyl groups do contribute to the suppression of NF-kB activation, also may be connected with their antioxidant potential, but there is a synergy between the components, the mixture is more active than CUR alone [4,5].

In addition to inhibiting NF-kB signaling in macrophages and lung cells *in vitro*, including decreased secretion of IL-6, curcumin was able to inactivate, block adsorption and inhibit influenza virus proliferation *in vitro*, decreasing the severity and mortality of influenza pneumonia in animals [6,7], as well as attenuating CAP/ ARDS caused by reovirus, inhibiting post-infection pulmonary fibrosis [8]. Curcumin also inhibits in vitro infection of SARS-CoV [9], and possibly SARS-CoV-2, according to in silico studies [10,11]. Drug repositioning studies are essential for rapid action and promising. In view of what is known today about SARS-CoV-2, it is desirable to use antithrombotic substances [12], which reduce pulmonary inflammation, have antiviral properties and have evaluated clinical safety, such as curcumin.

Previous studies have shown that the nanocurcumin formulation has demonstrated comparable or better in vitro antimicrobial efficacy compared to the curcumin solution in DMSO. Antibacterial activity was more pronounced against Gram-positive than Gram-negative bacteria. In vitro biological tests have clearly demonstrated that the transformation to the nanometric form significantly improves water solubility and the effectiveness of curcumin as an antimicrobial agent [13,14].

Curcumin antibacterial and anti-inflammatory activities are interesting to buccal application. Curcumin was successfully incorporated into oral wafers in a previous study (Item 3), but it was not possible to verify its release in aqueous media, which can hinder its action. Taking this into account, we believe that the formation of curcumin-cyclodextrin nanocomplexes will be able to improve or at least maintain curcumin's antimicrobial activity.

As stated above, the three compounds affect some important biological activities in a different manner, showing the importance of knowing the real quantity of each curcuminoid in the extract. In this paper we intended to enhance the curcumin water solubility by complexation with cyclodextrins, evaluating the affinity of cyclodextrins with each curcuminoid.

4.2 METHODS

4.2.1 **Materials**

Curcumin C3 complex (CC) was obtained by Infinity pharma (USA), containing 99.99% of total curcuminoids. Sulfobutyl-β-cyclodextrin (SBE-β-CD) was a gift of Cyclolab (Hungary). Hydroxypropyl-β-cyclodextrin (HP-β-CD), glacial acetic acid, acetonitrile, methanol and all other chemicals were purchased Sigma-Aldrich.

4.2.2 **Drug content**

The analytical methodology by HPLC for curcuminoids quantification was applied according to Wichitnithad et al. [15], with modifications, aiming to obtain a symmetrical peak and within the required standards. The analytical curve was constructed by taking increasing concentrations of total curcuminoids between 6 and 100 μg/mL. Table 1 shows the HPLC conditions.

Table 1. Chromatographic conditions for quantification of curcuminoids.

Sample dilution	Mobile phase
Mobile phase	Glacial acetic acid 2% in water and acetonitrile (3:2, v/v)
Injection volume	10 μL
Run time	16 minutes
Flow	2.0 mL/min
Detector	425 nm
Column	C18 – 250 mm x 4.6 mm x 5 μm (L1)

4.2.3 **Mass spectrometry**

5 mg of CC was dissolved in 1mL of Methanol: H_2O (1: 1). After homogenization by sonication for 5 min at room temperature, 2 μL of this solution was dissolved in 998 μL of Methanol: H_2O (1: 1). To the final solution, 1 μL of formic acid was added and directly infused in an ESI-LTQ-XL Discovery mass spectrometer (Thermo Scientific, Bremen, Germany) for analysis in the positive mode. At first, spectral data in the range of 50-1000 m/z were obtained for the evaluation of major signals using a flow of 10 μL.min^{-1}, capillary temperature at

280 °C, spray current at 5 kV, and carrier gas at 5 arbitrary units. Based on the information available in the literature on the main curcuminoids and with the aid of metabolomics databases such as METLIN (Scripps Center for Metabolomics, La Jolla, CA), three m/z values were selected for structural elucidation by mass spectrometry sequential (Tandem MSn). The experimental fragmentation of the selected m/z was performed using Helium, as collision gas, and collision energy (CID) in the range of 20 to 30 eV. The fragments obtained experimentally were compared with the theoretical fragmentation of the proposed molecules using the Mass Frontier software [16].

4.2.4   In silico studies – molecular docking

The tridimensional structures of the curcuminoids were downloaded from PubChem [17]. The structures of the HP-β-CD and the SBE-β-CD were drawn in Discovery Studio Visualizer [18] by modifying the crystallographic model of the β-cyclodextrin (PDB ID 1BFN). The geometries of the side chains of the designed structures were then refined via standard energy minimization in Spartan 14 [19], while keeping the geometries of the D-glucopyranonsyl residues constrained. Ligand preparation and docking simulations were performed as we previously described [20], while no constraints were used in any of the simulations. Dockings were carried out using the Extra Precision (XP) procedure settings and poses were ranked using the GlideScore fitness function [21]. The most probable binding mode for each curcuminoid was then assigned based on the best ranked pose, being the corresponding intermolecular interactions with the CD studied through visual inspection with the aid of the receptor-ligand interactions module of Discovery Studio Visualizer [18].

4.2.5   Complex formation

CC was dissolved in pure ethanol (2 mg/mL) until complete dissolution, then was added to the aqueous cyclodextrin solution under magnetic stirring (150 rpm) for 24 hours, protected from the light.

For the solubility test, CC powder, was added to the aqueous cyclodextrin (CD) solution under magnetic stirring (150 rpm) for 24 hours, protected from the light.

4.2.6   **Complex hydrodynamic diameter (size)**

The samples were analyzed by Dynamic Light Scattering (DLS; Zetasizer Nano ZS, Malvern Instruments Ltd, Malvern, England) and by nanoparticle tracking analysis (NTA; Nanosight, Malvern Instruments Ltd, Malvern, England). Both techniques analyze the Brownian movement of the particles to determine the diffusion coefficient, and use the Stokes-Einstein equation to calculate the hydrodynamic diameter of the particles (size). DLS calculates Brownian motion by the resulting fluctuations in the laser beam's diffraction intensity, at a given angle and for a set of particles; the NTA records this movement by image and for each particle.

DLS analyses were performed at an angle of 90 ° and at 25 °C, with samples diluted in ultrapure water (refractive index 1.333 – viscosity 0.8905 cP) until the correlation coefficient reaches a value between 0.7 and 1. Each sample were analyzed in triplicate, with number of runs in automatic mode, after preparing the complex. The results of average particle size, polydispersity index and D10/ D50/ D90 provided by the equipment were considered.

The NTA assays were performed at 25 °C, with samples diluted in ultrapure water to reach between 30-100 particles per frame, and 10^7-10^9 particles per mL. CC-CD complexes were read in NTA without dilution. Each sample were analyzed in triplicate, after preparing the complex. The results of average particle size, D10/ D50/ D90 and concentration of particles per mL provided by the equipment were considered.

4.2.7   **Phase solubility studies**

The effects of HP-β-CD and SBE-β-CD on the solubility of CC was investigated according to the phase solubility method described by Higuchi and Connors [22]. In this experiment increasing concentrations of CD (0–20 mM) were added to a saturated CC solution. The solutions were left under magnetic stirring for 24 h (150 rpm, 25 °C). Aliquots of each vial were centrifuged for 20 min (16000 × g) or the supernatant was filtered through 0.45 µm (Millipore, Burlington, Massachusetts, USA) and diluted to determine CC concentration by HPLC. The phase solubility diagram was obtained by plotting the solubility of CC, versus the concentrations of HP-β-CD or SBE-β-CD (M^{-1}). The complexation efficiency (CE) determines the adequate ratio of CDs to ensure maximum solubility of the

complexed drug [23]. The apparent stability constant (Ks) was calculated by Equation 1, where S0 is the aqueous molar solubility of the drug, taken from the Y intercept of the plot:

$$Ks = Slope/S0 * (1 - Slope) \quad \text{Equation 1}$$

For the CC-CD complex, CE was calculated from the phase solubility plots, according to Equation 2. The CE values allow drug/CD ratio in the formulation, according to Equation 3 [24]:

$$CE = Slope/(1 - Slope) \qquad \text{Equation 2}$$

$$Drug{:}CD = 1{:}\left(1 + \left(\frac{1}{CE}\right)\right) \qquad \text{Equation 3}$$

4.2.8   Freeze drying microscopy

To determine the collapse temperature of the samples, a microscope coupled to a lyophilization module, Lyostat 2, model FDCS 196, Linkam Instruments, Surrey, UK, equipped with a liquid nitrogen freezing system (LNP94/ 2) and temperature controller, was used programmable (TMS94, Linkam). The pressure was monitored through a Pirani valve. The equipment was calibrated with aqueous NaCl solution (eutectic temperature of –21.1 °C). Direct observation of freezing and lyophilization was performed using a Nikon polarized light microscope, model Elipse E600 (Nikon, Japan), and heating-cooling ramps of 2.5 °C/ min, 5 °C/ min and 10 °C/ min.

4.2.9   Freeze drying

The formulations were lyophilized in 7 mL vials or 24-well plate. The process was carried out in the Lyostar 3 lyophilizer (SP scientific), which contains shelves with computational pressure control and temperature ramps. The samples were subjected to different rates of freezing and heating, according to the previous results of the thermal analysis. From their evaluation, the formulations were lyophilized following the coming protocol: freezing at -40 °C for 5 hours, followed by primary drying at -40 °C for 24 hours, secondary drying at -20 °C for 16 hours and 20 °C for 20 hours, with 100 mTorr vacuum.

4.2.10 **Thermogravimetric analysis (TGA)**

The residual moisture of the lyophilized samples was determined using a thermogravimetric analyzer (TGA, model TGA-50M, Shimadzu, Kyoto, Japan). For weighing the samples in an alumina sample holder, a microanalytical balance was used (Mettler Toledo, model MX5, Schwerzenbach, Switzerland). The samples were heated from 25 to 150 °C at a rate of 10 °C per minute.

4.2.11 **Differential scanning calorimetry (DSC)**

The glass/ eutectic transition temperature was performed in DSC (Differential Scanning Calorimetry – Mettler Toledo, model DSC1, Schwerzenbach, Switzerland). For weighing the samples in an aluminum sample holder, a microanalytical balance was used (Mettler Toledo, model MX5, Schwerzenbach, Switzerland). The blank was automatically discounted in each analysis. The analyses were carried out in a nitrogen atmosphere, at a flow of 50 mL/min, in different temperature ranges.

4.2.12 **Minimum inhibitory concentration (MIC)**

The determination of the minimum inhibitory concentration (MIC) was made by the microdilution method in 96-well plates as described by the Clinical and Laboratory Standards Institute (CLSI) [25]. All tests were performed in triplicates. The bacteria and the medium used were described in the Table *2*.

Table 2. Culture media and conditions for bacterial growth.

Bacteria	Culture media	Growth conditions
S. sanguinis 3K36		
S. mitis NCTC 12261	Brain heart infusion	
S. aureus ATCC 29213	(BHI) and brain	CO_2 5 %, 37 °C, for 24
K. pneumoniae ATCC BAA1705	hearth infusion agar	hours
K. pneumoniae ATCC BAA1706	(BHI agar)	
K. pneumoniae ATCC 700603 (ESBL)		

CC was first dissolved in 50% absolute ethanol, while CD-CC was dissolved in sterile distilled water. The concentrations of CC varied from 500 to 0.24 µg/mL with ethanol with a final concentration in the wells of 5%. The plates

were incubated for 24 hours. The experimental groups tested were: A. Test group (culture medium + bacteria + CC in different concentrations); B. Vehicle control group (culture medium + bacteria + 5% ethanol); C. Substance control group (culture medium + CC); D. Culture medium control group and E. Inoculum control group (culture medium + inoculum). To verify the minimum inhibitory concentration, optical density readings were made on a spectrophotometer (550 nm) and then stained with 30 µL of resazurin in each well at 0.01% in aqueous solution, for better visualization of bacterial growth.

4.2.13   **Antiviral activity assay**

Briefly, 96-well plates were prepared with 5 x 10^5 cells/mL of Vero E6 or PBMC (200 µL per well), as previously described [26]. CC concentrations were added 4 h before infection. Vero E cells were infected with IHUMI-3 (a clinical SARS-CoV-2 strain obtained by Pasteur Institute – ongoing sequencing) at a MOI of 1. After 48h post-infection, the replication was estimated by RT-PCR using the Superscrit III platinum one step with Rox kit (Invitrogene) after extraction with the BIoExtract SuperBall kit (Biosellal, Dardilly, France). The primers used were previously described [27].

4.3   RESULTS AND DISCUSSION

4.3.1   **Curcuminoids content**

The HPLC method for curcuminoids contents was linear on the specified range (6 – 100 µg/mL), with correlation coefficient >0.99 (Sup. Table 1). The method was specific, without any other peaks in the same retention time, precise and reproductive.

It was determined the presence of 81.4% of CUR, 16.0% of DMC, and 2.6% of BDC (Sup. Figure 1).

4.3.2   **Mass spectrometry**

Table 3 and Figure 1 shows the results of mass spectrometry, corroborating the results of HPLC, showing greater abundance of CUR, followed by DMC, and BDC.

Table 3. Mass spectrometry results for curcuminoids present in Curcumin C3 complex (CC).

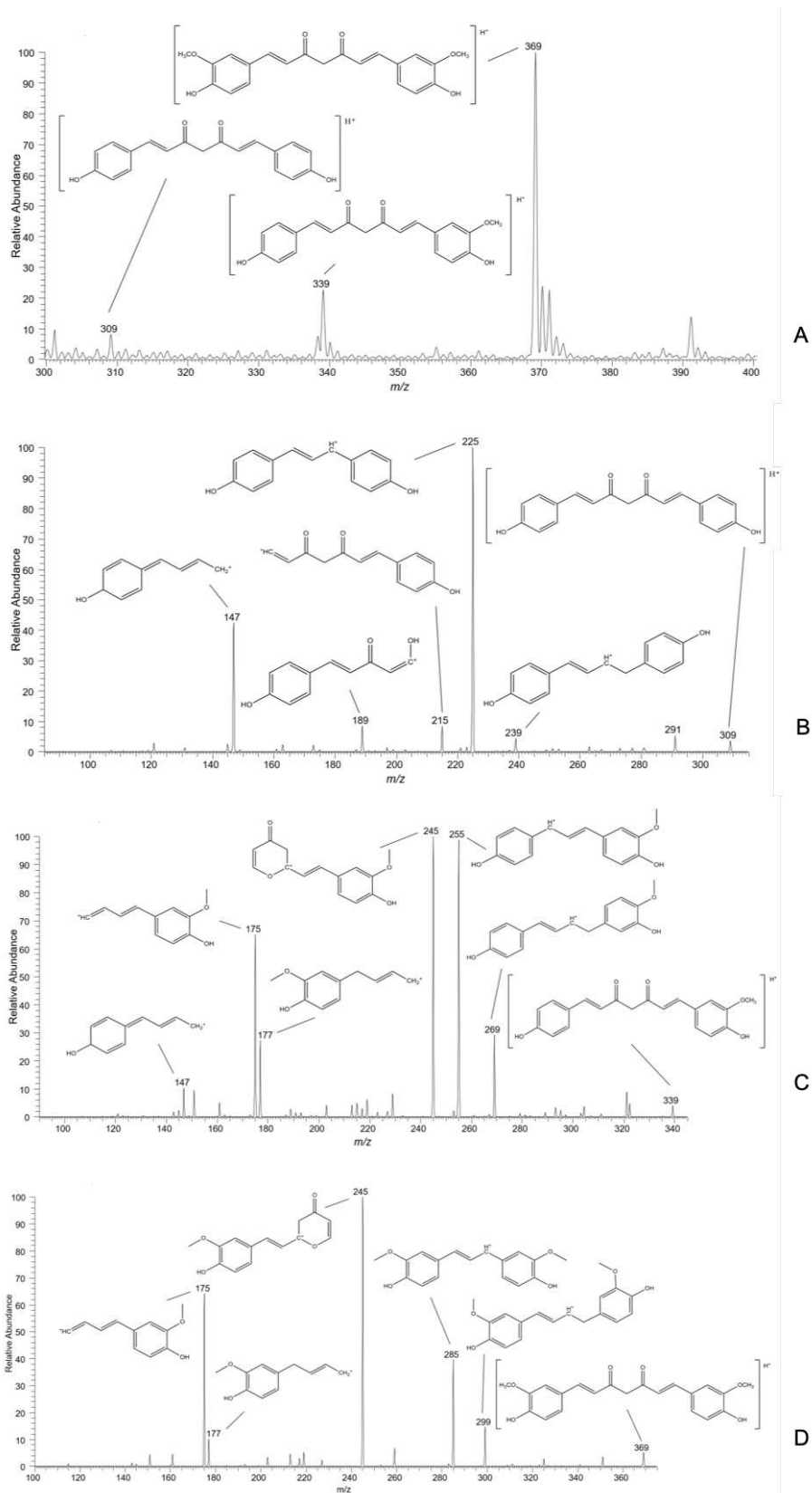| m/z	Curcuminoid	Adduct	MSMS
309	Bisdemethoxycurcumin (BDC)	[M+H]+	225-147-215-189-239-309
339	Demethoxycurcumin (DMC)	[M+H]+	245-255-175-269-177-147-339
369	Curcumin (CUR)	[M+H]+	245-175-285-299-177-369

Figure 1. Mass spectrum of three curcuminoids presents in Curcumin C3 complex (CC): (A) full spectrum; (B) Bisdemethoxycurcumin (BDC), (C) Demethoxycurcumin (DMC) and (D) Curcumin (CUR). Relative abundance in function of m/z.

4.3.3   **Molecular docking**

Considering Curcumin C3 complex contain around 80% of CUR, 16% of DMC and 3% of BDC, we must almost univocally affirm the affinities of these three compounds for the reversed phase C_{18} column observed in the RP-HPLC assay was: CUR > DMC > BDC, with the corresponding retention times BDC < DMC < CUR. However, when we add a CD to the mobile phase, the first compound to elute will be that with the highest affinity for the CD in the mobile phase and, of course, this will also depend on the structure of the CD. In our studies, we used two different CD, the 2-hydroxypropyl-β-cyclodextrin (HP-β-CD) and the sulfobutylether-β-cyclodextrin (SBE-β-CD), which have different 3-D arrangements. While the central channel of HP-β-CD is constricted at one side, making the molecule resemble a half coconut Figure 2A, the bulkier and charged side chains at SBE-β-CD produces a doughnut format Figure 2B, with a larger central cavity that, probably, will make ligands bind more loosely to it.
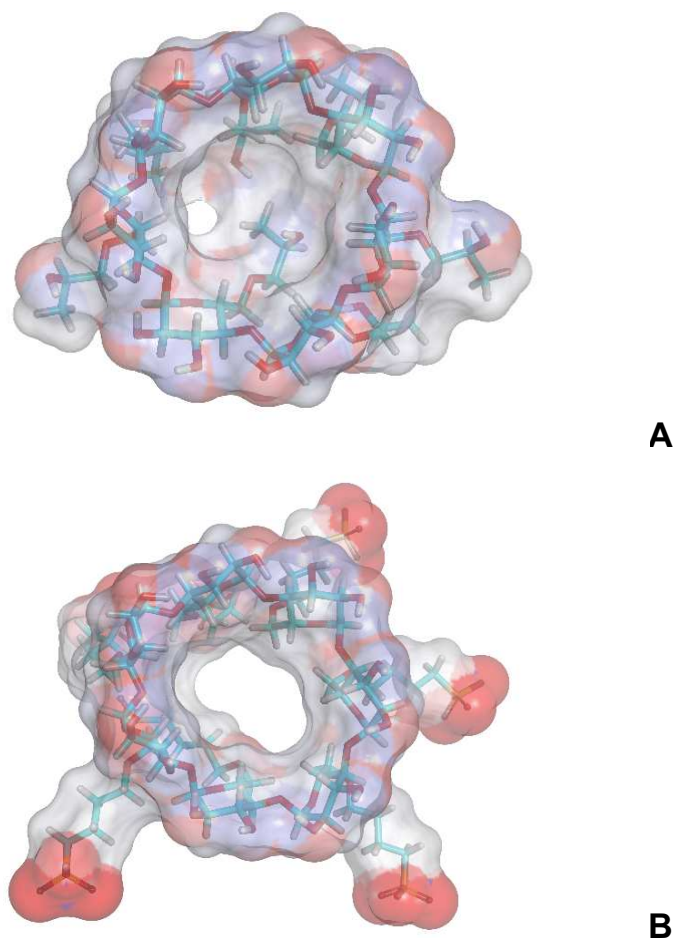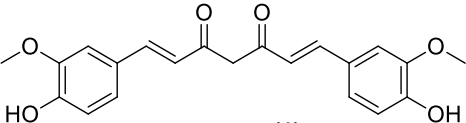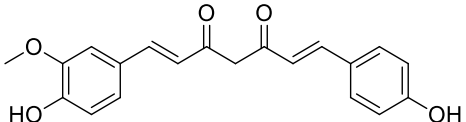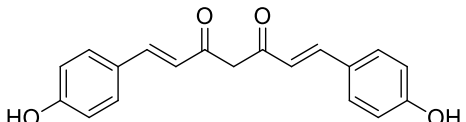
Figure 2. Three-dimensional structures of the 2-hydroxypropyl-β-cyclodextrin (HP-β-CD) (A) and the sulfobutylether-β-cyclodextrin (SBE-β-CD) (B), highlighting the surfaces exposed to the solvent.

However, we must highlight the manufacturer does not clearly state the actual substitution pattern/configuration for the SBE-β-CD [28] and we assumed in our model that all the OH groups at this cyclodextrin are substituted for sulfobutylethers, an assumption that, if incorrect, will affect the predictivity of the model. In this context, we performed molecular docking simulations to assess the potential of the three curcuminoids in interacting with these two cyclodextrins Table 4. According to the predicted binding affinities, the retention times expected for HP-β-CD would be CUR < DMC < BDC, which agree with the experimental observations but, for the SBE-β-CD the retention order would be BDC < DMC < CUR, with CUR only marginally interacting with this cyclodextrin.

Table 4. Docking scores for curcumin (CUR), demethoxycurcumin (DMC) and bisdemethoxycurcumin (BDC) for simulations using two different cyclodextrins, 2-hydroxypropyl-β-cyclodextrin (HP-β-CD) and sulfobutylether-β-cyclodextrin (SBE-β-CD). Docking scores are given in kcal/mol and calculated using the GlideScore function that expresses energy values as negative numbers aiming to reproduce the experimental binding affinities ($\Delta G_{bind} = -RT\ln K_b$).

Compound	ΔG_{bind} for HP-β-CD	ΔG_{bind} for SBE-β-CD
Curcumin (1)	−4.76	−1.51
Demethoxycurcumin (2)	−4.50	−3.69
Bisdemethoxycurcumin (3)	−3.21	−4.89

To confirm the predictivity of the docking models, we performed the visual inspection of the interactions between the docked poses of each curcuminoid and the two CD. Analyses of the predicted interactions of curcumin with HP-β-CD Figure 3A highlight the existence of hydrogen bonds and carbon hydrogen bonds anchoring both the aromatic rings of this compound to, consequently, make curcumin more tightly bind to the target. Carbon hydrogen bonds, represented as C − H ⋯ A hydrogen bonds (where A = O or N), usually display half of the strength of a traditional H bond (3-5 kcal/mol) and are much more frequent in the process of ligand-protein interactions than generally believed [29,30]. For CUR, we observe one regular H-bond and three carbon H-bonds at the phenolic hydroxyl and two more carbon H-bonds at the neighbor O-methoxy substituent of the aromatic ring buried at the central cavity of HP-β-CD. At the other aromatic ring of CUR, three classical H-bonds are observed for the OH/OCH$_3$ substituents of the ring Figure 3A, which aid in preventing the displacement of the CUR by the mobile phase.

Figure 3. Binding modes of curcumin (carbons highlighted in yellow) (A), demethoxycurcumin (carbons highlighted in orange) (B) and bisdemethoxycurcumin (carbons highlighted in magenta) (C) with the HP-β-CD. Classical hydrogen bonds are depicted as green dashed lines while carbon hydrogen bonds are represented as purple dashed lines. A weak H bond, where the aromatic ring acts as H bond acceptor, is also depicted as purple dashed line.

In the interaction of DMC with HP-β-CD Figure 3B, only two carbon H-bonds are observed for the buried (O-demethoxy) phenolic ring, while the solvent accessible part of the ligand are bind to the cyclodextrin via two regular H-bonds,

one at the carbonyl oxygen and other at the phenolic hydroxyl group. For BDC Figure 3C, two classical H bonds and one carbon H-bond are performed with the buried aromatic ring, which are reinforced by a regular but much weaker H bond, where the hydrogen bond acceptor is represented by the delocalized π cloud of the ring [31]. Additionally, one carbon H-bond and one classical H-bond are observed for each of the carbonyl oxygens of the molecule, which partially, but not totally, hinders the displacement of BDC by mobile phase.

When the interactions are estimated for the SBE-β-CD Figure 4A, except for one classical H bond (performed with the phenolic OH of the solvent-exposed ring), only weak interactions are observed for CUR, three carbon H-bonds and one sulfur-π interaction, which has been estimated to contribute between 0.5 and 2 kcal/mol to the total binding energy [32]. We believe this interaction pattern makes curcumin more loosely associated with the CD, then allowing an easy displacement by mobile phase to, possibly, co-elute with the other complexes.
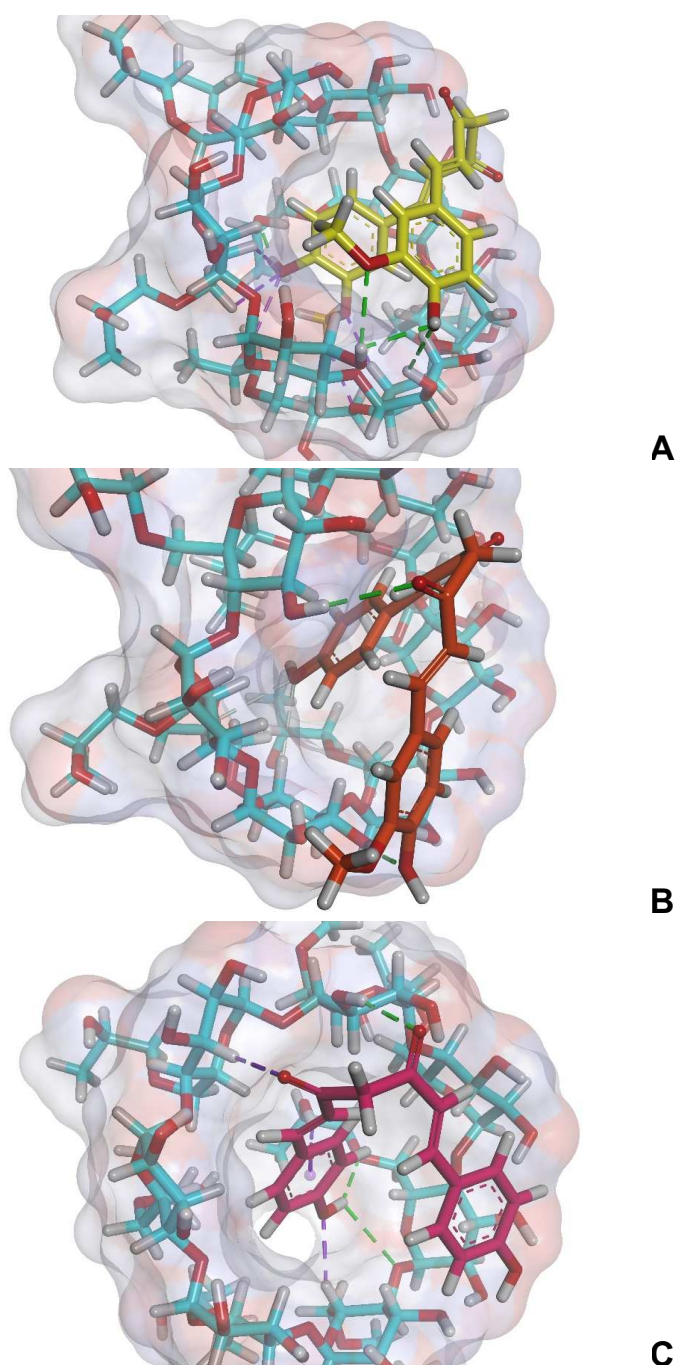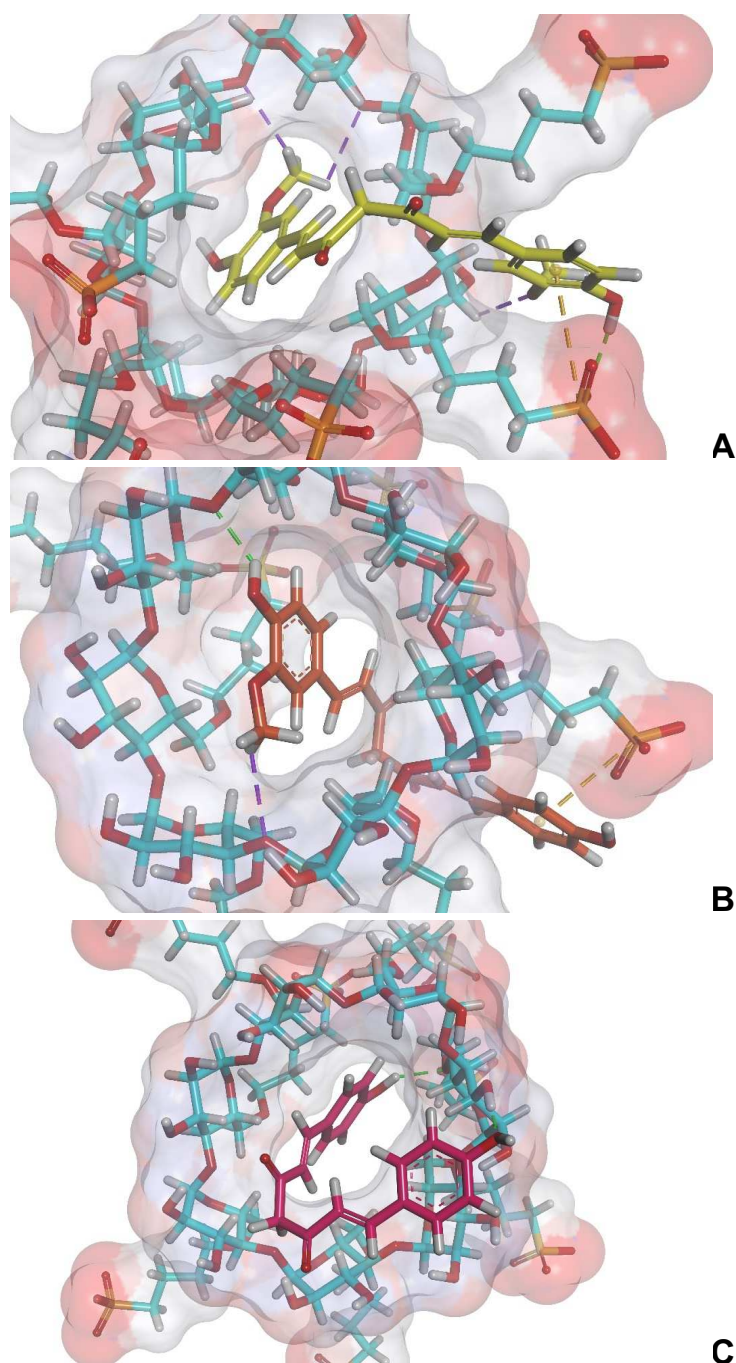
Figure 4. Binding modes of curcumin (carbons highlighted in yellow) (A), demethoxycurcumin (carbons highlighted in orange) (B) and bisdemethoxycurcumin (carbons highlighted in magenta) (C) with the SBE-β-CD. Classical hydrogen bonds are depicted as green dashed lines while carbon hydrogen bonds are represented as purple dashed lines. The sulfur-π interactions are depicted as orange dashed lines.

The binding mode of DMC with SBE-β-CD Figure 4B suggests the aromatic ring anchored at the central cavity of the CD by a classical plus a carbon H bond, while the other terminal moiety of the compound interacting via a sulfur-

π interaction. For BDC Figure 4C, both the phenolic groups are predicted to interact with SBE-β-CD via classical H bonds, making this compound less prone to be solvated by the mobile phase than DMC or CUR.

4.3.4   **Complex hydrodynamic diameter (size)**

The complex HP-β-CD 12 mM and CC was filtered (syringe filters of 0.45 μm) or centrifuged (16,000 rpm, 20 min, 25 ºC) after the equilibration period, followed by determination of hydrodynamic particle size and curcuminoid content (Table 5). There was a difference in the content of curcuminoids (16.77 μg/mL in the filtered complex *versus* 39.39 μg/mL in the centrifuged complex), showing possible interaction of the curcuminoids with the filter, indicating that centrifugation can be the best method to separate soluble from non-soluble curcuminoids.

Table 5. Complex (HP-β-CD 12 mM complexed with Curcumin C3 complex) hydrodynamic size measured by NTA, and curcuminoids content measured by HPLC, comparing the samples after filtration (0.45 μm) and after centrifugation (16,000 rpm, 20 min, 25 ºC).

		Filter	**Centrifugation**
NTA	Mean (nm)	169.9 ± 2.3	221.6 ± 3.1
	D10 (nm)	109.8 ± 1.3	152.9 ± 2.7
	D50 (nm)	149.4 ± 1.8	213.1 ± 4.2
	D90 (nm)	251.2 ± 6.0	301.0 ± 4.1
	Concentration (particles/mL)	$(8.41 \pm 0.20) \times 10^8$	$(1.21 \pm 0.04) \times 10^9$
HPLC	Bisdemethoxycurcumin (μg/mL)	2.48	3.48
	Demethoxycurcumin (μg/mL)	4.18	8.22
	Curcumin (μg/mL)	10.10	27.68
	Curcuminoids total (μg/mL)	16.77	39.39

We tried to measure the hydrodynamic size of the complexes by DLS. In the case of colored solutions, as long as the laser light is not absorbed completely by the solution, the sample can be measured. Emission spectra revealed that curcumin show emission bands at 571 nm, ranging from 500 to 650 nm approximately [33]. Fluorophores that absorb and emit within 600–700 nm interferes with DLS [34], which agrees with what we found: polydispersion index

(PDI) higher than 0.7, showing a high polydisperse sample, and a warning that the sample can be fluorescent, confusing the reading.

4.3.5   **Phase solubility studies**

CC is a drug practically insoluble in water [35]. For in vitro tests to be relevant, and the release of curcumin to be facilitated, an alternative to enable its solubilization is to complex it with CDs, such as HP-β-CD [36,37] and SBE-β-CD.

To verify its viability, the phase solubility study proposed by Higuchi & Connors [22] was carried out, in which increasing concentrations of HP-β-CD or SBE-β-CD were added to saturated solutions of CC. The phase solubility diagrams have two variables: type A occurs when the complex formed is soluble and type B when the complex formed becomes insoluble, from a certain concentration of ligand. In A_P and A_N formats, the ligand is more effective to increase solubility in higher and lower concentrations, respectively. The A_L profile indicates a linear increase in solubility as a function of the concentration of the ligand (CD) [38].

The phase solubility diagram showed an A_L-type phase-solubility profile, with a first order linear increase ($R^2 = 0.994$ for HP-β-CD, and $R^2 = 0.984$ for SBE-β-CD, for total curcuminoids – Table 6) in solubility as a function of the CD concentration (Figure 5) [22].

Table 6. Stability constant (Ks), complexation efficiency (CE), curcuminoid:cyclodextrin (drug:CD) ratio, and solubility of curcuminoids in 20 mM of cyclodextrins (HP-β-CD and SBE-β-CD).

		Curcumin	Demethoxy curcumin	Bisdemethoxy curcumin	Total curcuminoids
Ks_{min}*	HP-β-CD	> 2.1039	> 6.0314	> 9.6493	> 3.051
	SBE-β-CD	> 1.7824	> 6.4674	> 13.7011	> 3.030
CE	HP-β-CD	0.0078	0.0055	0.0019	0.0147
	SBE-β-CD	0.0066	0.0059	0.0027	0.0146
Drug:CD ratio	HP-β-CD	1:128	1:182	1:526	1:69
	SBE-β-CD	1:151	1:169	1:370	1:69
Solubility in CD 20 mM	HP-β-CD	0.1322 mM	0.0792 mM	0.0329 mM	0.2329 mM
	SBE-β-CD	0.1338 mM	0.0958 mM	0.0472 mM	0.2618 mM
R^2	HP-β-CD	0.9498	0.9892	0.7828	0.9941
	SBE-β-CD	0.9140	0.9634	0.8143	0.9838

* Quantification of curcumin in water was not possible, as its concentration was below the limit of quantification. Due to the difficulties in determining S_0 for curcumin, the apparent stability constant (Ks) for the curcumin/ cyclodextrin complexes could not be determined from the phase solubility diagram. In this case, an estimate of the minimum stability constant (Ks_{min}) was made, using the analytical detection limit as the highest possible value for S_0.
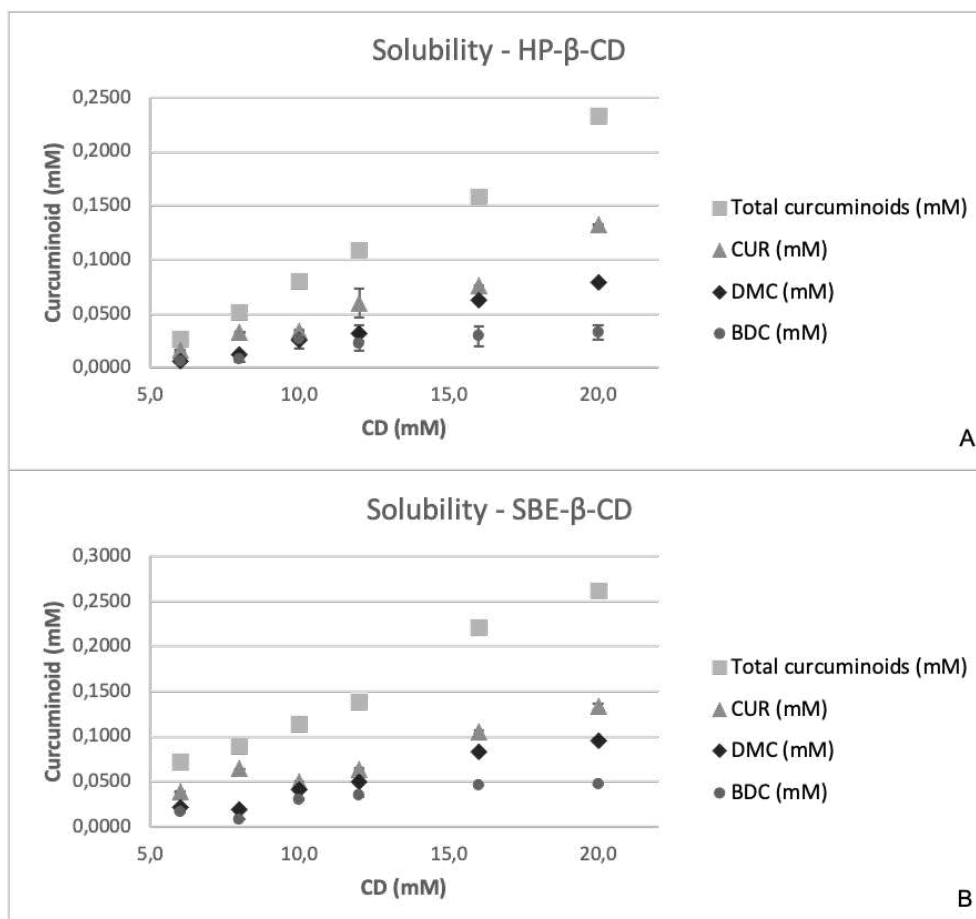
Figure 5. Solubility of three different curcuminoids (bisdemethoxycurcumin, BDC; demethoxycurcumin, DMC; and curcumin CUR) in (A) hydroxypropyl-β-cyclodextrin (HP-β-CD), and (B) sulfobutylether-β-cyclodextrin (SBE-β-CD).

CC dissolved in water (S_0) is lower than the detection limit ($S_0 < 0.005$ mM). The apparent solubility of CC improved up to 46 times (0.233 mM of CC) with 20 mM of HP-β-CD, and up to 52 times (0.262 mM of CC) with 20 mM of SBE-β-CD. Previous studies reached a solubility of 0.122 mM for total curcuminoids, with 79 mM of HP-β-CD [36], and 0.27 mM of CC with 70 mM of HP-β-CD [39]. With 46 mM SBE-β-CD, they found a solubility of 0.123 mM for total curcuminoids [36].

All curcuminoids dissolved in water showed a solubility lower than the detection limit ($S_0 < 0.0002$ mM for BMC, $S_0 < 0.0009$ mM for DMC, and $S_0 < 0.0041$ mM for CUR). The apparent solubility in 40 mM of HP-β-CD was improved up to 60, 28 and 16 times for BDC, DMC and CUR respectively, and in SBE-β-CD up to 49, 26 and 22 times for BDC, DMC and CUR respectively (Table 6).

One previous study reached a CUR solubility of 0.27 mM and BDC solubility of 1.94 mM in 65 mM of HP-β-CD [39].

4.3.6 **Freeze-drying microscopy**

An optimized freeze-drying process guarantees better product stability, shorter processing cycles and lower costs [40]. The improvement of the process depends on the physical and chemical properties of the product, such as the collapse temperature (Tc), determined by lyophilization microscopy. Starting drying above Tc generally results in the collapse of the lyophilized cake structure, which can impact residual moisture, reconstitution times and storage stability [41]. The frozen structure collapsed at −9.2 °C with HP-β-CD, and at −26.9 with SBE-β-CD (Table 7), similar to what was found for pure HP-β-CD (15% w/ w, −9.5 °C) [41], and for pure SBE-β-CD (15% w/ w, −27 °C Tn and −20 °C Tc) [42] in another studies. The resulting Tc is also suitable for an additional scale up, since most industrial freeze-dryers do not operate at temperatures below −40 °C.

Table 7. Freeze-drying microscopy.

Complex	CCCD_024 (HP-β-CD)	CCCD_025 (SBE-β-CD)
Tn	-17.9 °C	-23.4 °C
Tco	-10.7 °C	-28.2 °C
Tc	-9.2 °C	-26.9 °C

Tn: nucleation temperature, i.e. when the sample freeze; Tco: micro collapse temperature; Tc: total collapse temperature.

### 4.3.7 **Complex evaluation**

Curcumin-cyclodextrin complexes (CC-CD) were produced with 5 mM of CC, and 20 mM of CD (1:4), in 20% of ethanol. After equilibration time and centrifugation, the complexes were freeze-dried. The freeze-dried complexes were evaluated by thermogravimetric analysis to determine the residual moisture, and curcuminoids content (Table 8).

Table 8. Curcuminoids (bisdemethoxycurcumin – BDC, demethoxycurcumin – DMC, and curcumin – CUR) content and residual moisture of freeze-dried complexes (CCCD).

Complex	CCCD_024 (HP-β-CD)	CCCD_025 (SBE-β-CD)
BDC (µg/mL)	0.047	0.045
DMC (µg/mL)	0.276	0.270
CUR (µg/mL)	1.362	1.341
CC total (µg/mL)	1.684	1.656
CC total (mM)	4.57	4.50
Residual moisture (%)	5.37	6.82

4.3.8 Differential scanning calorimetry (DSC)

DSC analysis was carried out as a method to confirm that the complex CC-CD was formed. As seen in the figure below, the pronounced exothermic peak of curcumin (Figure 6A) appears in the physical mixture of SBE-β-CD and curcumin C3 complex (Figure 6B) in a minor endothermic peak due to the decrease in curcumin concentration in the total mass analyzed. However, it completely disappeared in the CC-CD complex (Figure 6C), showing curcumin complexation with cyclodextrin.
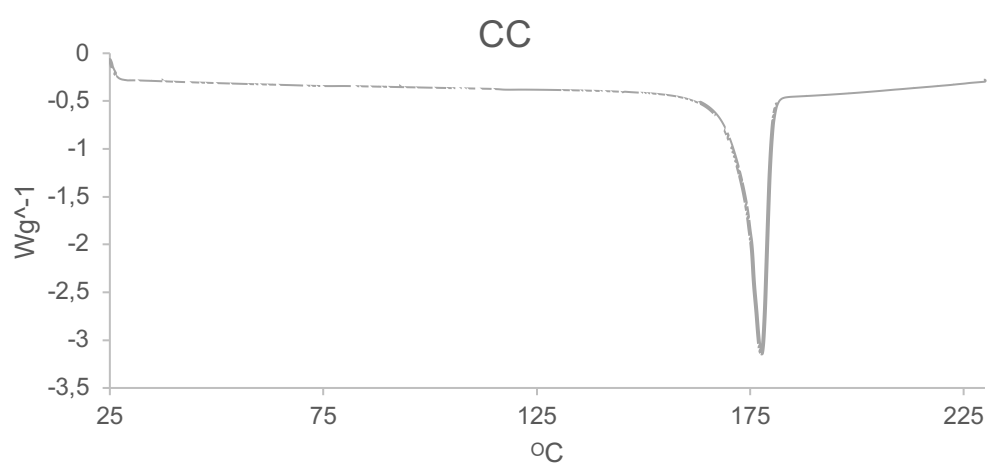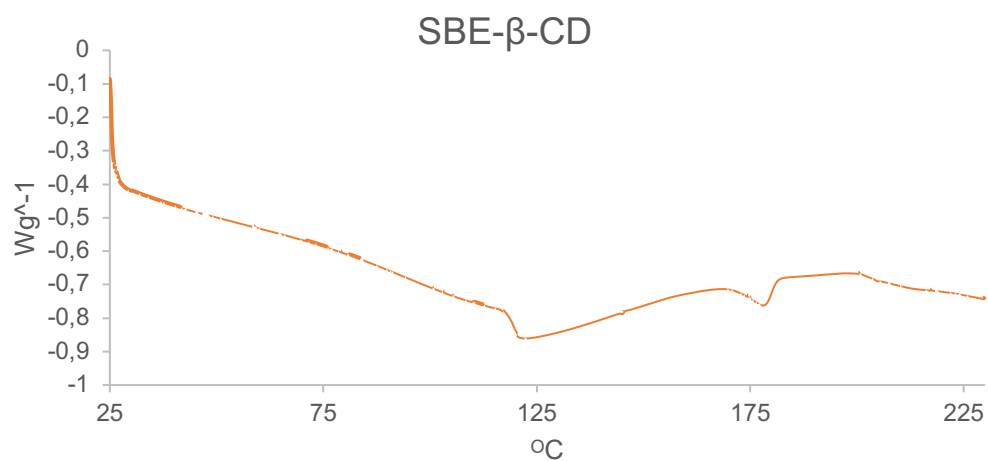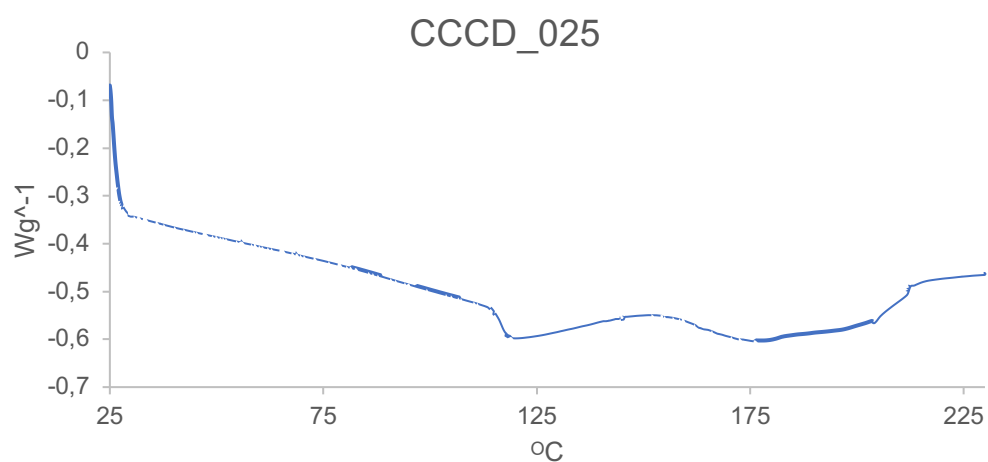
Figure 6. DSC (A) Pure curcumin C3 complex (CC), (B) physical mixture of CC and sulfobutylether-β-cyclodextrin (SBE-β-CD), and (C) CCCD_025 (CC and SBE-β-CD complex).

4.3.9 **Minimum inhibitory concentration (MIC)**

Minimal inhibitory concentration (MIC) experiments was conducted in order to explore the antimicrobial activity of curcumin. The results are in Table 9.

Table 9. Free and cyclodextrin complexed curcumin minimal inhibitory concentration (MIC, µg/mL) against oral and pulmonary bacterial strains.

Strain	MIC (µg/mL)		
	Curcumin (CC)	CCCD_024 (HP-β-CD)	CCCD_025 (SBE-β-CD)
S. sanguinis 3K36	250	>500	>500
S. mitis NCTC 12261	125	>500	125
S. aureus ATCC 29213	500	>500	>500
K. pneumoniae ATCC 700603	>500	200	100
K. pneumoniae BAA 1705	>500	>500	>500
K. pneumoniae BAA 1706	>500	>500	>500

Gunes et al. [43] showed that curcumin presents a MIC of 219 µg/mL, which is approximately 1-fold higher than the result that we found, and a MIC of 216 µg/mL against *K. pneumoniae* ATCC 700603, but the extract used had 67% of purity.

In previous studies, curcumin showed activity against *S. aureus* ATCC 25923: Tajbakhsh at al. [44] found a MIC of 187.5 µg/mL, and Mun et al. [45] a MIC of 250 µg/mL, but both studies diluted curcumin in DMSO.

Although the MIC values found were high when compared to other drugs, it is below the toxicity of curcumin, which has been shown to be safe at oral doses of up to 8 g per day in clinical trials [46,47].

We did not find previous studies with curcumin facing these oral bacteria to compare the results found in this work. We also plan to perform this test with more oral bacteria.

4.3.10 **Antiviral activity assay**

Despite the theoretical activity of CC against the SARS-CoV-2 [10,11], it was not possible to identify this action in the concentrations tested (10, 20 and 50 µg/mL) in test performed (Figure 7).
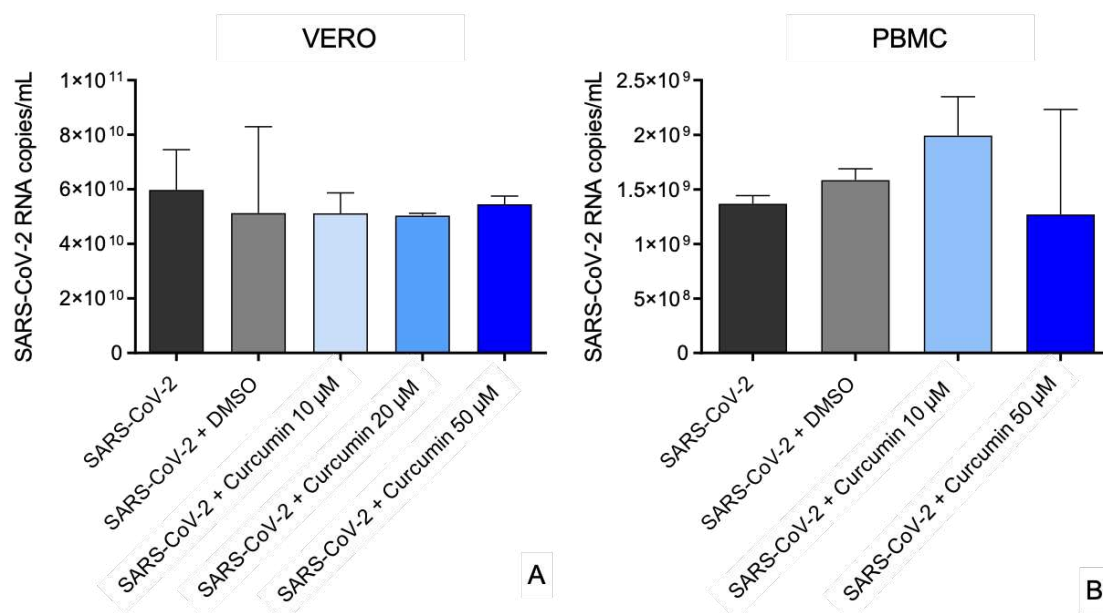

Figure 7. Antiviral activity of curcumin C3 complex (Curcumin) against SARS-CoV-2 in (A) Vero cells, and in (B) peripheral blood mononuclear cell (PBMC) cells.

4.4   CONCLUSION

Each curcuminoid was detected and quantified by the validated HPLC method, which was also suitable for quantifying the complexed species. Complexations were evaluated by phase solubility studies that indicated a linear increase in curcuminoids solubility as a function of the concentration of both cyclodextrins. From our knowledge, this is the first work to evaluate curcuminoids complexation individually. The curcumin-cyclodextrin complexes were formed and freeze-dried, with its formation confirmed by DSC, although it was not possible to identify separate complex curcuminoid entities. SBE-β-CD showed slightly greater capacity to increase the curcuminoids solubility.

The MIC results suggest that curcumin showed antimicrobial activity against *S. sanguinis* and *S. mitis*, common oral bacteria strains, while only the complex formed with SBE-β-CD showed activity against *S. mitis*. Both curcumin complexes have shown action against one strain of respiratory bacteria *K. pneumoniae*, increasing its activity comparing with free curcumin. There are no reports of activity modifications on bacteria upon cyclodextrin complexation of curcumin and more research is in need to understand the involved mechanisms of changing, since they are not equal to all tested bacteria. Unfortunately, it was not possible to achieve antiviral activity against SARS-CoV-2 in the concentrations tested.

Ongoing studies will improve complex understanding: X-ray diffraction, scanning electron microscopy, drug release, and *in vitro* anti-inflammatory activity. Also, future studies incorporating the complexes in buccal wafers will be carried out to evaluate its potential for buccal affections.

4.5 REFERENCES

1. Kocaadam, B. & Şanlier, N. Curcumin, an active component of turmeric (Curcuma longa), and its effects on health. *Critical Reviews in Food Science and Nutrition* **57**, 2889–2895 (2017).

2. Nagpal, M. & Sood, S. Role of curcumin in systemic and oral health: An overview. *J Nat Sci Biol Med* **4**, 3–7 (2013).

3. Kim, J. H., Gupta, S. C., Park, B., Yadav, V. R. & Aggarwal, B. B. Turmeric (Curcuma longa) inhibits inflammatory nuclear factor (NF)-κB and NF-κB-regulated gene products and induces death receptors leading to suppressed proliferation, induced chemosensitization, and suppressed osteoclastogenesis. *Mol Nutr Food Res* **56**, 454–465 (2012).

4. Sandur, S. K. *et al.* Curcumin, demethoxycurcumin, bisdemethoxycurcumin, tetrahydrocurcumin and turmerones differentially regulate anti-inflammatory and anti-proliferative responses through a ROS-independent mechanism. *Carcinogenesis* **28**, 1765–1773 (2007).

5. Tønnesen, H. H. Studies on curcumin and curcuminoids. XV. Catalytic effect of demethoxy- and bisdemethoxycurcumin on the peroxidation of linoleic acid by 15-lipoxygenase. *International Journal of Pharmaceutics* **51**, 179–181 (1989).

6. Dai, J. *et al.* Inhibition of curcumin on influenza A virus infection and influenzal pneumonia via oxidative stress, TLR2/4, p38/JNK MAPK and NF-κB pathways. *International Immunopharmacology* **54**, 177–187 (2018).

7. Han, S., Xu, J., Guo, X. & Huang, M. Curcumin ameliorates severe influenza pneumonia via attenuating lung injury and regulating macrophage cytokines production. *Clinical and Experimental Pharmacology and Physiology* **45**, 84–93 (2018).

8. Avasarala, S. *et al.* Curcumin Modulates the Inflammatory Response and Inhibits Subsequent Fibrosis in a Mouse Model of Viral-induced Acute Respiratory Distress Syndrome. *PLOS ONE* **8**, e57285 (2013).

9. Barnard, D. L. & Kumaki, Y. Recent developments in anti-severe acute respiratory syndrome coronavirus chemotherapy. *Future Virology* **6**, (2011).

10. Kandeel, M. & Al-Nazawi, M. Virtual screening and repurposing of FDA approved drugs against COVID-19 main protease. *Life Sciences* **251**, 117627

(2020).

11.   Jena, A. B., Kanungo, N., Nayak, V., Chainy, G. B. N. & Dandapat, J. Catechin and Curcumin interact with corona (2019-nCoV/SARS-CoV2) viral S protein and ACE2 of human cell membrane: insights from Computational study and implication for intervention. *Nature Research Journal* **(under review)**, (2020).

12.   Keihanian, F., Saeidinia, A., Bagheri, R. K., Johnston, T. P. & Sahebkar, A. Curcumin, hemostasis, thrombosis, and coagulation. *Journal of Cellular Physiology* **233**, 4497–4511 (2018).

13.   Shailendiran, D. *et al.* Characterization and Antimicrobial Activity of Nanocurcumin and Curcumin. in *2011 International Conference on Nanoscience, Technology and Societal Implications* 1–7 (IEEE, 2011). doi:10.1109/NSTSI.2011.6111984.

14.   Bhawana, Basniwal, R. K., Buttar, H. S., Jain, V. K. & Jain, N. Curcumin Nanoparticles: Preparation, Characterization, and Antimicrobial Study. *J. Agric. Food Chem.* **59**, 2056–2061 (2011).

15.   Wichitnithad, W., Jongaroonngamsang, N., Pummangura, S. & Rojsitthisak, P. A simple isocratic HPLC method for the simultaneous determination of curcuminoids in commercial turmeric extracts. *Phytochemical Analysis* **20**, 314–319 (2009).

16.   Thermo Scientific. *Mass Frontier*. (Thermo Fisher Scientific Inc.).

17.   PubChem. PubChem. https://pubchem.ncbi.nlm.nih.gov/.

18.   BIOVIA, Dassault Systèmes. *Discovery Studio Visualizer*. (Dassault Systèmes, 2016).

19.   Wavefunction. *Spartan*. (Wavefunction Inc., 2014).

20.   Kagami, L. P. *et al.* Identification of a novel putative inhibitor of the Plasmodium falciparum purine nucleoside phosphorylase: exploring the purine salvage pathway to design new antimalarial drugs. *Mol Divers* **21**, 677–695 (2017).

21.   Friesner, R. A. *et al.* Glide: A New Approach for Rapid, Accurate Docking and Scoring. 1. Method and Assessment of Docking Accuracy. *J. Med. Chem.* **47**, 1739–1749 (2004).

22.   Higuchi, T. & Connors, K. A. Phase-solubility techniques. *Adv. Anal. Chem. Instrum.* **4**, 117–210 (1965).

23. Loftsson, T., Hreinsdóttir, D. & Másson, M. Evaluation of cyclodextrin solubilization of drugs. *International Journal of Pharmaceutics* **302**, 18–28 (2005).

24. Loftsson, T., Hreinsdóttir, D. & Másson, M. The complexation efficiency. *J Incl Phenom Macrocycl Chem* **57**, 545–552 (2007).

25. CLSI. *Methods for Antimicrobial Susceptibility Testing of Anaerobic Bacteria; Approved Standard—Seventh Edition; CLSI document M11-A7*. vol. 27 (Clinical and Laboratory Standard Institute, 2007).

26. Andreani, J. *et al.* In vitro testing of combined hydroxychloroquine and azithromycin on SARS-CoV-2 shows synergistic effect. *Microbial Pathogenesis* **145**, 104228 (2020).

27. Amrane, S. *et al.* Rapid viral diagnosis and ambulatory management of suspected COVID-19 cases presenting at the infectious diseases referral hospital in Marseille, France, - January 31st to March 1st, 2020: A respiratory virus snapshot. *Travel Medicine and Infectious Disease* **36**, 101632 (2020).

28. Jain, A. S., Date, A. A., Pissurlenkar, R. R. S., Coutinho, E. C. & Nagarsenker, M. S. Sulfobutyl ether(7) β-cyclodextrin (SBE(7) β-CD) carbamazepine complex: preparation, characterization, molecular modeling, and evaluation of in vivo anti-epileptic activity. *AAPS PharmSciTech* **12**, 1163–1175 (2011).

29. Gilli, G. & Gilli, P. *The Nature of the Hydrogen Bond: Outline of a Comprehensive Hydrogen Bond Theory*. (OUP Oxford, 2009).

30. Freitas, R. F. de & Schapira, M. A systematic analysis of atomic protein–ligand interactions in the PDB. *Med. Chem. Commun.* **8**, 1970–1981 (2017).

31. Nolan, T., Singh, N. & McCurdy, C. R. Ligand macromolecule interactions: theoretical principles of molecular recognition. *Methods Mol Biol* **572**, 13–29 (2009).

32. Daeffler, K. N.-M., Lester, H. A. & Dougherty, D. A. Functionally Important Aromatic–Aromatic and Sulfur−π Interactions in the D2 Dopamine Receptor. *J. Am. Chem. Soc.* **134**, 14890–14896 (2012).

33. Ali, Z., Saleem, M., Atta, B. M., Khan, S. S. & Hammad, G. Determination of curcuminoid content in turmeric using fluorescence spectroscopy. *Spectrochimica Acta Part A: Molecular and Biomolecular Spectroscopy* **213**, 192–198 (2019).

34. Bhattacharjee, S. In relation to the following article "DLS and zeta potential

— What they are and what they are not?" Journal of Controlled Release, 2016, 235, 337–351. *Journal of Controlled Release* **238**, 311–312 (2016).

35.   Curcumin - DrugBank. https://www.drugbank.ca/drugs/DB11672.

36.   Tønnesen, H. H., Másson, M. & Loftsson, T. Studies of curcumin and curcuminoids. XXVII. Cyclodextrin complexation: solubility, chemical and photochemical stability. *Int J Pharm* **244**, 127–135 (2002).

37.   Mohan, P. R. K., Sreelakshmi, G., Muraleedharan, C. V. & Joseph, R. Water soluble complexes of curcumin with cyclodextrins: Characterization by FT-Raman spectroscopy. *Vibrational Spectroscopy* **62**, 77–84 (2012).

38.   Frömming, K.-H. & Szejtli, J. *Cyclodextrins in Pharmacy*. (Springer Science & Business Media, 1993).

39.   Singh, R., Tønnesen, H. H., Vogensen, S. B., Loftsson, T. & Másson, M. Studies of curcumin and curcuminoids. XXXVI. The stoichiometry and complexation constants of cyclodextrin complexes as determined by the phase-solubility method and UV–Vis titration. *J Incl Phenom Macrocycl Chem* **66**, 335–348 (2010).

40.   Franks, F. Freeze-drying of bioproducts: putting principles into practice. *European Journal of Pharmaceutics and Biopharmaceutics* **45**, 221–229 (1998).

41.   Meister, E., Šaši, S. & Gieseler, H. Freeze-Dry Microscopy: Impact of Nucleation Temperature and Excipient Concentration on Collapse Temperature Data. *AAPS PharmSciTech* **10**, 582–588 (2009).

42.   Liu, J., Viverette, T., Virgin, M., Anderson, M. & Dalal, P. A Study of the Impact of Freezing on the Lyophilization of a Concentrated Formulation with a High Fill Depth. *Pharmaceutical Development and Technology* **10**, 261–272 (2005).

43.   Gunes, H. *et al.* Antibacterial effects of curcumin: An in vitro minimum inhibitory concentration study. *Toxicol Ind Health* **32**, 246–250 (2016).

44.   Tajbakhsh, S. *et al.* Antibacterial activity of indium curcumin and indium diacetylcurcumin. *African Journal of Biotechnology* **7**, (2008).

45.   Mun, S.-H. *et al.* Synergistic antibacterial effect of curcumin against methicillin-resistant Staphylococcus aureus. *Phytomedicine* **20**, 714–718 (2013).

46.   Cheng, A. L. *et al.* Phase I clinical trial of curcumin, a chemopreventive agent, in patients with high-risk or pre-malignant lesions. *Anticancer research* **21**, 2895–900 (2000).

47.   Siviero, A. *et al.* Curcumin, a golden spice with a low bioavailability. *Journal of Herbal Medicine* **5**, 57–70 (2015).

48.   Brasil. ANVISA, I. Resolution RDC Nº 166. (2017).

49.   Abraham, J. International Conference On Harmonisation Of Technical Requirements For Registration Of Pharmaceuticals For Human Use. in *Handbook of Transnational Economic Governance Regimes* (eds. Brouder, A. & Tietje, C.) 1041–1054 (Brill, 2009). doi:10.1163/ej.9789004163300.i-1081.897.

50.   ICH. Validation of analytical procedures: text and methodology Q2 (R1). (2005).

4.6   SUPPLEMENTARY FILES

4.6.1   **Curcumin content method validation**

The validation of the analytical method was performed as described in the guideline from *Agência Nacional de Vigilância Sanitária* (Brazilian Health Regulatory Agency) [48] and the International Conference on the Harmonization of Technical Requirements for the Human Use [49] were used in order to direct the validation of the method.

4.6.1.1   Specificity

Specificity was assessed to ensure that the method has the ability to measure exactly the compound of interest when others are present (for example, impurities, degradation products and matrix components) [48,50]. The mobile phase was used as a dispersant in the determination of CC in CD complexes, to evaluate the specificity of the analytical method.

4.6.1.2   Linearity

The linearity of the method was determined in order to demonstrate that the results obtained were proportional to the concentration of the analyte in the sample, within the specified interval. Different concentrations, carried out in triplicate and in three days, were used for the construction of the analytical curve, and the linear regression calculation was performed using the least squares method [48,50].

4.6.1.3   Precision

The precision, expressed by Sup. Equation 1, assesses the proximity of the results generated in several experiments of a multiple sampling of the same sample.

$$CV = \frac{SD}{DMC} * 100 \qquad \text{Sup. Equation 1}$$

The precision of an analytical method can be expressed as a standard deviation (coefficient of variation, CV) of various measures, where SD is the standard deviation and DMC, the determined mean concentration. Values greater than 5% are not allowed, which must be defined according to the methodology

used, with the concentration of the analyte in the sample, with the type of matrix and the purpose of the method [48].

Repeatability was performed in 3 runs, using 3 standard concentrations (low, medium and high), on the same day, by the same analyst. The intermediate precision was performed in 3 runs, on 3 different days.

4.6.1.4   Accuracy

The proximity of the results obtained by the method under study to the true value defines the accuracy of an analytical method. After establishing the linearity and specificity of the analytical method, its accuracy is determined from at least nine determinations, considering the linear range of the procedure, that is, three concentrations: low, medium and high, with three replicates of each. Accuracy (A) was obtained using Sup. Equation 2, which relates the average concentration determined experimentally and the theoretical concentration [48],

$$A = \frac{DAC}{TC} * 100 \quad \text{Sup. Equation 2}$$

where, TC is the theoretical concentration and DAC is the determined average concentration.

4.6.1.5   Interval

The range between the limits of quantification used in the construction of the analytical curve is called the interval; this is derived from the linearity assessment, being dependent on the desired application [48,50]. The specified range was determined by confirming that the method has adequate accuracy, precision and linearity.

### 4.6.1.6   Detection and quantification limits

The detection limit (DL) refers to the smallest amount of the analyte in a sample that can be detected, but not necessarily quantified, under the established experimental conditions. By analyzing solutions of known and decreasing concentrations of the analyte, down to the lowest detectable level, the detection limit can be measured.

The limit of quantification (QL) is the smallest amount of the analyte in a sample to be determined with allowable precision and accuracy under the experimental conditions already determined.

In the case of instrumental methods (HPLC, gas chromatography, atomic absorption), the DL estimate can be made based on the ratio of 3 times the baseline noise. For the QL, the baseline noise is determined and the concentration that produces a signal-to-noise ratio greater than 10: 1 is considered as the limit of quantification [50].

4.6.2   Curcumin content method validation – Results

Sup. Figure 1 shows the chromatogram of a standard CC sample, the peaks of bisdemethoxycurcumin (BDC), demethoxycurcumin (DMC) and curcumin (CUR) can be visualized in a retention time of 10.1, 11.5 and 13.1 minutes, respectively, similar with found by Wichitnithad et al. [15]. No other peaks were observed at the same retention time when samples of CD without CC were evaluated under the same conditions of chromatographic analysis, as well as impurities of the components were not observed, thus demonstrating specificity in the established technique.
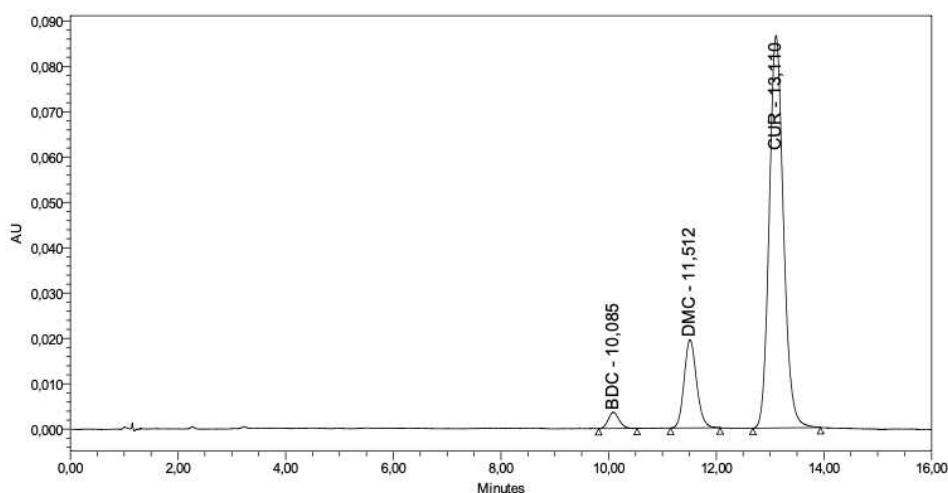
	Peak Name	RT (min)	Area (µV*sec)	% Area	Height (µV)	% Height
1	BDC	10,085	50052	2,57	3564	3,25
2	DMC	11,512	311712	16,01	19480	17,78
3	CUR	13,110	1584997	81,42	86531	78,97

Sup. Figure 1. Curcumin C3 complex (CC) chromatogram, showing the three curcuminoids: bisdemethoxycurcumin (BDC), demethoxycurcumin (DMC) and curcumin (CUR).

CC solutions were prepared containing between 6 µg/mL to 100 µg/mL. The correlation coefficients (R^2) were > 0.99, according to the recommendations of RDC 166 of ANVISA [48] (Sup. Table 1).

Sup. Table 1. Linearity, limit of detection (LOD) and limit of quantitation (LOQ) for the three curcuminoids: bisdemethoxycurcumin (BDC), demethoxycurcumin (DMC) and curcumin (CUR).

	BDC	DMC	CUR
Linear equation	y = 36804x − 1156	y = 37631x − 4368.8	y = 38420x − 27102
R^2	0.9998	0.9999	0.9999
Range (µg/mL)	0.18 – 2.80	1.07 – 17.12	5.31 – 84.95
LOD (µg/mL)	0.05	0.28	1.34
LOQ (µg/mL)	0.16	0.84	4.07

4.6.2.1 Precision

The data are presented in Sup. Table 2, showing CV values below 5%, and accuracy results according to ANVISA's determination (between 95% and 105%).

Sup. Table 2. Results of the precision analysis (mean and standard deviation (SD) of triplicate), and accuracy for the three curcuminoids: bisdemethoxycurcumin (BDC), demethoxycurcumin (DMC) and curcumin (CUR).

Curcuminoid concentration (µg/mL)		Intraday		Inter day		Accuracy (%)
		Mean ± SD (µg/mL)	CV (%)	Mean ± SD (µg/mL)	CV (%)	
BDC	2.8	2.79 ± 0.05	1.91	2.96 ± 0.12	4.12	99.6
	1.4	1.39 ± 0.02	1.40	1.44 ± 0.06	4.43	99.0
	0.4	0.36 ± 0.02	4.59	0.38 ± 0.01	1.14	102.6
DMC	17.1	17.10 ± 0.09	0.55	17.78 ± 0.68	3.81	99.9
	8.6	8.43 ± 0.03	0.36	8.85 ± 0.34	3.87	98.5
	2.1	2.18 ± 0.02	0.74	2.29 ± 0.10	4.18	101.7
CUR	85.0	85.02 ± 0.24	0.28	88.10 ± 2.93	3.32	101.1
	42.5	41.96 ± 0.11	0.27	43.8 ± 1.69	3.86	98.8
	10.6	10.94 ± 0.07	0.67	11.45 ± 0.46	4.05	103.0

4.6.2.2 Robustness

It was used the same column, in a different laboratory in another HPLC equipment (Shimadzu, LabSolutions software).

The method is linear on the specified range (6 – 100 µg/mL), with correlation coefficient >0.99 (Sup. Table 3). The method is specific, without any other peaks in the same retention time.

Sup. Table 3. Equations and correlation coefficients (R2) obtained for the three curcuminoids: bisdemethoxycurcumin (BDC), demethoxycurcumin (DMC) and curcumin (CUR).

	BDC	DMC	CUR
Linear regression	y = 41297x – 2036.2	y = 40424x – 2157.1	y = 41452x – 48598
R^2	0.9993	1.0000	0.9992

5 FINAL CONSIDERATIONS

The aim of this work was to develop mucoadhesive polymeric wafers and cyclodextrin complex to release drugs. We could formulate freeze-dried wafers with a good physical appearance with both drugs lidocaine and curcumin, and the quantification methods of lidocaine and curcumin were adapted and validated successfully. After the theoretical selection of the polymers, they were characterized by zeta potential, pH and thermal proprieties, leading to the better choice for the wafer polymers. Buccal wafers produced presented a good physical appearance, a porous surface, and a good drug entrapment.

Free lidocaine hydrochloride and curcumin presented antimicrobial activity against some common oral bacterial strains, notably against *P. gingivalis*. Future studies will evaluate antimicrobial activity of both drugs in the wafer. While lidocaine wafers presented a satisfactory drug release, in both methods tested, the same did not occur with curcumin wafers, leading the complexation of curcumin with cyclodextrin, to improve its water solubility.

Curcumin-cyclodextrins complexes were characterized, and through HPLC analysis it was possible to quantify the three main curcuminoids in the formulations. Nanocomplexes with both cyclodextrins showed improvement in curcumin solubility.

Curcumin-sulfobutylether-beta-cyclodextrin complex presented the same antibacterial activity against oral bacteria *S. mitis* than free curcumin, while it surpasses free curcumin activity facing *K. pneumoniae* ATCC 700603, as well as curcumin-hydroxypropyl-beta-cyclodextrin. This result showed that complexes formed with different cyclodextrins can show changes in antibacterial activity against free curcumin, implying as an important test.

Future studies will be conducted incorporating curcumin-cyclodextrin complexes in buccal wafer, enabling curcumin release in the aqueous medium. The antibacterial activity of the curcumin-cyclodextrin wafer will be evaluated, comparing with the free complexes.

15% match (publicações)
Juliana Souza Ribeiro Costa, Karen de Oliveira Cruvinel, Laura Oliveira-Nascimento. "A mini-review on drug delivery through wafer technology: Formulation and manufacturing of buccal and oral lyophilizates", Journal of Advanced Research, 2019

1% match (Internet a partir de 08-jan-2014)
http://guiacosmeceutico.com.br/index.php/component/attachments/download/3

1% match (Internet a partir de 06-mar-2021)
https://purehost.bath.ac.uk/ws/files/157825353/Thermal_comfort_in_refugee_camps_final_AAM.pdf

1% match (Internet a partir de 28-ago-2020)
https://www.mdpi.com/1422-0067/21/16/5741/htm

1% match (Internet a partir de 12-set-2019)
http://repositorio.unicamp.br/jspui/bitstream/REPOSIP/334889/1/Couto_VeronicaMuniz_D.pdf

1% match ()
https://www.ncbi.nlm.nih.gov/pubmed/31193385

< 1% match (publicações)
Janaína Artem Ataide, Danilo Costa Geraldes, Eloah Favero Gérios, Fernanda Mazon Bissaco et al. "Freeze-dried chitosan nanoparticles to stabilize and deliver bromelain", Journal of Drug Delivery Science and Technology, 2020

< 1% match (Internet a partir de 04-mar-2021)
https://idoc.pub/documents/paccon2017-proceedings-jlk9v02yg545

< 1% match (Internet a partir de 24-mar-2021)
https://www.ncbi.nlm.nih.gov/books/NBK526006/

< 1% match (Internet a partir de 29-mar-2019)
https://austinpublishinggroup.com/analytical-pharmaceutical-chemistry/fulltext/ajapc-v1-id1022.php

< 1% match (publicações)
Hanne Hjorth Tønnesen, Már Másson, Thorsteinn Loftsson. "Studies of curcumin and curcuminoids. XXVII. Cyclodextrin complexation: solubility, chemical and photochemical stability", International Journal of Pharmaceutics, 2002

< 1% match (Internet a partir de 23-ago-2016)
https://www.scribd.com/document/250553175/4-Encyclopedia-of-Pharmaceutical-Technology-Third-Edition-pdf

< 1% match (publicações)
Bhawana, Rupesh Kumar Basniwal, Harpreet Singh Buttar, V. K. Jain, Nidhi Jain. "Curcumin Nanoparticles: Preparation, Characterization, and Antimicrobial Study", Journal of Agricultural and Food Chemistry, 2011

< 1% match (Internet a partir de 26-mai-2020)
https://www.mediterranee-infection.com/wp-content/uploads/2020/04/Dox_Covid_pre-print.pdf

< 1% match (Internet a partir de 14-jan-2021)